Investigation of radon prevention and mitigation: from radon measurements to specification for soil depressurisation systems

by

Marta Fuente Lastra

Supervisor: Dr Mark Foley

Co-supervisor: Dr Jamie Goggins

A thesis submitted to the National University of Ireland Galway in accordance with the requirements for the Degree of Doctor of Philosophy

School of Physics

National University of Ireland Galway

September 2019

Declaration of authorship

I, Marta Fuente Lastra, declare that this thesis titled "Investigation of radon prevention and mitigation: from radon measurements to specification for soil depressurisation systems" and the work presented in it are my own, and that appropriate credit has been given to the work of others. The work in this thesis has not been submitted elsewhere for any other degree or qualification.

Signed: 

Date: 27/09/2019

Abstract

Reduction of indoor radon concentration in buildings is considered to be an important public health issue, since radon was recognised as the leading cause of lung cancer after tobacco smoking by the World Health Organisation. The study of radon protective measures for buildings has become more important recently, in accordance with the 2013/59/EURATOM BSS Directive, mandatory since February 2018 within the member states of the European Union. This thesis work was conceived within the National Radon Control Strategy for Ireland to investigate the effectiveness of radon prevention and mitigation measures, with the main aim to determine specifications for the optimum performance of soil depressurisation systems. For that purpose, a case study in an experimental house was conducted over a year to test the ability of active and passive soil depressurisation systems, focused on pressure field extension and the radon reductions achieved. Complementary laboratory-based experiments were conducted to examine the properties of granular fill materials used in the aggregate layer under the slab, which affects soil depressurisation. Main findings from the work were the permeability characterisation of various standard granular fill materials within the European context, the distribution of the pressure induced under the slab and its behaviour as a function of the extraction airflow. Additionally, radon reductions in relation to the soil depressurisation system features were quantified. Further, in order to assess the performance of instrumentation for radon in-air measurements, a benchmark study of radon monitors in a purpose-built radon chamber was carried out. The key finding from this research was that, although different radon monitors provide an accurate measurement, response time to fluctuation in the radon concentration can vary and, therefore, selection of the appropriate detector should be specific to the application. This work gives an insight into the understanding of the operation of soil depressurisation systems and the resulting findings contribute to specifications for optimum radon protection by soil depressurisation within an European context, which can potentially inform revision of the building regulations.

Acknowledgements

I would like to express my sincere thanks to my supervisor Dr Mark Foley for his guidance, support and encouragement over the past three years. Thank you for trusting in my work and inspiring me throughout the PhD. Thanks also to Dr Jamie Goggins for his expertise and support co-supervising this work. To both, thanks for giving me the opportunity to embark upon a PhD within the OPTI-SDS project, funded by the Irish Environmental Protection Agency (EPA), that granted me a scholarship. Thanks to Dr Le Chi Hung, also part of the OPTI-SDS, and special acknowledgements to the steering committee of the project: David Fenton (EPA), Eamonn Smyth (Department of Housing, Planning and Local Government, DHPLG), Stephanie Long (EPA) and Simon McGuinness (DHPLG).

To Dr Luis S. Quindós Poncela and Dr Carlos Sainz from the radon group at the University of Cantabria (Spain), thank you for your insight, encouragement and advice. Thanks to all the members of the radon group that helped me contributing to this work, especially during the experiments conducted in the radon chamber and at the pilot house. As well, I would like to acknowledge ENUSA Industrias Avanzadas S.A. for the support and help while conducting the experiment at the pilot house within their facilities.

I wish to express my gratitude to Dr Borja Frutos from the Eduardo Torroja Institute for Construction Science (IETcc-CSIC) in Madrid (Spain) and to Eduardo Muñoz for the work conducted together in Madrid and Galway. Thank you for the willingness to collaborate, it is always a pleasure working with you.

I would like to recognise the School of Physics and the Civil Engineering Department at the National University of Ireland Galway, thanks to all the colleagues, postgraduates and staff members, that I have found here and have been very kind and helpful over these years.

Coming to the end, I wish to acknowledge my friends. Thanks to my lifelong friends for their support in the distance (and also the visits) that helped me throughout the journey. Thanks also to my Spanish family in Ireland, the ones that are still here and those who already left from this wonderful place. You made this experience much better!

Y gracias a todos aquellos que me han enseñado algo, queriendo o sin querer, al cruzarse en mi camino a lo largo de estos tres años, de ese modo contribuyendo a la realización de esta tesis.

Last but not least, I would like to thank my family for all their support. Gracias a mis padres y a mi hermana María, sin vosotros esto no habría sido posible. Especialmente a mis padres, gracias por el apoyo y cariño, por enseñarme a ser perseverante y por ser inspiración en mi vida. Gracias por dejarme volar y animarme a conseguir lo que me proponga.

Nothing in life is to be feared, it is only to be understood.
Now is the time to understand more, so that we may fear less.

Marie Curie

Contents

Nomenclature

Abbreviations	
BSS	Basic Safety Standards
CAN	Canary monitor
CFD	Computational Fluid Dynamics
EPA	Environmental Protection Agency
EU	European Union
FEM	Finite Element Method
HRA	High Radon Areas
IETcc	Eduardo Torroja Institute for Construction Science
IRCP	International Commission on Radiological Protection
K-S	Kolmogorov-Smirnov
LaRUC	Laboratory of Environmental Radioactivity University of Cantabria
Loess	Locally Estimated Scatterplot Smoothing
MUMPS	MUltifrontal Massively Parallel sparse direct Solver
NUIG	National University of Ireland Galway
PTB	Physikalisch Technische Bundesanstalt
RPII	Radiological Protection Institute of Ireland
RS	Radon Scout monitor
RSH	Radon Scout Home monitor
SD	Soil Depressurisation
SDS	Soil Depressurisation System
TCD	Trinity College Dublin
PFE	Pressure Field Extension
UNSCEAR	United Nations Scientific Committee on the Effects of Atomic Radiation
WAV	Wave monitor
WHO	World Health Organisation

Symbol	
β	parameter - FEM simulations
γ	specific weight of fluid [kg/m^{2}s^2]
$\delta(\%)$	relative percentage difference
ε	soil porosity
λ_e	air exchange constant [s^{-1}]
λ_{Rn}	radon (^{222}Rn) decay constant [1/s]
μ	dynamic viscosity [kg/m·s]
ρ - ρ_{fluid}	fluid density [kg/m^3]
ρ_{b}	soil bulk density [kg/m^3]
τ	tortuosity factor
ϕ	radon emission rate from a source [Bq/s]
ϕ_{a}	advective radon flow density [Bq/m^{2}s]
ϕ_{d}	diffusion radon flow density [Bq/m^{2}s]
A	cross section [m^2]
c	Forchheimer factor [s/m]
C_0	initial radon concentration [Bq/m^3]
C_i	radon concentration at time i [Bq/m^3]
C_{Rn}	radon concentration [Bq/m^3]
$\bar{C}_{\mathrm{Rn}}$	mean radon concentration [Bq/m^3]
$\bar{C}_{\mathrm{ref}}$	mean reference radon concentration [Bq/m^3]
d - Δl	distance [m]
d_{p}	effective particle diameter [m]
D	diameter [m]
D_{e}	effective diffusion coefficient [m^2/s]
D_{M}	molecular diffusion coefficient [m^2/s]
E	radon emanation coefficient
F	pump flow rate [m^3/s]
G	radon generation rate [Bq/m^{3}s]
h	height [m]
$\Delta h/\Delta l$	hydraulic gradient
k	Darcy's permeability coefficient [m/s]
K	parameter - FEM simulations
K_{D}	Darcy's permeability [m^2]

K_{DF}	Darcy-Forchheimer specific permeability [m^2]
K_E	Ergun specific permeability [m^2]
Δm	water mass [kg]
n	porosity of the granular fill material
r	Pearson's correlation coefficient
R	mass activity of radium (^{226}Ra) [Bq/kg]
Re	Reynold's number
RE	relative error
P	pressure [Pa]
P_{atm}	atmospheric pressure [Pa]
ΔP	pressure difference [Pa]
Q	fluid flow rate [m^3/s]
t	time [s]
T	temperature [°C]
v	velocity [m/s]
v_{wind}	wind velocity [m/s]
V	volume [m^3]

Dissemination of research

Peer review research articles

Fuente, M., Long, S., Fenton, D., Hung, L.C., Goggins, J., Foley, M. (2019). OPTI-SDS: Review of radon research in Ireland and its impact on the National Radon Control Strategy. Submitted for publication.

Fuente, M., Rábago, D., Goggins, J., Fuente, I., Sainz, C., Foley, M. (2019). Radon mitigation by soil depressurisation case study: radon concentration and pressure field extension monitoring in a pilot house in Spain. Science of the Total Environment, 695, 133746. https://doi.org/10.1016/j.scitotenv.2019.133746

Fuente, M., Muñoz, E., Sicilia, I., Goggins, J., Hung, L.C., Frutos, B., Foley, M. (2019). Investigation of gas flow through soils and granular fill materials for the optimisation of radon soil depressurisation systems. Journal of Environmental Radioactivity, 198, pg. 200-209. https://doi.org/10.1016/j.jenvrad.2018.12.024

Fuente, M., Rábago, D., Herrera, S., Quindós, L., Fuente, I., Foley, M., Sainz, C. (2018). Performance of radon monitors in a purpose-built radon chamber. Journal of Radiological Protection, 38, pg. 1111-1127. https://doi.org/10.1088/1361-6498/aad969

Co-author (minor contributions)

Hung, L.C., Goggins, J., **Fuente, M.**, Foley, M. (2018b). Investigation of sub-slab pressure field extension in specified granular fill materials incorporating a sump-based soil depressurisation system for radon mitigation. Science of the Total Environment, Vol. 637-638, 1081-1097. https://doi.org/10.1016/j.scitotenv.2018.04.401

Hung, L.C., Goggins, J., **Fuente, M.**, Foley, M. (2018). Characterisation of specified granular fill materials for radon mitigation by soil depressurisation systems. Construction and Building Materials, Vol. 176 (10), 213-227. https://doi.org/10.1016/j.conbuildmat.2018.04.210

Conference proceedings

Fuente, M., Hung, L.C., Goggins, J., Foley, M. (2019). Passive soil depressurisation systems: current and future perspectives. *9th Conference on Protection against Radon at Home and at Work.* 16th-20th September 2019, Prague, Czech Republic. **(Oral presentation)**.

Foley, M., **Fuente, M.**, Hung, L.C., Goggins, J. (2019). OPTI-SDS project: contributions to the NRCS in Ireland and international collaborations investigating radon mitigation. *9th Conference on Protection against Radon at Home and at Work.* 16th-20th September 2019, Prague, Czech Republic. **(Oral presentation)**.

Fuente, M., Rábago, D., Goggins, J., Fuente, I., Sainz, C., Foley, M. (2019). Pilot house study on active and passive soil depressurisation for radon mitigation: radon concentration and pressure field extension monitoring. *9th Conference on Protection against Radon at Home and at Work.* 16th-20th September 2019, Prague, Czech Republic. **(Poster presentation)**.

Foley, M., Long, S., Fenton, D., Hung, L.C., Goggins, J., **Fuente, M.**. (2019). EPA funded radon research in Ireland and its impact on the National Radon Control Strategy. *10th Annual Scientific Meeting of the IAPM (Irish Association of Physicist in Medicine).* 23rd March 2019, Dublin, Ireland. **(Oral presentation).**

Fuente, M., Hung, L.C., Goggins, J., Foley, M. (2018). Ongoing research on radon mitigation by soil depressurisation in a Spanish pilot house. *ROOMS 2018.* 27th-28th September 2018, Lugano, Switzerland. **(Oral presentation).**

Hung, L.C., Croxford, C., Goggins, J., **Fuente, M.**, Foley, M. (2018). OPTI-SDS Project: An experimental investigation of the pressure field extension in a granular fill material for radon mitigation by soil depressurisation systems. *ROOMS 2018.* 27th-28th September 2018, Lugano, Switzerland. (Oral presentation).

Rábago, D., **Fuente, M.**, Herrera, S., Quindós, L., Fuente, I., Foley, M., Sainz, C. (2018). Response time of radon monitors under controlled conditions. *14^{th} International workshop GARRM 2018.* 18^{th}-20^{th} September 2018, Prague, Czech Republic. (Oral presentation).

Fuente, M., Hung, L.C., Goggins, J., Foley, M. (2018). Radon mitigation in Spanish pilot house: results overview and measurement plan. CERI 2018 Conference Proceedings, pg. 518-522. ISBN 978-0-9573957-3-2. **(Conference paper)**

Fuente, M., Hung, L.C., Goggins, J., Foley, M. (2018). Radon mitigation in Spanish pilot house: results overview and measurement plan. *CERI (Civil Engineering Research in Ireland) 2018.* 29^{th}-30^{th} August 2018, Dublin, Ireland. **(Oral presentation)**.

Foley, M., Goggins, J., **Fuente, M.**, Hung, L.C. (2017). An investigation of the optimum specification for soil depressurisation (SD) systems (active and passive) that take account for Irish building practices. *ENVIRON 2018.* 26^{th}-28^{th} March 2018, Cork, Ireland. (Oral presentation).

Fuente, M., Muñoz, E., Foley, M., Frutos, B. (2017). Behaviour study of air flow through gravels based on laboratory experimentation and contrast with fem models. *ROOMS 2017.* 18^{th}-19^{th} October 2017, Galway, Ireland. **(Oral presentation)**.

Foley, M., Goggins, J., **Fuente, M.**, Hung, L.C. (2017). OPTI-SDS: An investigation of the optimum specification for soil depressurisation (SD) systems (active and passive) that take account for Irish building practices. *ROOMS 2017.* 18^{th}-19^{th} October 2017, Galway, Ireland. (Oral presentation).

Foley, M., **Fuente, M.**, Goggins, J., Hung, L.C. (2016). An investigation of the optimum specification for soil depressurisation (SD) systems (active and passive) that take account for Irish building practices. *Environment & Health Conference: Our Environment, Our Health, Our Wellbeing. EPA-HSE.* 30^{th} November 2016, Dublin, Ireland. **(Poster presentation)**.

Hung, L.C., Goggins, J., Foley, M., **Fuente, M.** (2016). An investigation of the optimum specification for soil depressurisation (SD) systems (active and passive) that take account for Irish building practices (OPTI-SDS Project). *ROOMS 2016.* 6^{th}-7^{th} October 2016, Concarneau, France. (Oral presentation).

Chapter 1

Introduction

Radon ^{222}Rn is a naturally occurring gas formed as a decay product of radium ^{226}Ra, which belongs to the uranium ^{238}U radioactive decay series (see Figure 1.1). Radon is a radioactive alpha-particle emitter noble gas, it is generated after several disintegrations from ^{238}U, i.e., the most common natural isotope of uranium. Traces of both radium and uranium are present in the soil and rocks of the Earth's crust, in varying amounts depending on their nature and composition, and thus provide a continuous radon source.

Radon is colourless, odourless and tasteless, and its half-life is approximately 3.8 days. There are two more naturally occurring isotopes of the Rn element: thoron ^{220}Rn and actinon ^{219}Rn; which belong to the thorium ^{232}Th and uranium ^{235}U decay series respectively. Their half-lives are shorter when compared to ^{222}Rn, thoron has a half-life of 55.6 s and actinon has a half-life of 3.96 s. Due to this fact, ^{222}Rn is normally the only isotope considered and it is the one called radon (Quindós et al., 1994; Audi et al., 2017).

Because of its noble gas character, radon has a stable atomic structure and it is chemically inert. Hence, its behaviour is determined by physical processes instead of chemical interactions. This property along with its half-life and its gaseous nature make it highly mobile, being able to migrate from its origin and release into the atmosphere. Emanating from rocks or soil, radon can move through interconnected pores and reach the ground surface where it is exhaled.

In the outdoor environment radon levels are not considered a health hazard because the radon that diffuses into the atmosphere normally disperses rapidly. However, if radon gas enters the air space of a building or a cavity it can be

accumulated, causing an elevated indoor radon concentration, which can lead to health risks due to high radioactive dose when inhaled. The average outdoor radon concentration is estimated globally between 5-15 Bq/m^3 (Gunning et al., 2014). Indoor radon concentrations can be significantly higher and vary widely depending on different factors such as the underlying geology, atmospheric conditions or the building characteristics. The global average indoor radon concentration is 40 Bq/m^3 according to UNSCEAR (2000), but in Ireland the national average indoor radon concentration for homes is 77 Bq/m^3 (Dowdall et al., 2017). Large range variations of indoor radon levels have been reported, a concentration of 49,000 Bq/m^3 was measured in a dwelling in Castleisland (Ireland) and it is among the highest recorded in the world (Organo and Murphy, 2007).

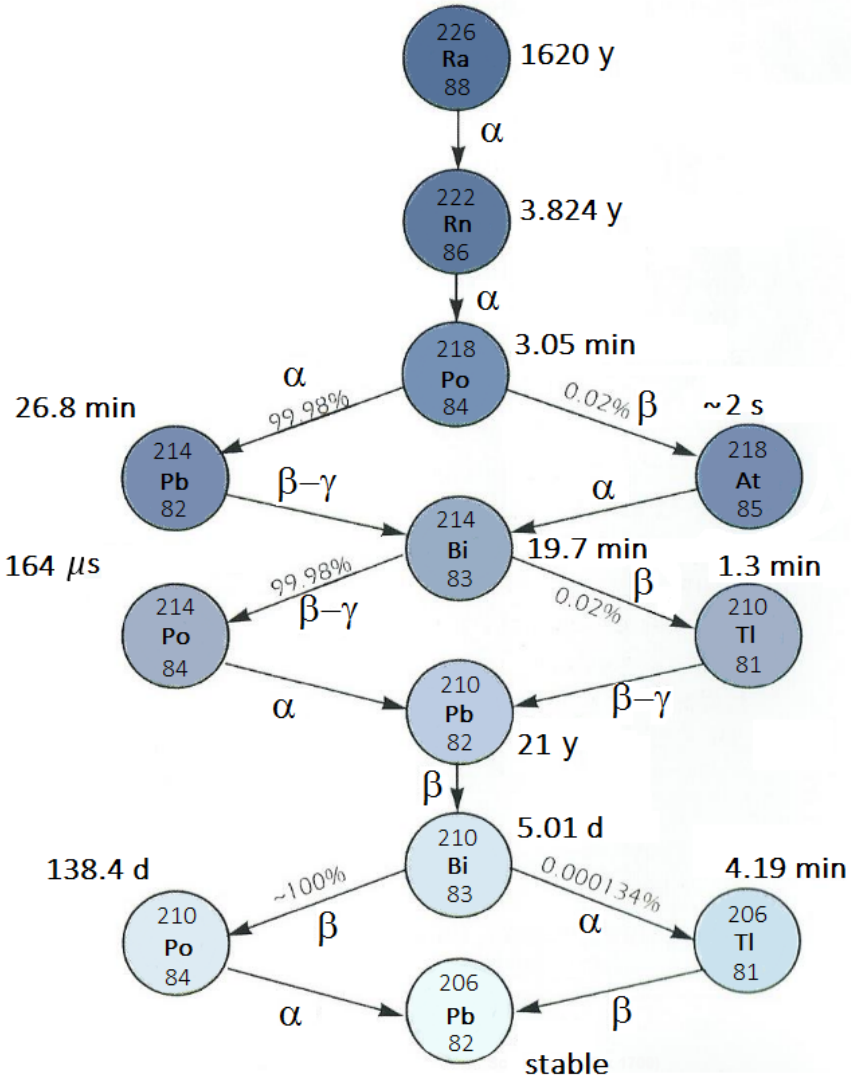

Figure 1.1: Diagram of ^{238}U decay series from ^{226}Ra element, modified from Quindós (1995).

Radon is the largest source of exposure to ionising radiation for the general public and the second greatest cause of lung cancer only after tobacco smoking, according to the World Health Organization (WHO). The WHO identified radon as a carcinogen agent in 1986 (Pacheco-Torgal, 2012) and it has been shown to cause lung cancer through the inhalation of its short lived alpha decay products, such as alpha emitting ^{218}Po and ^{214}Po, which induce pulmonary cell DNA damage (WHO, 2009). In the European Union alone, radon in homes is responsible for around 20,000 lung cancer deaths each year (Darby et al., 2005) and in Ireland, it is estimated that radon exposure accounts for approximately 14% of all lung cancers; this equates to 300 cases per year approximately (NRCS, 2019a).

To regulate indoor radon exposure, a reference level was defined. This level represents the annual mean radon concentration in a home above which it is strongly recommended to reduce the occupants' exposure, but it does not define a rigid boundary between safety and danger (WHO, 2009). International organizations recommend different indoor radon concentration thresholds, the International Commission on Radiological Protection (IRCP) recommends a reference level for radon gas in dwellings of 300 Bq/m^3 and WHO proposes a reference level of 100 Bq/m^3, but also specifies that if this level cannot be reached in some countries, the chosen reference level should not exceed 300 Bq/m^3 (ICRP, 2009; WHO, 2009; Bochicchio, 2011). The 2013/59/EURATOM Basic Safety Standards (BSS) Directive, mandatory since February 2018, advises that national reference levels of all European Union Member States for indoor radon concentrations shall not exceed 300 Bq/m^3 (2013/59/EURATOM). The government in Ireland, following the advice of the RPII (Radiological Protection Institute of Ireland) and the Nuclear Energy Board, adopted an annual average radon gas concentration of 200 Bq/m^3 as the national Reference Level above which remedial action to reduce indoor radon concentration should be considered in dwellings (DELG, 2002).

1.1 Radon generation and transport

Radon generation occurs in the radium ^{226}Ra soil grains, the radon atoms that reach the pore space as a result of the recoil when ^{226}Ra decays can be transported to the soil surface and then exhaled to the atmosphere (see Figure 1.2). Radon generation rate G can be defined as:

$$G = \frac{\lambda_{\mathrm{Rn}} E R \rho_{\mathrm{b}}}{\varepsilon} \tag{1.1}$$

where λ_{Rn} is the radon decay constant (2.1×10^{-6} 1/s), E is the emanation coefficient, R is the mass activity of radium ^{226}Ra (Bq/kg), ρ_{b} is the soil bulk density (kg/m^3) and ε is the soil porosity.

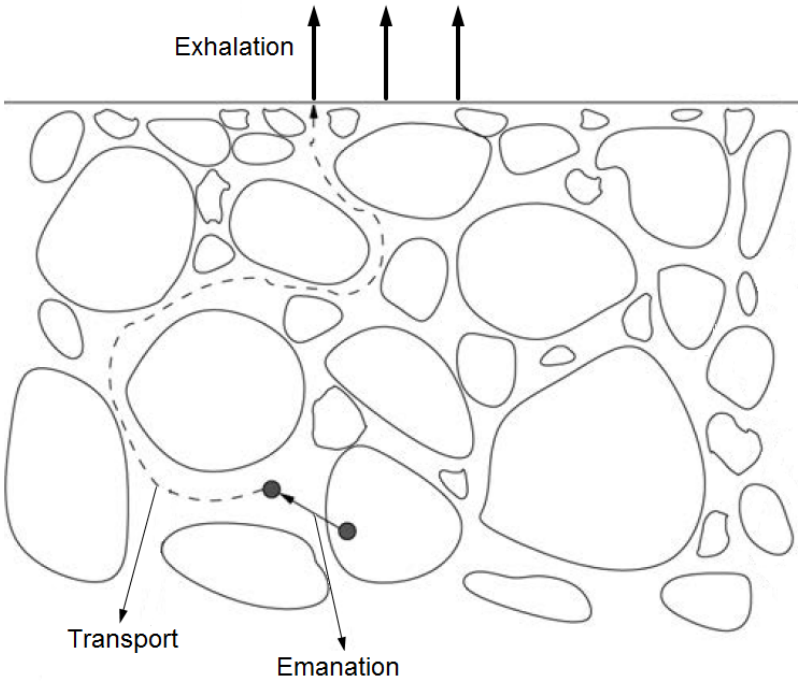

Figure 1.2: Diagram of processes leading to radon release to the atmosphere, modified from Ishimori et al. (2013).

The emanation coefficient E is the fraction of the total number of radon atoms formed from the alpha decay of ^{226}Ra that can escape into the pore volume between the grains and become free to migrate. Emanation coefficient depends basically on the soil grain-size distribution, porosity and water content, and has a typical value of 0.2 for soils (de Oliveira Loureiro, 1987; Nero et al., 1990).

Once in the pore volume, radon can travel across the soil towards the surface by means of two transport mechanisms: diffusion and advective flow. The diffusive transport of radon is affected by moisture, porosity and tortuosity, and it can be expressed by Fick's law of diffusion in terms of a diffusion coefficient.

Fick's law of diffusion states that radon flow density is linearly proportional to its concentration gradient under assumption of a steady state:

$$\phi_{\mathrm{d}} = -D_{\mathrm{e}} \nabla C_{\mathrm{Rn}} \tag{1.2}$$

where ϕ_d is the diffusion flow density (Bq/m^{2}s), D_e is the effective diffusion coefficient (m^2/s), and C_{Rn} is the radon activity concentration (Bq/m^3). The negative sign arises from the fact that radon diffuses from high to low concentrations (Ishimori et al., 2013).

Radon diffusion coefficient depends on the soil type, pore size distribution, water content, position and compaction. The effective diffusion coefficient can be described as:

$$D_e = \varepsilon \tau D_M \tag{1.3}$$

where τ is the tortuosity factor, which is typically less than unity in soils (e.g. 0.6 for closely packed uniform spheres) and D_M is the molecular diffusion coefficient (m^2/s) Ishimori et al. (2013).

Advective transport of radon is influenced by air permeability of the soil, moisture and pressure gradient, and it can be described by Darcy's law in terms of air permeability, which strongly depends upon the pressure differential (Nazaroff, 1992; Chauhan and Kumar, 2015).

Darcy's law relates the apparent velocity of fluid flow through the soil to the pressure gradient:

$$\vec{v} = -\frac{K_D}{\mu} \nabla P \tag{1.4}$$

where $\vec{v}$ is the superficial velocity vector (m/s), K_D is the Darcy's permeability of the soil (m^2) that shows the ability of a fluid to transmit through the soil (porous material), P is the pressure (Pa) and μ is the dynamic viscosity of the gas-phase of the soil pores (kg/m·s) (Nazaroff, 1992). The advective flow density ϕ_a is obtained by multiplying Darcy's velocity by the radon activity concentration in the soil pores and dividing by the soil porosity (Font, 1997).

$$\phi_a = -\frac{C_{Rn}}{\varepsilon} \frac{K_D}{\mu} \nabla P \tag{1.5}$$

A general differential equation to describe soil radon transport, considering diffusion and advection mechanisms, radon generation and the radioactive decay can be written as (Jiránek and Svoboda, 2007; Muñoz et al., 2017):

$$\frac{\partial C_{Rn}}{\partial t} = D_e \nabla^2 C_{Rn} + \frac{\nabla C_{Rn}}{\varepsilon} \frac{K_D}{\mu} \nabla P + G - \lambda_{Rn} C_{Rn} \tag{1.6}$$

1.1.1 Radon entry into buildings

The main source of indoor radon is the soil and geology under the building, but also, it is generally accepted that a very small percentage is due to building materials (Pacheco-Torgal, 2012). Thus, radon entry into a building is the addition of contributions from exhalation from the soil and from building materials (Vasilyev and Zhukovsky, 2013; Schubert et al., 2018). Another possible source of indoor radon can be the water supply, but it is usually a negligible contribution.

Initially, radon diffusion through soil and building materials was considered to be the controlling mechanism of radon entry into buildings. However, indoor radon concentrations found in many houses were much higher than the prediction based on the diffusion theory (Minkin, 2002), which led to believe that the extent to which diffusion through soil pores contributes to radon entry into buildings is less important than advection.

The dominant mechanism of radon entry from the soil into the indoor air of a building is pressure-driven airflow (i.e., advection) (Abdelouhab et al., 2010; Jelle, 2012; Chauhan and Kumar, 2015). As air pressure indoors is generally lower than that in the ground, soil gas in drawn from the ground into the building. Pressure gradients are created either by thermal difference, due to different indoor-outdoor temperature, wind effects, household activities or mechanical ventilation systems and foster the soil gas to flow into dwellings through joints, gaps and other leakage routes existing in the foundation structures (Turk et al., 1991; Arvela, 2001; Collignan et al., 2012). Typical ingress routes for radon are through cracks in walls and floors, construction joints, wall cavities and gaps around service piping and cables. Some examples of key entry routes for radon are shown in Figure 1.3.

Indoor radon concentration is affected by different factors such as the ground potential, which is the ability of the soil to generate and transport radon, and it is determined by the content of radium in the soil, the emanation coefficient, soil permeability, porosity and moisture content among others. The characteristics of the building, including airtightness of the foundation, and the ventilation or air exchange rate, related to the occupancy behaviour and atmospheric conditions, also influence indoor radon concentration (Makelainen et al., 2001; Wang and Ward, 2002). Normally, radon is not a problem in the upper stories or high rise buildings, as it comes from the ground and is a gas heavier than air, it tends to accumulate in the lower levels (DELG, 2002).

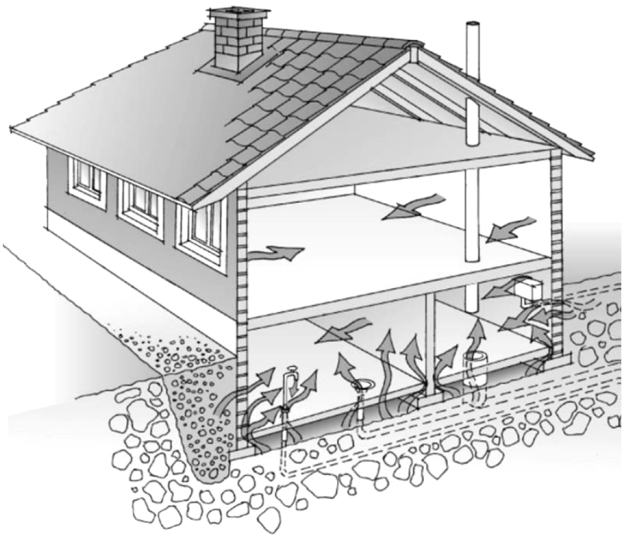

Figure 1.3: Possible radon entry routes, modified from Nilson (2017).

1.2 Radon prevention and mitigation

Radon prevention and mitigation are aimed at reduce indoor radon levels to the lowest concentration possible in order to achieve an overall risk reduction in the population (Angell, 2011). Measures for radon reduction are based on either preventing radon entering the building or removing it after entry. Radon prevention refers to the radon control measures that can be taken during the construction of new buildings, while mitigation or remediation deals with reduction of radon in existing buildings (DELG, 2002).

The correct design and installation of prevention and mitigation measures must provide radon reductions below the reference level. The appropriate radon control system for a particular building depends on the site and building conditions, which must be considered in the design, along with compliance with a series of requirements to assure safety, durability and functionality during the building expected life. The design criteria also requires that the system should be quiet and unobtrusive for the occupants, its performance should be easy to monitor and the costs of installation, operation and maintenance low (WHO, 2009; EPA, 2019).

1.2.1 Prevention and mitigation techniques

There are different strategies to address radon prevention and mitigation. Techniques to prevent radon entry and limit infiltration due to pressure-driven airflow include sealing of entry routes into the building, installation of barriers or

membranes and soil depressurisation (SD) (e.g. radon sumps), which is used to draw radon away before it can enter the building by reversing the pressure gradient between the soil and the building. To remove radon once it has entered the building, the common technique employed is ventilation (e.g. natural ventilation of living spaces) that allows dilution of indoor radon concentration with external air.

Sealing entry routes

This strategy involves sealing the possible infiltration pathways through which radon ingress is produced, including all cracks, gaps, joints and pipe penetrations in the building foundation, floors and adjoining walls. Sealing radon entry routes contributes to obtain higher airtightness of the building envelope, which prevents radon entry due to pressure-driven airflow from the soil to the indoors (EPA, 2001).

The sealant materials used for this purpose require specific characteristics, for instance, being flexible and permanently elastic, to avoid any cracks to reappear as a consequence of building settlement over time, and being able to adhere to different type of surfaces. Among the high quality sealant materials employed are silicone, polysulphide and polyurethane (DELG, 2002).

This technique can be very demanding as radon is able to enter the indoor air of a building through openings that are too small to locate and effectively closed off and thus, only satisfactory results are found when entry routes are almost completely sealed (Holmgren and Arvela, 2011). Sealing entry routes has limited potential as a stand-alone radon prevention strategy, but it can improve the performance of other protection strategies. Therefore, it is recommended to use this method in combination with other protection techniques (WHO, 2009).

Barriers and membranes

This radon protection measure involves provision of a radon barrier such as a membrane of a radon proof material between the soil and the indoor space of the building to limit radon entry. In order that radon barriers and membranes are effective, they must be installed airtight, but this is normally difficult to achieve under common construction practices (Angell, 2011).

Characteristics that should be taken into account in the design and installation of radon barriers include the diffusion coefficient, which determines the resistance to radon, strength, durability and thickness (Jiránek and Hulka, 2001; WHO, 2009).

In many cases, damp-proof membranes used for moisture can provide a sufficient radon-proof barrier if well installed (Holmgren and Arvela, 2011).

The installation of radon barriers and membranes requires special care at joints, pipe penetrations and connection to walls so that airtightness is achieved (Frutos Vázquez, 2009) (see Figure 1.4). Damage during installation should be avoided in all possible ways, as imperceptible holes could act as a trap to funnel soil gas into the building (Angell, 2011).

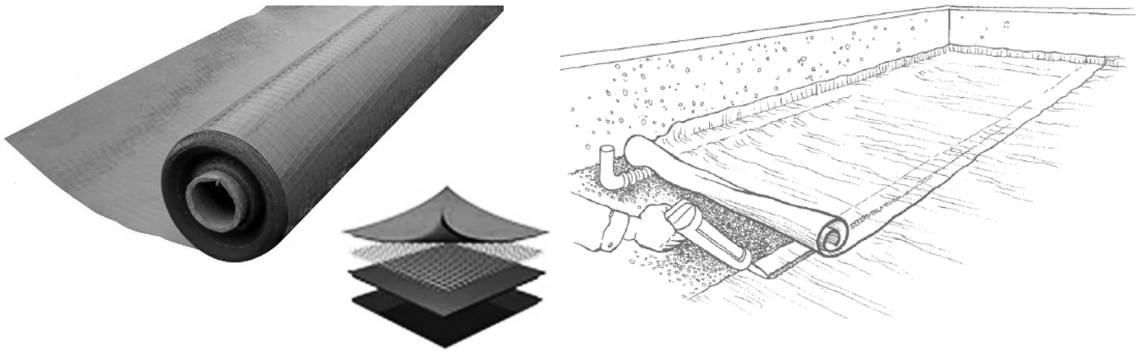

Figure 1.4: Example of a multilayer comercial radon-proof membrane (Monarflex) and diagram of installation, extracted from (EPA, 2001).

This technique can be used as a stand-alone strategy to reduce radon. However, as barriers do not address pressure-driven airflow, they should be used together with other radon protection measures and not as the only measure against radon (Angell, 2011).

Soil depressurisation

Soil depressurisation is a radon protection strategy that focuses on reversing the pressure gradient between the soil beneath the building and the indoor space, as advection is the primary driving force for radon entry (DELG, 2002). Depressurisation is created under the slab in such a way that radon can be drawn out before it enters the indoor air of the building (see Figure 1.5).

Soil depressurisation systems (SDS) consist of three basic components: a suction point located below the slab and connected to a continuous and uniform permeable aggregate layer, an exhaust pipe to extract soil gas and a means of extraction (WHO, 2009). The suction point of a SDS is normally a sump, which can be dig out through the slab or the foundation walls; an alternative to the radon sump is

placing drain perforated pipes in the aggregate layer beneath the slab. Depending on the extraction method, SDS can be classified as active or passive. A mechanical extractor (e.g. an electrical fan) can be used in the case of forced extraction (active SD), while for natural extraction (passive SD) there are different types of chimney cowls (Holmgren and Arvela, 2011). Active SDS are generally installed with a mechanical fan which maintains a constant depressurisation beneath the building, but passive soil depressurisation is obtained naturally by means of thermal buoyancy and wind effect (Diallo et al., 2015).

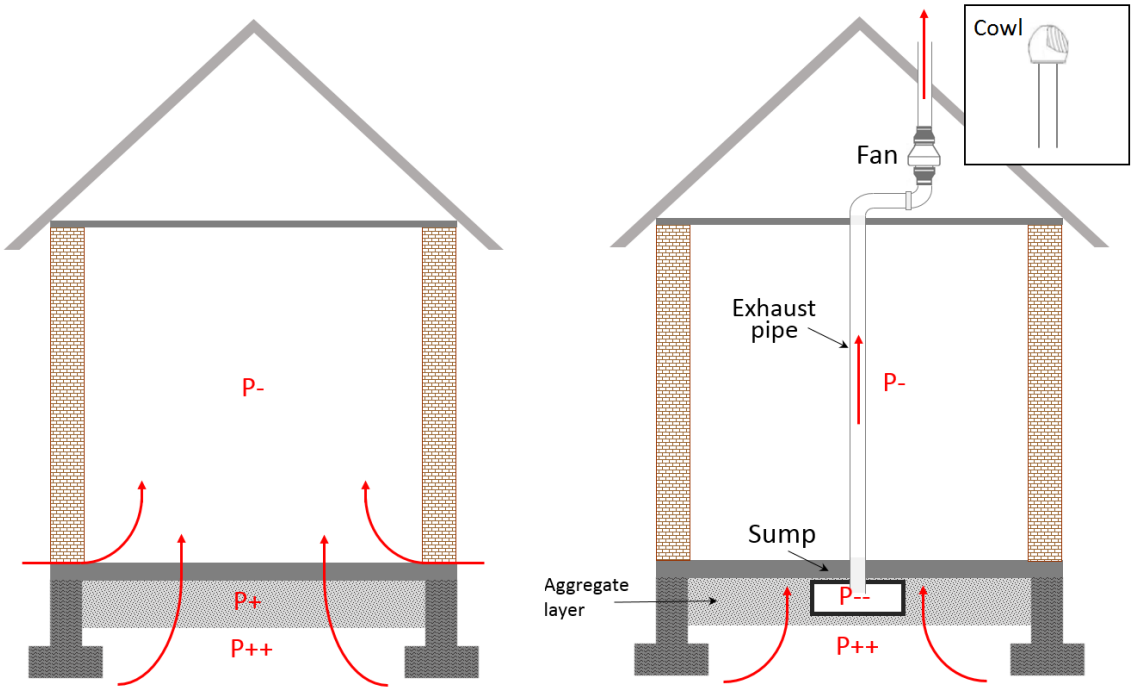

Figure 1.5: Diagram of the working principle of a soil depressurisation system; red arrows indicate radon flow.

There are many variations of SDS and in the design of a specific SDS configuration, the building and foundation characteristics should be considered. Among the factors that influence SD effectiveness are building airtightness, aggregate layer and soil permeability, location and size of sumps or pipes, exhaust pipe diameter and height, and type of extractor (natural or mechanical) (Abdelouhab et al., 2010).

Active and passive soil depressurisation contribute both to dilute radon in the air space under the slab and to prevent the transfer of radon due to the advective soil gas flow from the ground towards the building (Holmgren and Arvela, 2011). SD is a very effective method for radon reduction and, in general, active systems

are more effective than passive. However, although the high effectiveness of SDS, combination with other strategies such as radon barriers is recommended to obtain better results (WHO, 2009).

Pressurisation

This technique consist in creating an indoor overpressure compared to that in the soil beneath the building by means of a mechanical fan. Thereby, the normal airflow from soil gas into the building is reversed and radon is forced to reach the surface through other routes far from the building, see Figure 1.6 (Frutos Vázquez, 2009). Positive pressurisation throughout the building reduces radon entry due to pressure-driven airflow and also contributes to the increase of the air exchange rate so that radon is diluted (DELG, 2002; Holmgren and Arvela, 2011).

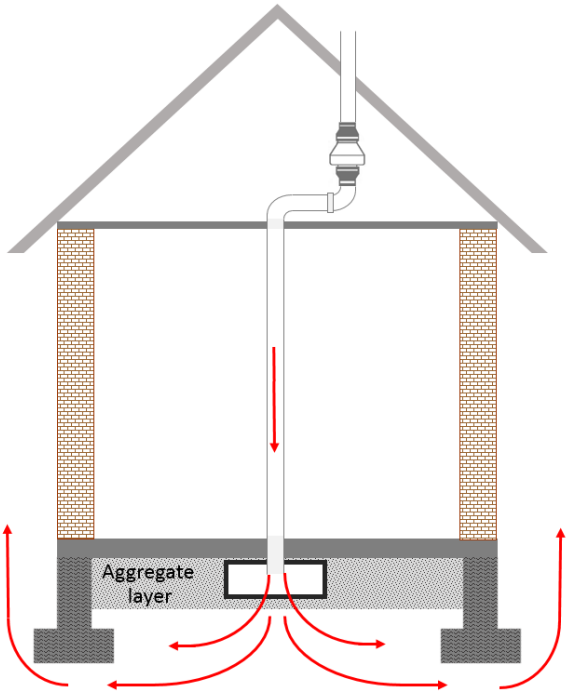

Figure 1.6: Diagram of the operation principle of a pressurisation system, red arrows indicate radon flow.

To ensure that this technique is effective the building must be well sealed and relatively airtight. If the building airtightness is high, low airflow provides sufficient indoor pressure level (Holmgren and Arvela, 2011). This technique is also a good alternative in some situations where soil depressurisation is not recommended because it may cause radon extraction in quantity from a wide area. In such cases, reversing the action of the fan to cause positive pressurisation can be effective in reducing indoor radon concentration (DELG, 2002).

Ventilation

Ventilation is a radon protection measure based on the exchange of indoor radon-laden air and outdoor air to dilute radon and thereby reduce indoor radon concentration (Angell, 2011). There are two ventilation approaches that can be considered, improving ventilation of the indoor living areas and ventilation of unoccupied spaces between the soil and the indoor occupied space (e.g. cellar ventilation, vented crawlspaces, under-floor vents, ...) (WHO, 2009).

Increasing ventilation of living spaces can be achieved actively by using a mechanical fan or naturally by opening windows and doors manually, providing air vents and installing trickle vents through walls or windows (Hodgson and Pudner, 2019). Besides radon reduction due to dilution with outdoor air, ventilation of occupied spaces also can lower radon concentration by reduction of the pressure gradient between the soil and the indoor space and so, limiting radon entry due to pressure-driven airflow (EPA, 2019). On the other side, ventilation of unoccupied spaces allows interception of the rising soil gas and removal before entering the building, thereby reducing radon entry (DELG, 2002). To this effect, a strong current of fresh air to constantly replace the soil gas as it emerges from the ground is created (WHO, 2009).

Active ventilation can be achieved using three different mechanical systems, namely exhaust ventilation, supply ventilation and balanced ventilation. Exhaust ventilation basically consists in extracting air, which depressurises the indoor space in relation to the soil and outdoors, while supply or positive ventilation tends to pressurise by blowing air into the indoor space, along as diluting radon after it has entered. Balanced ventilation introduces and extracts air at similar rates, resulting in a neutral pressure within the building (WHO, 2009).

This radon protection approach may lead to energy losses during cold seasons or in extreme climates, but there is the possibility to install a ventilation system with heat recovery (Angell, 2011). Normally, ventilation on its own may not be effective to remedy high levels of radon, but it could be used in combination with other radon protection measures and it also generally improves the overall indoor air quality.

Other methods

Apart from the radon protection techniques described above, other methods to reduce radon levels in buildings have been used in some countries across Europe,

such as radon wells, mitigation by soil ventilation through existing drainage piping, installation of active floor air gap ventilation, use of waterproof concrete instead of normal concrete and installation double radon-proof membrane (Holmgren and Arvela, 2011).

The working principle of a radon well is to extract air from soil at a depth of approximately 5 m within a large area to reduce radon concentration in the soil gas, see Figure 1.7. This technique is effective in high enough permeable soils, where the effect of a single radon well can reduce radon levels in dwellings within a 20-30 m radius (Holmgren and Arvela, 2011).

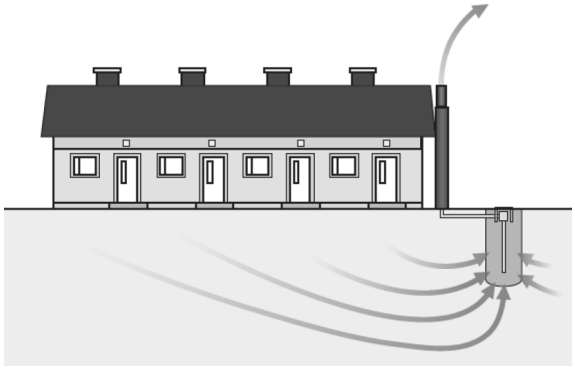

Figure 1.7: Diagram of working principle of a radon well, modified from (Holmgren and Arvela, 2011)

1.2.2 Discussion about effectiveness

A review of studies on radon prevention and mitigation interventions around the globe resulted in a general effectiveness classification of the radon prevention and mitigation techniques. Among the existing radon prevention and mitigation techniques, active soil depressurisation system was found to be the most effective technique, reaching radon reductions up to 60-95% (Jiránek and Svoboda, 2007; Jelle, 2012; Long et al., 2013; Jiránek, 2014). This was followed by active ventilation measures and pressurisation, reported to provide reductions of the radon concentration within 40-80%.

Passive methods, including sealing entry routes, radon barriers and membranes, and simple ventilation were found to be less effective (Khan et al., 2019). Efficiency of passive soil depressurisation is typically between 20–50%, and for sealing entry routes and naturally improving ventilation in living spaces and unoccupied spaces, radon reductions reported are in the range of 10-60%. Regarding the use of radon barriers, it is shown that they have a significant failure rate (Synnot et al., 2004; Denman et al., 2005). Effectiveness reported is varied due to bad installation in some cases, but if well installed significant radon reduction is achieved. On average, 50% reduction of the radon concentration is provided by a radon-proof barrier with a membrane (Holmgren and Arvela, 2011; Denman et al., 2018).

Although active soil depressurisation is the most effective technique, sometimes it is necessary to combine it with another measures to ensure radon concentration is below the Reference Level. A typical combination recommended for high radon areas in many countries is the use of a radon barrier along with acive or passive soil depressurisation. An overall recommendation to use a combination of prevention and mitigation techniques is given (Khan et al., 2019).

Soil depressurisation effectiveness

Abdelouhab et al. (2010) performed an extensive experimental investigation on the ability and efficiency of SDS in a pilot house in France, with dimensions of 9×9 m^2 and a 40 cm thick aggregate layer placed below the concrete slab. Ten different holes were drilled from the slab into the soil to test the induced pressure under the slab during soil depressurisation operation. As a result of the study, it was found that passive SDS running time could be mainly during the cold season, later confirmed in the work of Diallo et al. (2015), and also it was stated that passive SDS can be much more cost effective than active if a proper design is produced.

Frutos Vázquez et al. (2011) studied the effectiveness of active and passive SDS, examining also the positioning of the sump and exhaust pipes, in a pilot house in Spain with dimensions of 5×5 m^2 and two radon sumps, one in the centre of the house and the other at the side. The pilot house was built on a 10 cm thick concrete slab on top of a 15 cm thick gravel layer. Similar conclusions to those of Abdelouhab et al. (2010) were drawn from the investigation in the Spanish experimental house.

Jiránek et al. (1999) studied the impact of air permeability of the aggregate layer under the slab on the SDS effectiveness in dwellings. It was found that the lower radon concentration existed for dwellings with higher permeability of the aggregate layer. The same finding was observed in the work of Pennell et al. (2009) using computational fluid dynamic (CFD) simulations. As well, the indoor air concentration was found to be largely dependent on the air permeability of the soil beneath and surrounding the slab. Therefore, permeability of the soil and aggregate layer are among the most important factors to increase the effectiveness of a SDS, as Jiránek (2014) postulated after an experimental and numerical analysis on SDS effectiveness for remediating existing houses in the Czech Republic.

In contrast with previous analytical models which simply assumed an SDS as a homogeneous cylinder layer with impermeable layers at the top and bottom of the cylinder, Diallo et al. (2015) developed an analytical model to design the SDS that covered a wide range of boundary conditions such as the thickness of the slab, permeability of the slab or cracks. They validated the model by comparison with the data measured from a passive SDS and also confirmed a significant impact of the air permeability of the slab, soil and aggregate layer, and the environment temperature, on the efficiency of the SDS.

Impact of energy performance in buildings

Energy retrofit interventions in buildings influence indoor radon concentration. Evidence from different European countries shows that radon levels increase after building refurbishment (Jiránek and Kacmarikova, 2014; Ringer, 2014; Collignan et al., 2016; Meyer, 2019), in particular when involving windows replacement (Long and Smyth, 2015; Pampuri et al., 2018). However, retrofitting measures including purpose-provided ventilation compensation, e.g. mechanical ventilation with heat recovery, can overcome the accumulation of indoor radon and other pollutants (Collins and Dempsey, 2018; McGrath and Byrne, 2019).

New building concepts in line with the implementation of EU Directive 2010/31/EU on energy performance of buildings, aimed at reaching high energy efficiency and sustainability, have been implemented in new dwellings (2010/31/EU, 2010). The main characteristics of energy efficient dwellings are high airtightness, mechanical ventilation systems and high quality insulation, oriented to minimise energy losses through transmission and ventilation (Ringer and Graser, 2011). In general, new energy efficient builds present lower indoor radon concentrations compared to conventional new houses, due to a better airtight building shell being provided, preventing radon entry, in combination with an appropriate controlled ventilation system, to evacuate pollutants (Ringer and Graser, 2011; Poffijn et al., 2012; Ringer, 2014; McCarron et al., 2019).

1.3 Modelling radon entry

Modelling is a powerful tool for studies of soil gas and radon entry into houses. The equations governing radon generation and transport are reasonably well understood, as mentioned in section 1.1. Models of radon entry attempt to solve the equations under different approximations to the physical structure of the soil, entry pathways

and boundary conditions, either using analytical solutions or numerical methods (Gadgil, 1992).

Radon entry simulations were developed starting in the 1970s (Yao et al., 2013). Modelling was initially focused on simple models with one or two spatial dimensions that only considered advective transport of radon into buildings through a single and well-defined pathway. Later, these models were expanded to include diffusion as a secondary transport mechanism, multiple cracks, some simple geological variations in close proximity to the building foundation and also allowing full three-dimensional and time dependency (Pennell et al., 2009).

The ultimate motivation of model development is to understand the phenomenon of radon entry in terms of measurable properties of the soil and house construction and operation, but the specific near term goals can be different (Gadgil, 1992). Many models have been developed to characterise the ability and efficiency of soil depressurisation systems (some examples are discussed below) and there are also other models intended for more specific studies, such as the impact of slab thickness, joints and membranes on indoor radon concentration (Muñoz et al., 2017).

Reddy et al. (1991) used an analytical airflow SDS model based on non-Darcy flow. This model is limited by the assumption that there is no slab peripheral crack and the sub-slab/soil interface is impermeable, thus, is valid only when soil permeability is much lower than gravel permeability under the slab. Jelle (2012) presented an analytical model that may be applied as a tool in the process of selecting the most efficient and cost-effective measure to achieve a radon level that is well below the action level set by the authorities. Diallo et al. (2015) developed an analytical airflow model to the effective design SDS, integrated in a multizone airflow building code to consider the influence of meteorological conditions, building characteristics and ventilation systems.

Regarding numerical modelling, Gadgil et al. (1994) and Bonnefous (1992) used a three dimensional finite element model to study the performance of SDS, taking into account the diffusive and advective transports in the soil and the sub-slab gravel. Although this model does not consider the transport through the slab, only the airflow through the slab peripheral crack, it identifies the mechanisms and factors contributing to the performance of SDS (Diallo et al., 2015).

Muñoz et al. (2017) also proposed a finite element model, validated with several analytical and numerical solutions from the literature, to study the impact of slab thickness, joints and membranes on indoor radon concentration. The main finding of this study is that the soil and sub-slab permeability under the dwelling, along with the sub-slab layer tightness, are the key to extend the pressure field below the slab.

Wang and Ward (2000) developed a radon entry model for a house with a cellar using CFD, which is a useful tool based on numerical analysis and data structures able to solve and analyse problems that involve fluid flows, such as the radon generation and transport in the soil and its entry through complex substructures of a building. Other studies also used CFD to simulate radon entry into houses with different substructures (Akis et al., 2004; Pennell et al., 2009), leading to several findings related to the factors affecting optimum operation of SDS.

There is also a different approach to model radon, related to indoor radon measurements in the housing stock and directed towards a geographical characterization. It normally consists of developing an index to describe the propensity of housing stock to have high levels of indoor radon and is based on the use of relevant geological information (i.e. bedrock geology, radium content, soil permeability, radon emanation coefficient, etc.) combined with indoor radon measurements and sometimes including characteristics of the housing construction (Gadgil, 1992; Sainz et al., 2017; Elio et al., 2017).

1.4 Radon in air measurements

Performing a radon measurement is the only possible way to know the radon concentration and, for that reason, it is recognised that radon testing is essential to assess the levels of radon in buildings (George, 1996). Measurement of radon in air can be conducted by means of different detection techniques, depending on the purpose of the measurement and the type of radon detection device used, which can be classified into active and passive (WHO, 2009).

The percentage of measured dwellings is low in some countries and could be increased with policies including legal requirements to test radon levels in new and existing dwellings. A recommendation to perform radon tests during the conveyancing process is given in many countries, but it is not normally a legal

requirement (Gunning et al., 2016). Radon tests are conducted in dwellings or public buildings commonly due to surveys of radon levels at regional or national scale, or for diagnosis before and after mitigation works. In general, passive detectors are used for radon surveys, whereas active radon monitors are used in radon diagnostic measurements and in quality control programmes (Jílek and Marušiaková, 2011).

Radon tests are also discussed in terms of short-term or long-term measurements, as indoor radon concentration varies over time, including daily and seasonal fluctuations. To estimate the annual average indoor radon concentration in a building, tests are required for a period of at least three months and longer periods are preferred (WHO, 2009). Short-term measurements only can give a first idea of the indoor average long-term radon concentration, in many cases radon levels can be either underestimated, due to short-term measurements carried out during periods when the building had increased ventilation, or overestimated in the opposite situation (WHO, 2009).

Passive detectors are frequently used to perform long-term measurements while active radon monitors can be used for continuous monitoring and grab sampling (Espinosa et al., 2013). Regarding active monitors, there is a great diversity available in the market based on several detection techniques. Some of them are designed for homeowners while other are marketed to radon professionals working in testing and mitigation or for research purposes.

Quality control of the radon detectors is very important to ensure confidence in the measurement results. The accuracy and precision of all kind of radon detectors is key to guarantee reliable measurements. In order to evaluate the performance of different radon detectors both active and passive, comparison exercises are normally carried out within a controlled radon atmosphere. Active radon monitors traceable to primary ^{222}Rn gas standards can be used as a reference for quality assurance comparison exercises (Espinosa et al., 2013).

1.4.1 Passive radon detectors

Passive radon detectors based on different detection techniques have been widely used to perform measurements of integrated radon exposures and indoor radon concentration. The most common passive radon detection techniques are etched track detectors, activated charcoal detectors and electret ion chambers (WHO, 2009;

Howarth, 2017).

Etched track detectors

The detection principle of etched track detectors is the strike of alpha particles from the radon and its decay products in the surface of a plastic medium, leaving microscopic tracks (Howarth, 2017). Passive etched detectors are generally made of three materials: cellulose nitrate (LR-115), polycarbonate (Makrofol) and, the most popular, poly allyl diglycol carbonate (PADC), commonly known under the trademark as CR-39 (Wasikiewicz et al., 2019).

The widely used etched track detectors consist of the track-detecting material, e.g. CR-39, within a small container that acts as a diffusion chamber, excluding the entry of radon progeny. Therefore, only the alpha particles emitted by the radon entering the container and its decay products are recorded in the track detector (WHO, 2009). After a chemical, e.g. in a NaOH solution, or electrochemical etching process of the plastic detector, the latent alpha tracks are revealed (see Figure 1.8) and then can be counted by optical microscopy (Miles, 2004; Howarth, 2017). Generally, an optical microscope with an automated image analysis software is used to obtain the track density. Once the density of tracks in the detector is known, the radon exposure and hence the radon concentration can be obtained, by applying a conversion factor normally given by the manufacturer (De Pin et al., 2016).

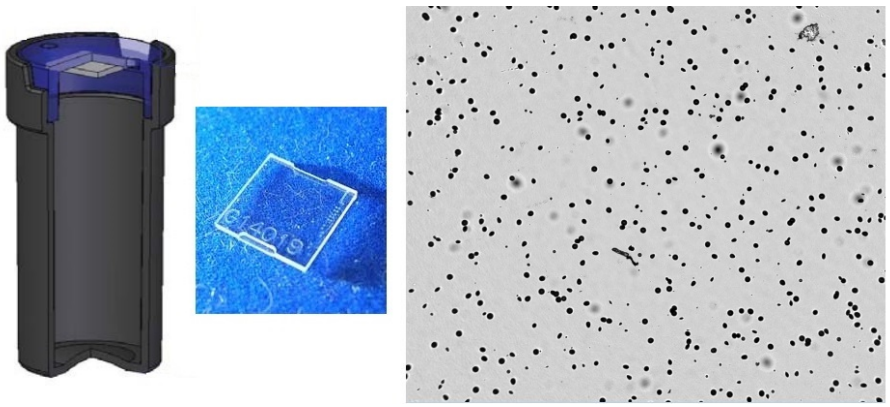

Figure 1.8: Diagram of an example of etched track detector diffusion container, CR-39 track detector and picture of the alpha tracks in the plastic surface seen through an optical microscope.

The use of etched track detectors provides reliable measurements at a low cost and thus, it is the most popular passive radon measuring technique (El-Badry and Al-Naggar, 2018).

Activated charcoal detectors

This technique is based on the adsorption of radon by the activated charcoal. Detectors usually consist of a bed of granulated activated charcoal within a collector. Following sampling, the detector is sealed to be analysed once secular equilibrium is reached between the ^{222}Rn collected and its short-lived decay products, after a three hour period approximately. The radon concentration is normally obtained by gamma spectroscopy of the emissions from the ^{214}Pb and ^{214}Bi radon progeny (WHO, 2009).

Activated charcoal allows adsorption and desorption of radon, i.e. radon adsorbed at the start of the exposure decays and it it partially desorb from the charcoal during the exposure period (Miles, 2004). As radon half-life is 3.8 days and due to desorption, recommended exposure periods for activated charcoal detectors are normally between 2 to 7 days. Also, activated charcoal is affected by humidity and therefore these detectors should be calibrated accordingly.

Electret ion chambers

The detection method of electret ion chambers is based on the gradual discharge of the electret produced because of the air ionisation in the chamber volume caused by radon and its progeny. Detectors consist of an electret placed within a chamber where radon enters by diffusion through a filtered inlet to avoid radon decay products. The average radon concentration can be obtained from the measurement of the electret charge before and after radon exposure (Miles, 2004; WHO, 2009; Howarth, 2017).

1.4.2 Active radon monitors

Active radon monitors are mainly distinguished from passive detectors because they require electric power to operate, but also, some of them are able to directly show the readings, chart the concentration and record the fluctuations of radon over the exposure period (Lin et al., 2013). Active detectors can be used for continuous monitoring or grab sampling and their typical detection methods are ionisation chambers, scintillation cells with ZnS(Ag) and electrostatic collection with solid state detectors (Miles, 2004).

Ionisation chambers

The detection principle of an ionisation chamber is the collection of ion pairs coming from decay of radon and its decay products inside the chamber (Jílek and Marušiaková, 2011). Radon is diffused or pumped into the chamber, in which an electric field is established between two or more electrodes. Then, ionisation of the gas inside the chamber volume is produced, due to the decay of radon and its short-lived progeny. The current generated by the total ionisation in the chamber or, alternatively, the pulses produced by individual alpha particles are counted and from them, radon concentration can be calculated. In the case of pulse ionisation chambers, alpha spectrometry is possible as the pulses generated by different decay products can be distinguished (Miles, 2004).

Scintillation cells

The detection method of scintillation cells, e.g. Lucas cells, consists of counting scintillations produced from alpha radon decay inside the cell. Cells consist of a cylinder coated in the internal surfaces with a scintillator, usually silver-activated zinc sulfide, ZnS(Ag). Radon enters the cell and decays, emitting alpha particles that interact with the scintillator, resulting in light pulses that can be recorded by a photomultiplier tube. The number of scintillations is counted, once the radon is in secular equilibrium with its short-lived decay products and then the radon concentration can be obtained (Quindós-Poncela et al., 2003). Scintillation cells are widely used for grab sampling measurements but also can be used as a continuous radon monitor if air is continuously pumped or diffused into the cell (Miles, 2004).

Electrostatic collection with solid state detectors

This technique is based on counting the radon decay alpha particles collected on the surface of a solid state detector, generally a silicon detector, under the effect of an electric field (Jílek and Marušiaková, 2011). Radon enters a chamber, either by diffusion or by means of a pump, where a solid state silicon detector is located. During decay of radon inside the chamber, ionisation of its progeny is produced, and then the charged radon decay products are directed towards the solid state detector yielding electrostatic collection. The collection is produced by an electric field generated when applying a high voltage between the solid state detector and the chamber wall (see Figure 1.9).

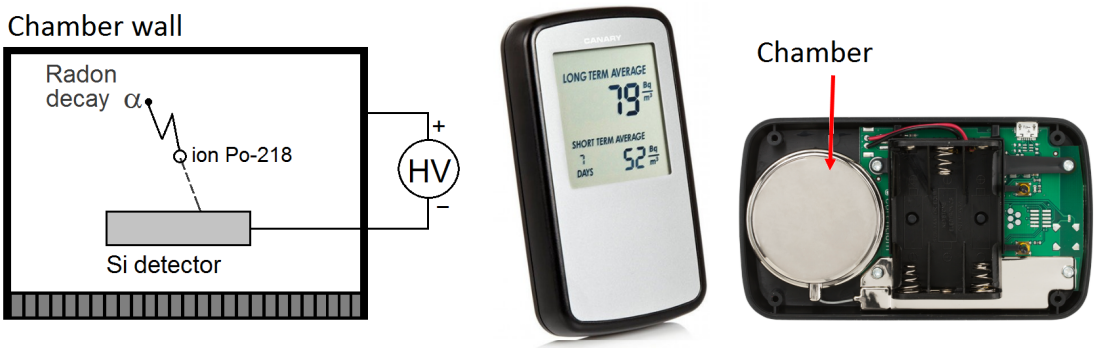

Figure 1.9: Scheme of the detection method for radon inside a diffusion chamber with a solid state Si detector, modified from (Rábago, 2013) and picture of an example of radon monitor (Canary, Airthings) that uses this detection method, extracted from (Airthings, Accesed date: 28 August 2019).

A number of alpha particles emitted by the collected decay products (e.g. ^{218}Po ion) enter the silicon detector and their energies are measured. Radon concentration can be obtained from the counting of alpha particles based on the measured energies. Alpha spectrometry is possible when using solid state silicon detectors, which allow to discriminate among the different decay products (WHO, 2009).

1.5 Radon programmes

Indoor radon exposure is a significant public health concern, identified as the most significant contribution to ionising radiation exposure for the general public and the leading cause of lung cancer for non-smokers, it is responsible for 9% of the deaths from lung cancer per annum only in the European Union (Darby et al., 2005). An increasing number of radon programmes and policies for protection against the dangers from exposure to radon gas have been developed over the past few years, aiming at reducing the overall population exposure to this human carcinogen and raising public awareness of the indoor radon associated risks.

In January 2014, the 2013/59/EURATOM Basic Safety Standard Directive was issued by the Council of the European Union. This BSS Directive, aimed at offering protection for people in dwellings and workplaces, introduced radon gas into the radiological protection system for the first time. Its implementation is mandatory since February 2018 for all Member States of the European Union (2013/59/EURATOM).

Article 2 of the document describes the scope and mentions that this Directive applies in particular to the exposure to indoor radon from workers or members of the public. Articles 54, 74 and 103 are related to radon exposure and among them it is stated that EU Member States shall establish national reference levels for indoor radon concentrations not exceeding 300 Bq/m^3 and also it is required to establish a national action plan addressing long-term risk from radon exposures in dwellings, buildings with public access and workplaces for any source of radon ingress (2013/59/EURATOM).

The WHO advises that radon programmes should be developed and established at a national level. A wide range of policies and cooperative efforts from government departments, public bodies, technical experts and other stakeholders are required for the implementation of effective national radon programmes, which should include monitoring of indoor radon levels, in order to identify high radon exposure potential areas, introduction of radon prevention and mitigation measures in the building codes and provision of services on radon risk communication to inform the general public and other stakeholders. To design successful national plans, collaboration with existing health promotion programs should be considered and also, development of training programs targeted at building professionals and stakeholders involved in radon prevention and mitigation implementation (WHO, 2009).

In Ireland, a national radon survey with measurements in over 11,000 homes was conducted during the 1990s by the RPII. A representative distribution of the radon concentration in Irish dwellings was obtained from the survey results, predicting that 7% of the existing housing stock had radon concentrations over the national Reference Level of 200 Bq/m^3 (RPII, 2002). After completion of the national radon survey, more than 44,000 additional measurements were carried out in the following years, all together resulting in a reliable guide to indoor radon levels in Ireland. A map of radon in Irish dwellings was developed and published (see Figure 1.12), identifying High Radon Areas (HRAs), defined as the areas in which over the 10% of the homes are predicted to exceed the national reference level.

In line with the findings from the national radon survey, the Building Regulations were revised in 1997 to include requirements on radon protection (DEHLG, 1997). All new dwellings built since July 1998 must incorporate radon protection measures, and in HRAs a radon barrier should be provided over the entire footprint of the

building. Additionally, it is necessary to have a potential means of extracting radon from the substructure, such as a standby radon sump or sumps with connecting pipework that could be activated later if necessary. In areas other than HRA, a potential means of radon extraction should be provided. Specific guidance on radon remediation measures for new buildings was included in 2004 in the "Technical Guidance Document C - site preparation and resistance to moisture" (DEHLG, 2004).

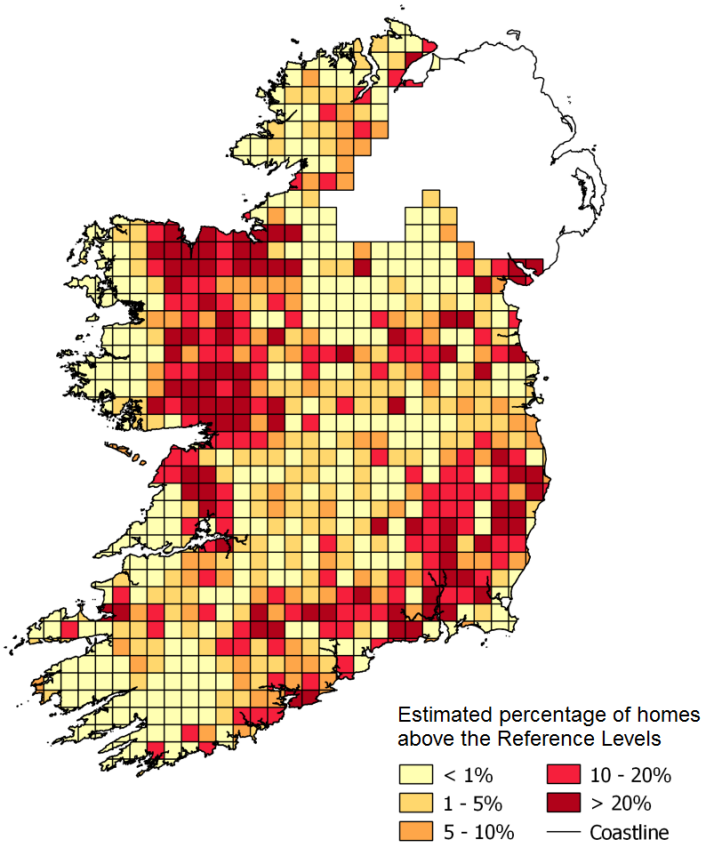

Figure 1.10: Prediction map of Radon in dwellings in Ireland, modified from (Dempsey et al., 2018). Source: Environmental Protection Agency.

By the 2000s, significant progress was made in Ireland in terms of radon policies compared to other European countries, but still many challenges to address the radon problem remained. In November 2011 the then Minister for the Environment, Community and Local Government, announced the Government decision to establish an interagency group to address the radon problem by developing a National Radon Control Strategy (NRCS) for Ireland.

1.5.1 National Radon Control Strategy for Ireland

The main aim of the national action plan would be to reduce the radon exposure for the Irish population and to decrease incidence of radon related lung cancers. Representatives from several different government departments and agencies, with the Department of Environment, Community and Local Government at the head, formed initially the interagency group, which worked between November 2011 and September 2013 to identify the main issues to tackle and design policies in a wide range of thematic areas to set the necessary interventions to effectively respond to the problem (NRCS, 2014).

In February 2014, a report of the interagency group to develop a National Radon Control Strategy was published (see Figure 1.11). The report contained three chapters: the first one set out the background on the scale of the radon problem and the need to develop a NRCS for Ireland, the second chapter addressed recommendations to reduce the risk from radon to people living in Ireland and the last chapter detailed the implementation process of the NRCS (NRCS, 2014).

A total of 48 recommendations were given in the NRCS report, divided in the following thematic areas:

- Radon prevention in new buildings;
- Use of property transactions (sales and rental) to drive action on radon;
- Raising radon awareness and encouraging individual action on radon;
- Advice and guidance for individual householders and employers with high radon results;
- Promoting confidence in radon services; and
- Addressing radon in workplaces and public buildings.

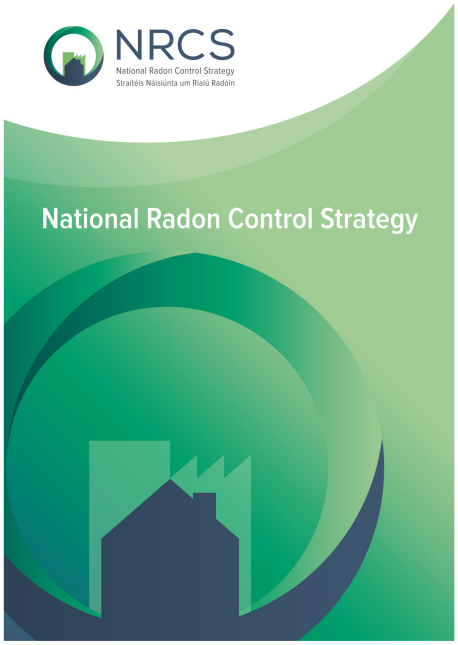

Figure 1.11: Front page of the first NRCS report, extracted from (NRCS, 2014).

From the recommendations across the six thematic areas, 31 specific actions were identified and set out in the NRCS. Initially, it was proposed that all actions would be delivered within a 4-year period.

In order to identify the existing knowledge gaps that would affect the effective implementation of the NRCS and to highlight the topics where targeted research could be focussed to support and improve the effective delivery of the strategy, a research working group was established by the interagency group. This group reviewed the research ideas from the NRCS development and set out four research themes (NRCS, 2019b):

1. Establish baseline values, considering the previous baseline surveys and to inform the update of the radon map;
2. Better targeting of measures and resources, including improvement of the radon map for Ireland;
3. Improve the effectiveness of radon preventive measures and radon remedial work, considering the design of better preventive systems, use of new construction technologies and remediation systems improvement; and
4. Develop better strategies for communicating radon risk and raising awareness, focused on radon awareness among stakeholders and the use of effective communication channels.

The strategy envisaged addressing all the recommendations within a four year period from 2014 to 2018, designated as Phase 1 of the NRCS. From the 31 actions identified, 18 were fully complete at the end of Phase 1, 7 were on-going and the remaining 6 were incorporated into a Phase 2 (NRCS, 2019a). Phase 2 was launched in 2019 to continue addressing public exposure to radon, in fulfilment of the 2013/59/EURATOM BSS Directive requirements, implemented in the Irish laws under Regulation 64 of S.I. No. 30 of 2019, Radiological Protection Act 1991 (Ionising Radiation) Regulations 2019 (NRCS, 2019c).

Many achievements were accomplished in Phase 1 of the NRCS. Among the key highlights, in relation to raising awareness, a dedicated website (www.radon.ie) was launched in 2016 and local radon awareness campaigns were held across the country, resulting in an increase of radon measurements in HRAs and identifying almost a thousand homes with radon levels over the Reference Level. Also, an annual "Radon Day" was established to be celebrated in November of each year.

Regarding the use of property transactions, contracts in the conveyancing process include three radon questions since 2017. Different training courses on radon prevention and remediation were developed and are running, some targeted at construction site staff and other targeted at local authorities, public bodies and radon contractors. A research survey was developed to evaluate the response to free radon testing offered in conjunction with a 50% grant for remedial work if needed, in order to inform the development of a national grant scheme. Lastly, to promote confidence in radon services, registration schemes for radon remediation and measurement were established (NRCS, 2019a).

A significant body of research was also completed, highlighting that a 13% reduction of the average level of exposure to radon was found as a result of the Building Regulations implementation in 1998 and the updated figure of 300 radon related lung cancers per year in Ireland. Regarding research theme 1, geographic and population weighted national average radon concentrations were updated to 77 Bq/m^3 and 98 Bq/m^3, respectively, as a result of new resource efficient survey protocols. From the research conducted on theme 2, a refined radon risk map incorporating geological parameters was published by Trinity College Dublin (TCD) and a project to understand ventilation and radon in Irish energy efficient buildings was completed by researchers at NUIG (National University of Ireland Galway). This NUIG project found an increase in radon levels associated with energy retrofitting measures to reduce ventilation, while for the cases of maintained ventilation levels, radon concentration was unaffected (NRCS, 2019b). Research theme 3 involved a three-year project to investigate the optimum specifications for soil depressurisation systems conducted by researchers at NUIG and research on long-term effectiveness of radon remediation systems in TCD, which led to a re-testing policy development, giving a recommendation to test remediated buildings every 5 years. From the study at NUIG, characterisation of granular fill material was conducted, contributing to the understanding of optimum aggregate layer specifications for the design of SD systems in practice. Finally, from research theme 4, it was found that stronger government regulation is required to effect real change on the responsibilities for addressing radon, which should not rest only on the householder, and a market research survey revealed that although 75% of the Irish public have heard of radon, the probability to have their home tested for radon is only 21% of those surveyed (NRCS, 2019b).

1.6 Thesis aims

This thesis was conceived within one of the research themes identified in the National Radon Control Strategy for Ireland, in line with the 2013/59/EURATOM BSS Directive implementation of required compliance since February 2018 by all European Union member states (see section 1.5). The research theme was focused on the improvement in the effectiveness of radon preventive measures and radon remedial work, considering the design of better prevention and mitigation systems and the use of new construction technologies (see section 1.5.1).

From the literature review, the soil depressurisation technique for radon reduction in new and existing buildings has been recognised as the most efficient technique to protect buildings from radon. However, specification for practical design and optimum operation of soil depressurisation systems are limited. Therefore, the need to thoroughly investigate features affecting the performance of soil depressurisation systems was established.

This work aimed at determining specification for the optimum performance of radon prevention and mitigation by soil depressurisation technique through collaborative projects with European partners. Given the factors known to affect the effectiveness of soil depressurisation systems (see section 1.2.1), the aims were to investigate the impact of the aggregate layer under the building slab on the depressurisation induced, the pressure distribution and the consequent radon reduction achieved. One specific objective was to characterise granular fill materials utilised in construction for the aggregate layer under the concrete slab of buildings and benchmark standards against the international European context. A secondary aim of this work included evaluation of instrumentation for measurement of radon in air used for research and other purposes.

To achieve these aims, laboratory based experiments were conducted and a case study in an experimental building with very high radon concentrations. The pursuit of the aims is presented in this thesis in three articles that have been accepted for publication in three peer reviewed journals (Journal of Radiological Protection, Journal of Environmental Radioactivity and Science of the Total Environment) and in one conference paper that was published in the proceedings of the Civil Engineering Research in Ireland 2018.

1.7 Thesis outline

Chapter 2 focuses on a radon instrumentation investigation. An experiment to benchmark different types of radon detectors was conducted in a purpose-built radon chamber. A selection of continuous radon monitors was tested under periods of stable radon concentration, quantifying accuracy and sensitivity of the radon concentration recorded. The response time of the monitors was also investigated, by analysing the performance of the detectors under controlled variations of the radon concentration within the chamber, for which several response time analysis methods were proposed and discussed.

Chapter 3 describes a characterisation of granular fill materials used in building construction for the aggregate layer under the slab, which has an impact on the effectiveness of soil depressurisation systems for radon prevention and mitigation. Flow through different aggregates and a soil sample was analysed in the laboratory, using an experimental set up similar to one previously developed to conduct tests of this kind on Irish standard granular fill materials. Benchmark analysis of European standard granular fill materials (Spanish, Irish and British) was also proposed.

Chapter 4 introduces the facilities used for the main experiment of this research (detailed in Chapter 5), a continuous monitoring study in an pilot house to test the ability of active and passive soil depressurisation technique for radon mitigation. The initial research conducted at the pilot house for which it was originally built is summarised and the testing plan proposed, details of the experimental set up and instrumentation utilised are then presented.

The main focus of this thesis is contained in Chapter 5. A long-term experiment conducted over a year in a pilot house with extremely high radon levels to investigate specifications for SDS is presented. Radon concentration behaviour in the experimental house and soil depressurisation performance were studied. The depressurisation induced and its distribution under the slab area were analysed and the radon reduction was quantified.

Finally, general conclusions drawn from the work presented in Chapters 2 to 5 and future research considered are discussed in Chapter 6.

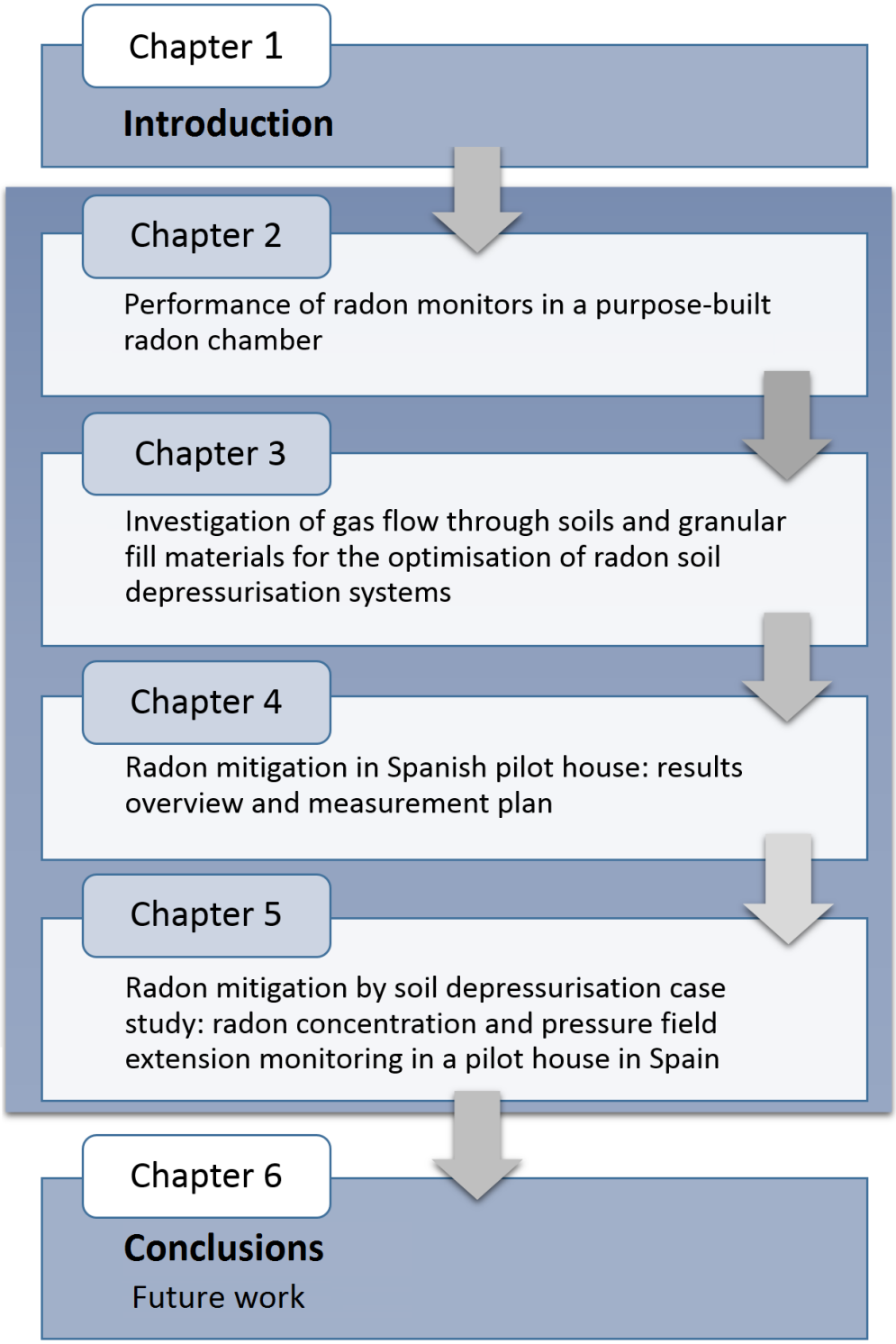

Figure 1.12: Flow chart showing the thesis outline.

Chapter 2

Paper I

Performance of radon monitors in a purpose-built radon chamber

Journal of Radiological Protection, 38, pg. 1111-1127 (2018)

Fuente, M., Rábago, D., Herrera, S., Quindós, L., Fuente, I., Foley, M., Sainz, C.

As highlighted in the introduction Chapter, radon measurements are key to assess indoor radon levels in buildings, which is determinant to tackle radon risk assessment and consequent actions in radon control programmes. To conduct radon measurements in air, there are different types of radon monitors based on several detection methods (see section 1.4), and used for a range of different applications, such as householder's radon control, measurement of radon levels pre- and post-mitigation works by radon testing service providers or research applications (e.g. pilot house case study presented in Chapters 4 and 5).

Envisaging the experiments to study ability of soil depressurisation technique for radon prevention and mitigation in a pilot house (see Chapter 5), which would require continuous radon monitoring to quantify radon reductions, along with the opportunity to use the facilities of the Laboratory of Environmental Radioactivity at the University of Cantabria (LaRUC) equipped with a purpose-built radon chamber, an experiment to investigate performance of several types of radon detectors was developed and carried out.

Different radon monitors were exposed to a controlled radon environment inside the radon chamber, two periods of stability during while radon concentration was maintained were alternated with pronounced variations in the radon concentration.

The former was used to evaluate accuracy and precision and the latter to quantify the response time of the detectors to fluctuations in the radon concentration. The devices under study were benchmarked against a reference monitor traceable to a ^{222}Rn primary standard.

From the results, mean radon concentration within the ±10% of the reference monitor was obtained for all detectors during the periods of stable radon concentration, which indicates that all monitors tested are appropriate for long-term measurements. Regarding the response time evaluation, four different analysis methods were proposed and discussed, and the slowest response time was found for a general purpose application monitor. A general recommendation deduced from the experiment is that the choice of detector to measure radon in air should depend on the accuracy and response time required for the application needed.

The results of the radon monitors performance experiment were submitted and accepted for publication to the Journal of Radiological Protection.

Author's contributions

Marta Fuente and Daniel Rábago designed the experiment with the support from Ismael Fuente, Mark Foley and Carlos Sainz. The experiment was conducted by Marta Fuente with the help from Daniel Rábago, Luis Quindós and the technical staff at the Laboratory of Environmental Radioactivity, University of Cantabria. Analysis of the experimental data was carried out by Marta Fuente with support from Daniel Rábago and contribution from Sixto Herrera. Marta Fuente wrote the manuscript. Mark Foley and Carlos Sainz reviewed the manuscript and all authors read and approved the final manuscript.

IOP Publishing | Society for Radiological Protection Journal of Radiological Protection

J. Radiol. Prot. **38** (2018) 1111–1127 (17pp) https://doi.org/10.1088/1361-6498/aad969

Performance of radon monitors in a purpose-built radon chamber

Marta Fuente[1], Daniel Rabago[2,4], Sixto Herrera[3], Luis Quindos[2], Ismael Fuente[2], Mark Foley[1] and Carlos Sainz[2]

[1] School of Physics, National University of Ireland Galway, Ireland
[2] Radon Group, University of Cantabria, Spain
[3] Meteorology Group, Department of Applied Mathematics and Computer Sciences, University of Cantabria, Spain

E-mail: mark.foley@nuigalway.ie and daniel.rabago@unican.es

Received 25 April 2018, revised 18 July 2018
Accepted for publication 30 July 2018
Published 31 August 2018

Abstract

The purpose of this paper is to benchmark several different radon monitors, by quantifying their accuracy and response time. Radon monitors with different characteristics were tested in a purpose-built radon chamber under reference conditions. The radon concentration in the chamber was controlled and maintained at a stable radon concentration of (2648 ± 85) Bq m^{-3} to evaluate the accuracy and precision of these monitors. The response time of the monitors was analysed for two time intervals. To assess the response time of the monitors, radon concentration was varied from a theoretical value of 0–6441 Bq m^{-3} and then from 6441 to 2648 Bq m^{-3}. The results from this study show that general purpose radon monitors are less accurate than those used by radon testing service providers and the research community. All monitors tested reported a mean radon concentration within the ±10% of the reference detector value at the radon equilibrium concentration. Different response time analysis methods were proposed and discussed, and for the particular time intervals analysed, response time was found to be slower for those radon monitors intended for general purpose applications.

Keywords: radon, radon monitor, chamber, response time

(Some figures may appear in colour only in the online journal)

[4] Author to whom any correspondence should be addressed.

0952-4746/18/0301111+17$33.00

1. Introduction

Radon is the second leading cause of lung cancer in the general population after smoking according to the World Health Organisation (WHO 2009). Inhaling radon has been shown to cause this disease through the decay of its short lived alpha decay products, such as alpha emitting ^{218}Po and ^{214}Po, which induce pulmonary cell DNA damage.

Radon comes from the decay chain of uranium (^{238}U), present in the soil and rocks of the Earth. It is a naturally occurring gas with half-life of 3.8 days, which can permeate through the soil and release into the atmosphere. Outdoor levels of radon do not pose a health risk because it is diluted in the atmospheric air. However, if it enters buildings and accumulates, indoor levels can be significantly higher reaching in average 40 Bq m^{-3} at global scale (UNSCEAR 2006) but higher levels at national scale (e.g. 77 Bq m^{-3} in Ireland, Dowdall *et al* 2017).

To regulate indoor radon exposure, a reference level for radon concentration is defined. This level represents the annual mean radon concentration in a house above which is strongly recommended to take action to reduce the occupants' exposure. Different indoor radon reference levels have been recommended by international organisations. The International Commission on Radiological Protection (ICRP) recommends a reference level for radon gas in dwellings of 300 Bq m^{-3}, the WHO proposes a reference level of 100 Bq m^{-3}, but also specifies that if this level cannot be reached in some countries, the chosen reference level should not exceed 300 Bq m^{-3}. The 2013/59/EURATOM Basic Safety Standards (BSS) Directive, mandatory since February 2018 for all European Union Member States, outlines that members should establish national reference levels for indoor radon concentration that shall not exceed 300 Bq m^{-3} (ICRP 2009, WHO 2009, Bochicchio 2011, Council of the European Union 2014).

Measuring radon is essential to control radon levels in any type of building and to do so there are different radon detectors, active and passive (George 1996, Tunno *et al* 2017). Long-term measurements are usually carried out by using passive detectors such as etched track detectors, which give a time-integrated radon concentration, from which average concentration is derived (Espinosa *et al* 2013). Active radon detectors are typically used to continuously monitor radon concentration and they are also used for grab sampling.

Most surveys of radon levels in dwellings are carried out using passive detectors. Active radon monitors are frequently used in radon diagnostic measurements and in some control programmes (Jilek and Marušiakova 2011, Gunning *et al* 2016).

There is a wide variety of radon monitors in the market based on various detection techniques, which have different performance characteristics. Some radon monitors are marketed to the general public for radon in home testing and some others are marketed towards the research community and professionals working in radon testing and remediation. Reference radon values can also be obtained from monitors which are traceable to primary ^{222}Rn gas standards (Espinosa *et al* 2013). Due to the great diversity of devices available in the market to measure radon, and their relative ease of use, there is a need to conduct periodic quality controls to guarantee the accuracy and precision of the provided results. Quality controls are typically carried out in controlled radon atmosphere chambers. The accuracy and precision of a monitor are usually evaluated by comparison with the values obtained from a reference device, with known traceability to ^{222}Rn primary standards. However, it is not common to evaluate the temporal response of radon monitors, which is a key parameter when testing in an environment with high fluctuations in concentration.

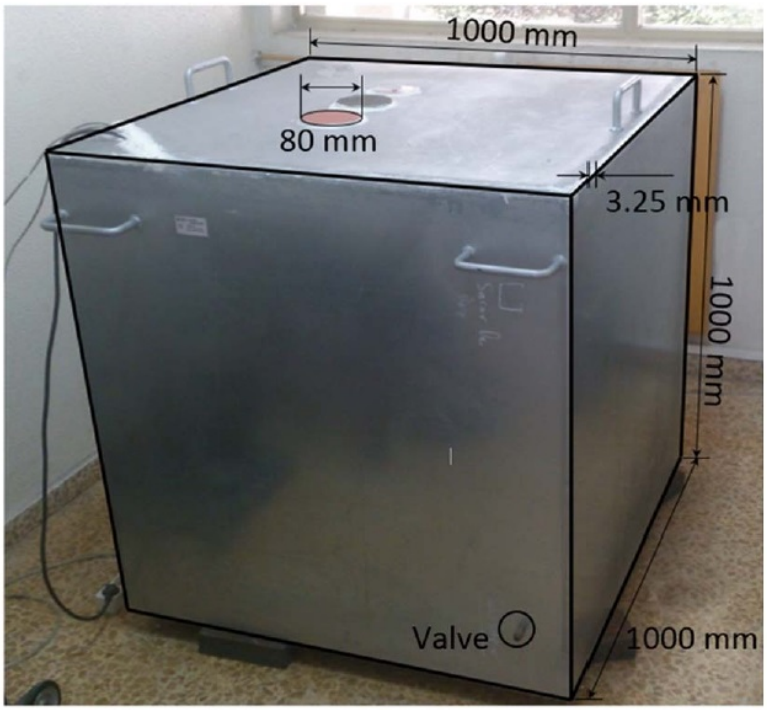

Figure 1. Picture of the radon chamber and dimensions.

The aim of the present work is to benchmark several different radon monitors, looking at their accuracy and response time. For this purpose, measurements were performed in a radon chamber which provides a controlled indoor radon environment.

2. Materials and methods

2.1. Radon chamber

The radon chamber (figure 1) used for this work is located at the LaRUC (Laboratory of Environmental Radioactivity, University of Cantabria) in Cantabria, Spain. It is a purpose-built stainless steel radon chamber with an internal volume of one cubic metre and wall thickness of 3.25 mm. The top face of the chamber is a lid that can be removed to place detectors inside. Also, on the top face there are three circular 80 mm diameter openings for inserting and removing etched track detectors without significant disturbance of the concentration inside the chamber.

Radon detectors in the chamber can be exposed to different concentrations by using several different radon sources, reaching radon concentrations of tens of $\mathrm{kBq\,m^{-3}}$ after a few days. The radon atmosphere is controlled by means of the source used each time, emission rate of the available radon sources ranges from 30 to 1100 $\mathrm{Bq\,h^{-1}}$, and also by the gas exchange with the outside air, which is controlled with a pump connected to a valve in the chamber wall.

The purpose of radon sources is to generate a specific radon concentration in the chamber and they are made up of dry soil powder with a high radium content enclosed in a cylindrical plastic container with high radon diffusion. Radon sources used in the study are not traceable, but the reference detector used to measure radon concentration is traceable to international standards, as described below.

Homogeneity of the radon concentration in the internal volume is achieved using a small fan that ensures concentration differences within the chamber are less than 3%. The air tightness of the assembly is guaranteed by seals made of acrylic material with a low diffusion coefficient for radon gas ensuring a leakage rate lower than 0.01 h^{-1} (Sainz *et al* 2018).

Radon concentration in the chamber is monitored using an Atmos 12 (Gammadata Instruments AB), which is the LaRUC's reference monitor traceable to the PTB (Physikalisch Technische Bundesanstalt) in Germany. Environmental conditions, temperature and relative humidity, are also recorded inside and outside the radon chamber.

2.2. Radon detectors

In addition to the Atmos 12 reference monitor, five different radon monitors were used in this study: two Radon Scout (SARAD GmbH), hereinafter referred as RS1 and RS2, one Radon Scout Home (SARAD GmbH) named RSH, a Canary (Airthings) and a Wave (Airthings), referred as CAN and WAV respectively. Several etched track detectors, CR-39 (Radosys Ltd) were used as well. Operation mode and features for each device are described below. All monitors used in this study have been calibrated.

The Atmos 12 is based on pulsed ionisation-chamber technology and alpha spectrometry to detect radon concentration. It has a measurement range 0–100 kBq m^{-3} and its sampling method is a pump with 1 l min^{-1} airflow. The uncertainty associated with the measurement performed by this device varies from 10% to 4% in the concentration range 100–1000 Bq m^{-3} with 1 h of integration time (Gammadata Instrument AB 2015). The one used for this study was calibrated at the Swedish Radiation Safety Authority (SSM). The difference between the SSM's reference instrument, calibrated at PTB radon chamber using a radon standard, and the Atmos 12 is less than 3%.

The detection system of the Radon Scout consists of a silicon detector in a chamber with high voltage collection. Radon gas enters a chamber and decays, high voltage is applied and radon daughters ionise and move towards the silicon detector surface that creates a pulse. Then, using gross alpha detection, radon concentration is obtained. The sampling method is by diffusion and the measurement range of this monitor is 0–2 MBq m^{-3}. The uncertainty with 1 h of integration time for range 200–1000 Bq m^{-3} is reported in 20%–10% range by the manufacturer (Sarad GmbH 2017). The prime use of this monitor is aimed at research or professional measurements. RS1 and RS2 devices used for the study were calibrated by the manufacturer just 2 months before the study started, using a reference instrument annually recalibrated by the German federal office for radiation protection BfS (Bundesamt für Strahlenschutz).

The Radon Scout Home is an instrument designed for general purpose long-term indoor measurements of the radon concentration and its principle of operation for radon measurements is a silicon detector and alpha spectroscopy. The measurement range of this monitor is 0–1 MBq m^{-3} and the preset integration time is 4 h with a 15% uncertainty after 7 days of measurements at 200 Bq m^{-3} (Sarad GmbH 2016).

The Wave and Canary radon monitors are designed for the general public. Radon sampling and detection method is the same for both, detection of radon is based on a passive diffusion chamber with a silicon photodiode and alpha spectrometry. The measurement range is 0–9999 Bq m^{-3} and after 7 days of measurements at 100 Bq m^{-3} the uncertainty of these devices is quoted as lower than 20% (Airthings 2017a, 2017b).

CR-39 etched track detectors are composed of a diffusion container and a 100 mm^2 plastic polymer placed inside, with an effective surface of 51.69 mm^2. Alpha particles from radon and its progeny decay strike the plastic leaving tracks that can be counted after etching in a NaOH solution (Ali *et al* 2009, Gillmore *et al* 2017). The track density on the plastic (obtained using a microscope with image analysis software) can be related to radon exposure and radon concentration by using a conversion factor, given by the manufacturer and verified by LaRUC. For calibration purposes the radon etched track detectors are exposed to a reference atmosphere for a defined time duration. The LaRUC is accredited according to UNE-EN ISO/IEC 17025 (2005) for integrated radon in air measurements with CR-39, which implies rigorous quality control of the entire measurement process (UNE-EN ISO/IEC 17025 2005).

2.3. Experimental method

The radon concentration variation over time in a closed space, such as the chamber used in this study, is described as the following exponential equation (Sainz *et al* 2016):

$$C(t) = C_0 e^{-\lambda t} + \frac{\phi}{V\lambda}(1 - e^{-\lambda t}), \tag{1}$$

where $C(t)$ is radon concentration in Bq m^{-3} at time t (h), C_0 (Bq m^{-3}) is the initial radon concentration, ϕ (Bq h^{-1}) is the radon emission rate from the source, $V = 1$ m^3 is the internal volume of the chamber, $\lambda = \lambda_{Rn} + \lambda_e$ (h^{-1}), $\lambda_{Rn} = 0.0076\,h^{-1}$ is ^{222}Rn decay constant and λ_e is a constant that reflects the air exchange in the chamber per unit time, controlled with the pump. λ_e can be derived from the pump flow rate F as $\lambda_e = F/V$.

The source chosen for this study, with a radon emission rate of (162 ± 5) Bq h^{-1}, was placed at the bottom and radon monitors were set up on a bench inside the radon chamber. All monitors were set to take readings every hour except for the RSH monitor (with a preset sampling interval of 4 h). Measurements were started at the same time in order to minimise extra temporal uncertainties due to differences between integration times.

The study was divided into different phases, initially the pump was set to extract air at $F = (0.9 \pm 0.1)$ 1 min^{-1} rate. A stable radon concentration of (2648 ± 85) Bq m^{-3}, hereinafter referred as equilibrium radon concentration, measured by the Atmos 12 reference monitor was reached after three days. Then, four CR-39 etched track detectors were placed in the radon chamber through the openings on the lid.

One week after reaching the equilibrium radon concentration, the chamber was opened and data from the monitors was downloaded. CR-39 etched track detectors were removed from the chamber and analysed. The monitor CAN does not have a data memory function, so the weekly and daily average concentrations were manually recorded during the week, through a transparent cover on the chamber lid.

A few days after, the chamber was closed again using the same radon source but this time without connecting the pump, therefore λ_e was negligible. Radon concentration increased for

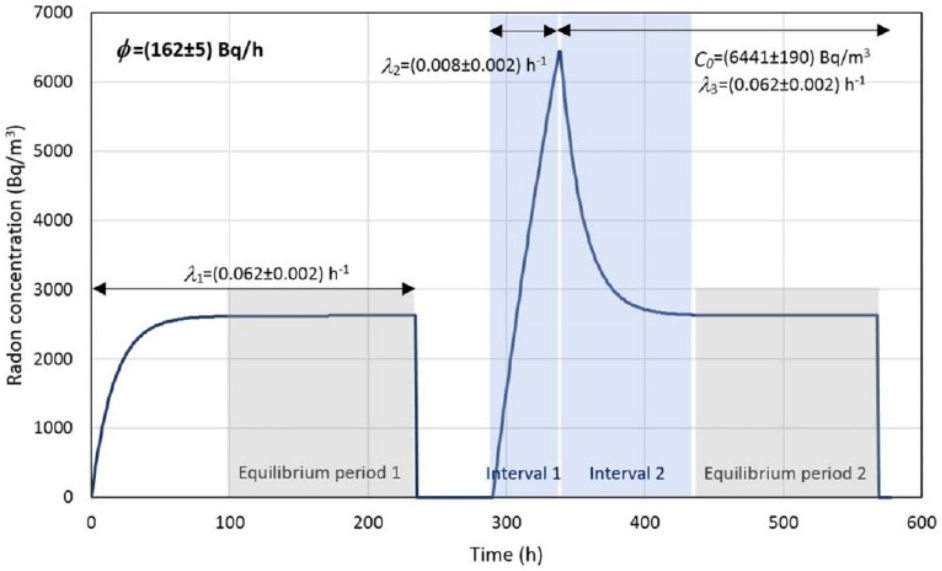

Figure 2. Plot of the theoretical radon concentration over time during the experiment in the radon chamber, values for the radon emission rate of the source ϕ, constant λ for each period and initial concentration C_0 are indicated.

two days up to (6441 $\pm$ 190) Bq m^{-3} and then, the extraction pump was set again to extract air at (0.9 $\pm$ 0.1) l min^{-1} rate, in order to reach the same radon equilibrium concentration as the first week. Once again, it took three days to reach the equilibrium concentration of (2648 $\pm$ 85) Bq m^{-3} and after that the chamber remained closed for another week. Finally, it was opened and all the data collected.

The theoretical curve of the radon concentration variation during the experiment calculated from equation (1) is shown in figure 2. The different phases of the study are depicted, grey shaded areas were intended to compare radon monitors measurement in equilibrium and blue shaded area to assess response time.

2.4. Response time analysis

Different methods are proposed to quantify the response time of the radon monitors during two time intervals, interval 1: increase of the radon concentration the second time the chamber was closed and interval 2: the following decrease when the pump was set to extract air, which corresponds to the blue shaded area in figure 2.

Method 1 suggested is to analyse the time that it takes for each monitor to reach a percentage of the final reference radon concentration in a given time interval. Corresponding time is obtained from the exponential fit (equation (1)) applied to each detector data set. Key percentages proposed are 10%, 50% and 90%, chosen to be at the beginning, middle and end of each time interval. Then, the time ratios between each monitor and Atmos 12 reference monitor are calculated.

Methods 2 and 3 proposed are based on the analysis of the radon concentration relative error (RE) from the Atmos 12 reference, obtained for each monitor as

$$\mathrm{RE} = \frac{(C_i[\mathrm{monitor}] - C_i[\mathrm{reference}])}{C_i[\mathrm{reference}]}, \tag{2}$$

where C_i is the radon concentration at time *i*.

Relative errors are obtained in three different ways, A: from the experimental radon concentration data, B: from the smooth local regression (Loess) curve of the experimental radon concentration data, using Loess regression to smoothen the experimental data series with a 0.2 degree of smoothing (Cleveland *et al* 1992), and C: from the radon concentration given by the exponential fit (equation (1)) applied to each experimental data set.

For method 2, response time is defined as the time it that takes for each detector to reach a relative error within ±10%. It is assumed that in the ±10% relative error range there is no significant difference between the measurement of the monitor and the Atmos 12 reference, and fluctuations are not considered as significant.

Method 3 hypothesizes that two radon monitors are comparable when their relative errors fluctuate around the zero. To this aim, this method compares the rescaled relative error data distribution for each radon monitor with a normal distribution centred in 0 with standard deviation equal to 1 using the statistical Kolmogorov–Smirnov (K–S) test (Conover 1971) and considering progressively the different measurements. Response time is identified as the time in which it is possible to reject the null hypothesis (same distribution) with a 95% confidence level.

Finally, method 4 is based on changing the analysis from concentration to the time corresponding to a given concentration. For each radon concentration data point, the corresponding time is calculated by inverting the exponential function given by equation (1) (see equation (3)) and using parameters C_0, ϕ and λ from the fit applied to Atmos 12 reference data set

$$t = -\log\left(\frac{C(t) - \frac{\phi}{\lambda}}{C_0 - \frac{\phi}{\lambda}}\right)/\lambda. \tag{3}$$

When the time difference is lower than one, the measurement given by the monitor is considered equivalent to the reference.

3. Results and discussion

The Atmos 12 was set as the benchmark to compare the rest of the detectors. Two period in which radon concentration was stable, referred as equilibrium periods, have been considered to evaluate the accuracy of the monitors. The Atmos 12 had an overall average radon concentration in equilibrium of (2648 ± 85) Bq m^{-3}, considering first and second equilibrium concentration periods. Theoretical radon concentration for equilibrium, obtained from equation (1) based on the source radon generation rate and the air exchange set on the chamber during the period under study, was estimated (2613 ± 167) Bq m^{-3}, which is in good agreement with the Atmos 12 average value.

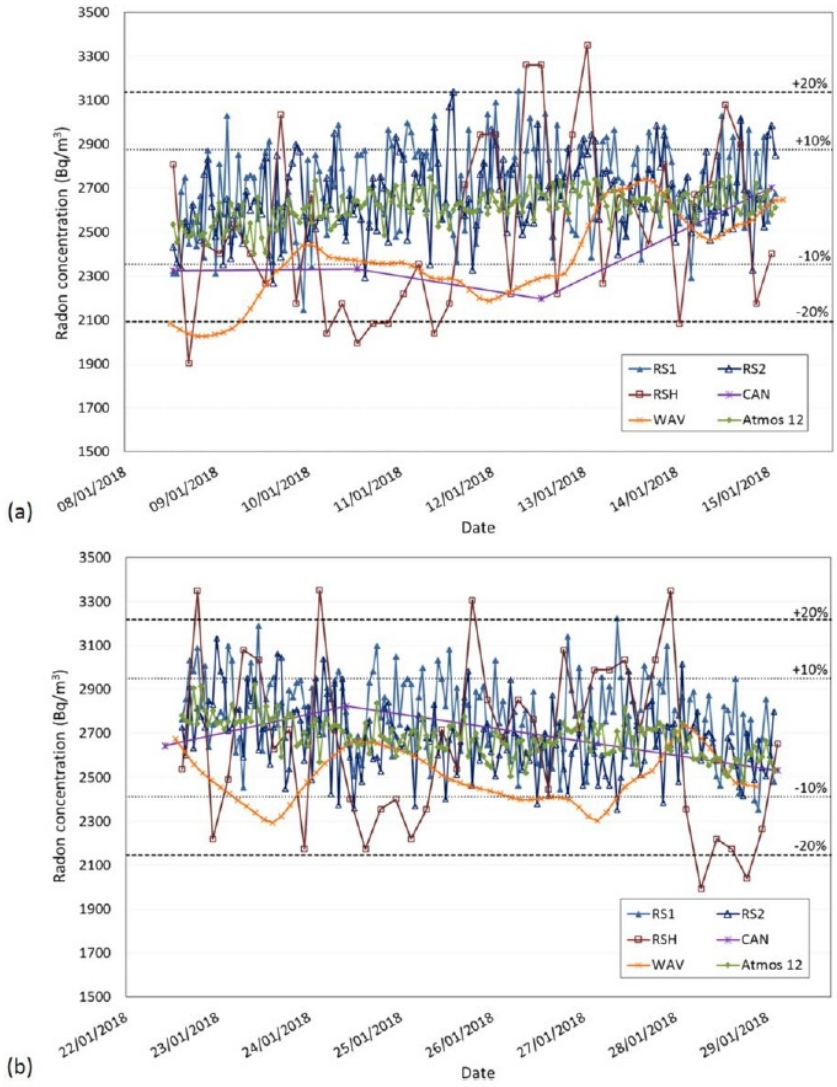

Figure 3. Plot of the radon concentration over time recorded by the radon detectors in the chamber during (a) radon concentration equilibrium period 1 and (b) equilibrium period 2. Data are indicated by lines and symbols for the different detectors.

Figure 3 shows the radon concentration over time recorded for each detector in the radon chamber during the equilibrium concentration periods 1 and 2. Reference lines of ±10% and ±20% for the Atmos 12 reference average concentration are included in the figure. RSH monitor displays fluctuation outside the ±20% as does the WAV in the beginning of the period 1, after 24 h all other radon detectors fell within ±20%.

Table 1 summarises mean radon concentrations $\overline{C}$ for each detector with associated uncertainties for equilibrium periods 1 and 2, corresponding to figures 3(a) and (b) respectively. Uncertainties are obtained as the standard deviation of the data points during

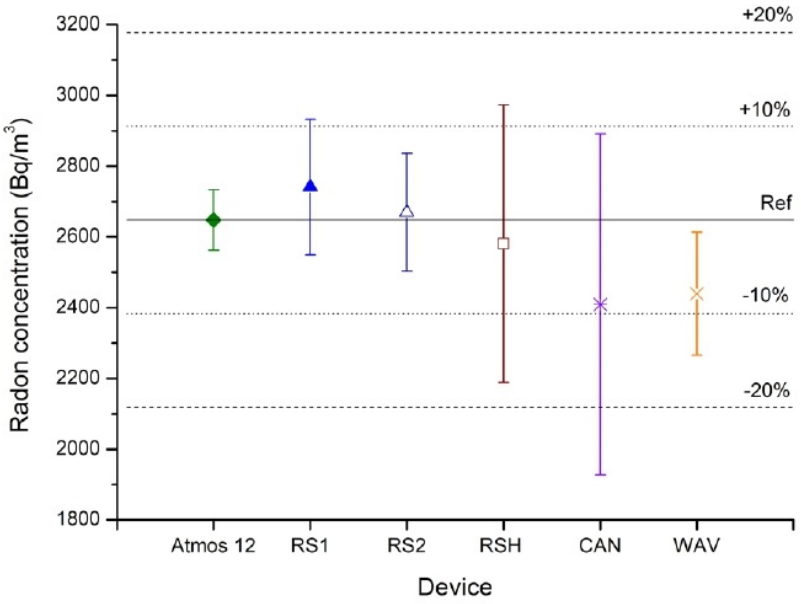

Figure 4. Plot of the total mean radon concentration in the chamber for each radon detector during equilibrium radon concentration periods, reference value given by Atmos 12 is $C_{ref} = (2648 \pm 85)$ Bq m^{-3}. Error bars show uncertainty associated with mean values which is the standard deviation, except for the monitor CAN with a 20% uncertainty.

Table 1. Mean radon concentration and relative percentage difference $\delta(\%)$ from the Atmos 12 reference equilibrium radon concentration in the chamber for equilibrium periods 1 and 2. Uncertainty associated to mean concentration is the standard deviation, except for the monitor CAN with an associated uncertainty of 20%.

	Equilibrium period 1		Equilibrium period 2	
	Mean radon concentration (Bq m^{-3})	$\delta(\%)$	Mean radon concentration (Bq m^{-3})	$\delta(\%)$
Atmos 12	2615 ± 73		2681 ± 83	
RS1	2696 ± 198	+3%	2787 ± 175	+4%
RS2	2664 ± 172	+2%	2675 ± 163	−0.2%
RSH	2512 ± 393	−4%	2649 ± 384	−1%
CAN	2348 ± 470	−10%	2471 ± 494	−8%
WAV	2383 ± 198	−9%	2500 ± 116	−7%
CR39	2757 ± 187	+5%	—	—

equilibrium period, except for the CAN monitor. CAN monitor records daily and weekly average concentrations and hence $\overline{C}$ presented in the table for each period is the weekly average given by the monitor and the uncertainty associated is 20% according to the manufacturer's manual. Relative percentage difference $\delta(\%) = 100 \times (\overline{C} - \overline{C}_{ref})/\overline{C}_{ref}$ from the Atmos 12 reference for each period is also quantified (table 1).

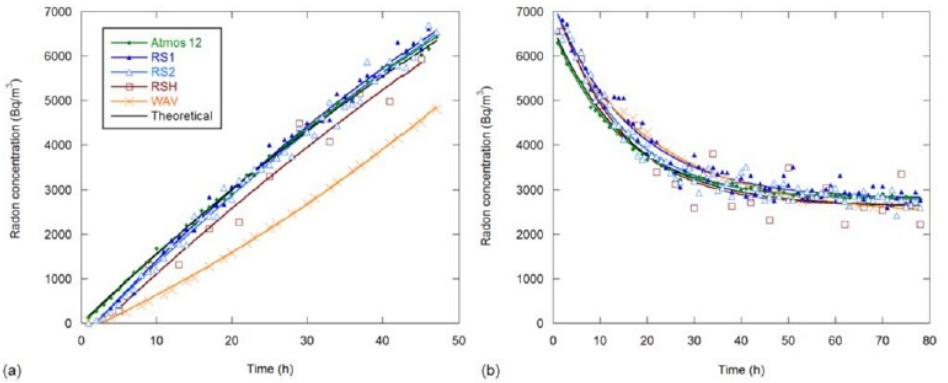

Figure 5. Plot of the radon concentration over time recorded by the radon detectors in the chamber during (a) interval 1 and (b) interval 2 selected to assess response time of the radon monitors. Data are indicated with symbols for each detector, lines correspond to the exponential fit of each data set and the theoretical radon concentration.

Differences between mean radon concentrations in each equilibrium period are not significant. However, mean values appear slightly lower for period 1 compared to period 2 and this can be due to dependency on previous concentration, as concentration was increasing from a lower value before period 1 while it was decreasing from a higher value before period 2. It is also noted that RSH, CAN and WAV monitors mean radon concentration is lower than the reference value, whilst RS1 and RS2 monitors present higher mean values than the reference, except for RS2 in period 2 with a percentage difference of −0.2%. Relative percentage differences are found to be higher for CAN and WAV detectors and lower for RS1 and RS2 devices, which means that their measurements are more accurate.

The mean radon concentration obtained from the CR-39 etched track detectors placed in the chamber during the first equilibrium period is (2757 ± 187) Bq m^{-3}, which is within 5% of the mean radon concentration given by Atmos 12 reference detector in the equilibrium period 1.

Figure 4 depicts the total mean radon concentration in the chamber for each radon detector during equilibrium radon concentration periods. In accordance with results from table 1, more accurate total mean radon concentrations are found for the RS1 and RS2 devices, followed by the RSH, WAV and CAN monitors. Looking at the measurements dispersion given by the standard deviation in such equilibrium periods, RS1 and RS2 devices and WAV have about 6%–7% dispersion and RSH monitor has 15% dispersion. As stated above, CAN monitor dispersion is given by the 20% uncertainty indicated in the manual.

In this investigation the RS monitor is found to be the most accurate and sensitive radon monitor relative to the reference Atmos 12 monitor with a 3% dispersion found for the analysed equilibrium periods.

3.1. Response time analysis

To assess the response time of the radon monitors, variation of radon concentration was analysed for two different time intervals, at interval 1: increase of the radon concentration during 47 h from 0 to (6441 ± 190) Bq m^{-3} and at interval 2: for 78 h the following decrease down to (2648 ± 85) Bq m^{-3}. Figure 5 shows the radon concentration over time

Table 2. Time that it takes for each radon monitor to reach a 10%, 50% and 90% of the final concentration $t_{10\%}$, $t_{50\%}$ and $t_{90\%}$ in hours and Ratio $= t_{\%}$[reference]$/t_{\%}$[monitor], for intervals 1 and 2 under study.

Interval		$t_{10\%}$ (h)	Ratio	$t_{50\%}$ (h)	Ratio	$t_{90\%}$ (h)	Ratio
1	**Atmos 12**	4	1.00	21	1.00	41	1.00
	RS1	6	0.67	22	0.95	41	1.00
	RS2	6	0.67	22	0.95	41	1.00
	RSH	7	0.57	25	0.84	45	0.91
	WAV	10	0.40	35	0.60	>47	–
2	**Atmos 12**	2	1.00	11	1.00	42	1.00
	RS1	5	0.40	15	0.73	50	0.84
	RS2	4	0.50	13	0.85	42	1.00
	RSH	4	0.50	13	0.85	35	1.20
	WAV	–	–	16	0.69	45	0.93

recorded for each detector in the radon chamber during the described intervals 1 and 2. An exponential fit of the theoretical exponential model (equation (1)) was applied to each data set. CAN monitor measurements were not analysed here, as only a few data points were recorded.

3.1.1. Method 1. Method 1 proposed to analyse response time considered three percentages of the final concentration namely, 10%, 50% and 90%. The ratio between the Atmos 12 reference time to reach the percentages of the final concentration $t_{10\%}$, $t_{50\%}$ and $t_{90\%}$ and the corresponding times for each radon monitor gives a qualitative and quantitative idea of the response time, whereby a lower ratio means a slower response of the device. Table 2 summarises the times and ratios for each radon monitor.

From table 2 it is observed that as the radon concentration increases during interval 1, measurements of the radon monitors tend to reach the same trend as the Atmos 12 reference, except for the WAV which never reaches the final concentration during interval 1 (see figure 5(a)). The ratios obtained for the analysed 50% and 90% of the final concentration are higher than for the 10% of the final concentration. Also, for each percentage of the final concentration case studied, RS1 and RS2 present the best response time followed by the RSH and the WAV monitors. Results are similar for interval 2, ratios increase with the percentage of the final concentration analysed, but the numbers obtained vary from interval 1 to interval 2. RS2 monitor presents the best response time for interval 2, RSH also presents a quick response, but the ratio found for the 90% of the final concentration is higher than the unit which means it is ahead the Atmos 12 reference, thus RSH monitor trend is different than the reference.

Relative error of the radon concentration obtained from equation (2) for the three cases considered, A: using the experimental radon concentration data, B: using the smooth Loess curve of the experimental radon concentration data, and C: using radon concentration data given by the exponential fit applied to each experimental data set, is shown in figure 6.

The benefit of this approach is that from RE it is possible to better observe and quantify the zones where measurements of the different radon monitors are deviating from the reference, rather than looking at the variation of radon concentration with time. Figure 6 reveals that in the beginning of both intervals studied, radon monitors do not follow the

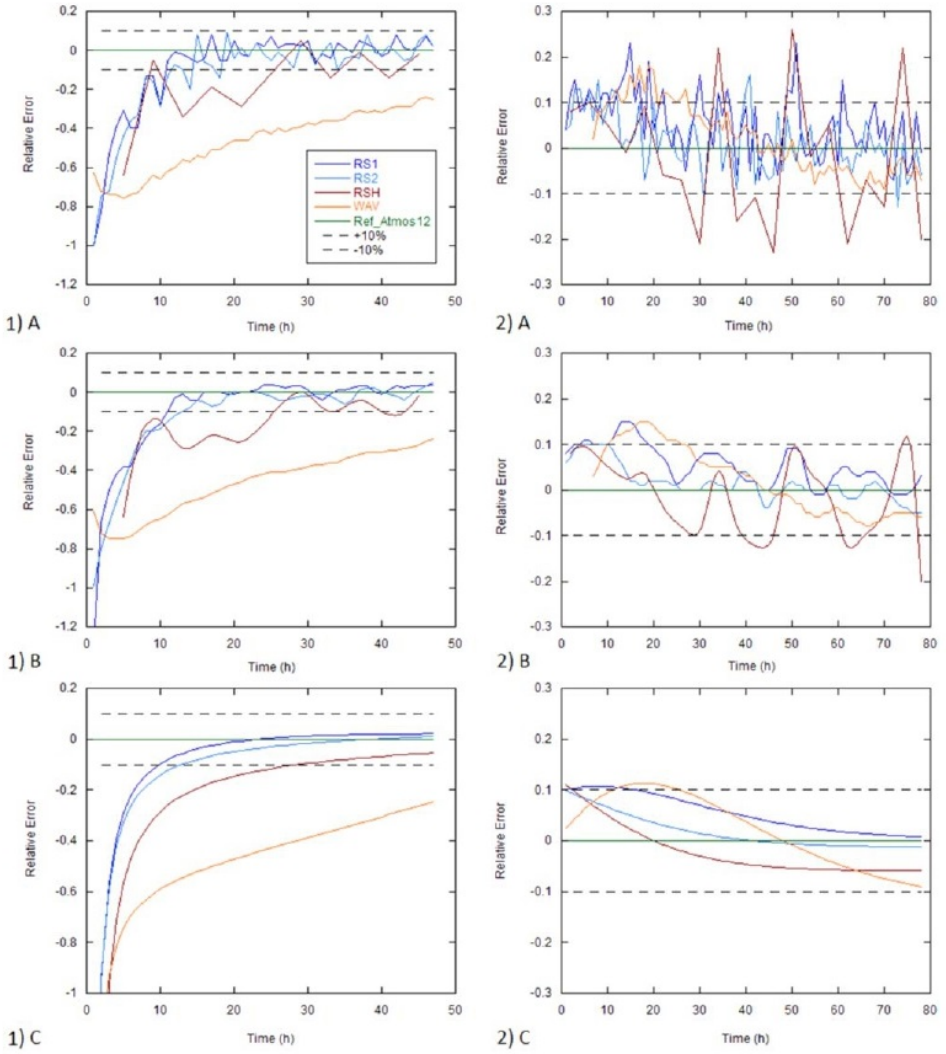

Figure 6. Plot of the radon concentration relative error over time during intervals (1) [LHS] and (2) [RHS] obtained for cases A: from experimental data, B: from smoothed Loess curve of the experimental data and C: from exponential fit applied to the experimental data. Data are indicated with lines for each detector.

increase/decrease trend of the Atmos 12 reference monitor. After some time, monitors' trends reach the Atmos 12 reference and then the relative error fluctuates around the zero. Also, it is observed from figure 6 that for case C, in which RE is obtained from the data of the fitted curves, the fluctuation of the measurements is reduced artificially, while for case B the smoothed data seems reasonable.

3.1.2. Method 2. Results for method 2 to analyse response time are presented in table 3. Response time is defined in this method as the time that it takes for each detector to reach a

Table 3. Time that it takes for each radon monitor to reach a relative error lower than 10% RE, for interval 1 and 2 under study. Three cases are presented, A: relative error obtained from the experimental data, B: relative error obtained from the smoothed Loess curve of the experimental radon concentration data, and C: relative error obtained from the radon concentration given by the exponential fit.

	t (h), interval 1			*t* (h), interval 2		
	A	B	C	A	B	C
RS1	11	11	10	22	19	16
RS2	14	13	13	12	10	<0
RSH	26	26	29	6	4	3
WAV	>47	>47	>47	28	27	26

Table 4. Time from which the relative error data distribution for each radon monitor cannot be considered different from a normal distribution with mean 0 and standard deviation 1, with a 95% confidence level, for interval 1 and 2 under study. Three cases are presented, A: relative error obtained from the experimental data, B: relative error obtained from the smoothed Loess curve of the experimental radon concentration data, and C: relative error obtained from the radon concentration given by the exponential fit.

	t (h), interval 1			*t* (h), interval 2		
	A	B	C	A	B	C
RS1	6[a]	9[a]	10[a]	26	3	—
RS2	9	18[a]	22[a]	3	32	—
RSH	9–12	—	>47	0	—	—
WAV	>47	>47	>47	47	>78	—

[a] Indicates cases where differences with the normal distribution (mean = 0, SD = 1) are encountered after the time presented.

Table 5. Times when measurements given by each radon monitor cannot be considered different from the Atmos 12 reference, for interval 1 and 2 under study. (Criteria: working in the time space of analysis, difference between a monitor data point and the Atmos 12 reference lower than the unit.)

	t (h), interval 1	*t* (h), interval 2
RS1	11, 12, 13, 14, 16, 21, 22, 24, 26, 29, 35, 36, 39, 41, 43, 44	18, 24, 33, 46
RS2	21, 22, 24, 26, 30, 32, 39, 42	13, 14, 15, 21, 37, 50, 57
RSH	9, 37	14
WAV	1	7

relative error within ±10%. During interval 1, results obtained for the three cases considered are in good agreement and the best response time is found for RS1 monitor followed by RS2, RSH and WAV monitor. The WAV monitor does not reach the Atmos 12 reference trend

during interval 1. The results obtained for interval 2 show response times varying for cases A, B and C, and they do not agree with results for interval 1. The best response time during interval 2 is found for RSH monitor, followed by RS2, RS1 and finally the WAV monitor.

3.1.3. Method 3. Method 3 is based on the comparison of relative error data distributions for each radon monitor (figure 6) with a normal distribution with mean zero and standard deviation 1 by means of the statistical K–S test. Different data distributions (e.g. RSH relative error data set considering times from 5 to 47 h, RSH relative error data set considering times from 6 to 47 h, etc) are tested to find the time from which we cannot reject the null hypothesis, i.e. both distributions cannot be considered as different with a 95% confidence level. Resulting times are summarised in table 4, those times marked with a superscript denote the cases in which, after the time presented, differences with the normal distribution (mean = 0, SD = 1) are encountered.

Contrary to expectations, this method does not provide relevant results. Consistent values are not obtained due to the great variability of experimental and smoothed data. Besides, K–S test are not sensitive for case C (relative error obtained from the radon concentration given by the exponential fit) considered in interval 2.

3.1.4. Method 4. Method 4 consists of changing the analysis from concentration to time, and then comparing times with the Atmos 12 reference. When the time difference between a monitor data point and the Atmos 12 reference is lower than the unit, we establish that the measurement given by the monitor cannot be considered different from the reference. Table 5 shows an overview of the times when measurements given by each radon monitor are equivalent to the reference.

It is observed from table 5 that RS1 and RS2 monitors present a higher number of times in which measurements can be considered equivalent to the reference, while for RSH and WAV monitors this happens just in one or two occasions. This means, that RS1 and RS2 monitors have a better time response. Now, if we look at the first time when the RS1 and RS2 satisfy the criterion established, for interval 1 the RS1 monitor has the best response time and for interval 2 is the RS2 monitor.

Similar results are found for methods 1 and 2, resulting RS1 and RS2 monitors the ones with the best response time, followed by the RSH and the WAV monitors. These methods work well for both time intervals analysed, although for interval 1 results are better because the increase of the radon concentration is similar to a linear trend while this does not happen for interval 2. Method 3 can be highlighted as the least sensitive for this study, and finally method 4 shows results in good agreement with the results obtained for methods 1 and 2.

4. Conclusions

A comparison between continuous radon monitors was conducted in a radon chamber in a controlled radon atmosphere. The equation that describes radon concentration variation over time in a closed space was used to check radon behaviour in the chamber during the study, with the reference radon concentration given by the Atmos 12 monitor.

Features, operation mode and purposes are different for each radon monitor, but all of them should satisfy minimum requirements. From the radon monitors tested, RSH, CAN and

WAV are aimed at the general public for house testing while RS1 and RS2 devices are intended for research or diagnostic measurements, and Atmos 12 is a reference monitor which must provide highly reliable and accurate measurements. Due to the nature of their applications, general purpose radon detectors are not expected to have the same level of accuracy, sensitivity and response time.

The methodology used to benchmark radon monitors was by comparing mean radon concentration in the chamber during equilibrium radon concentration periods. This ensures the radon concentration fluctuations are minimised and measurement dispersion intrinsic to each detector is evident. Also, the equilibrium radon concentration value was chosen to be in the order of 2 kBq m^{-3} to reduce statistical fluctuation in the measurements caused by the random nature of radioactivity.

Derived from the results analysis during radon equilibrium concentration periods, the RS monitor is the most accurate when compared to the reference monitor Atmos 12. Mean values for all detectors fell within the $\pm 10\%$ from Atmos 12 reference, but RSH monitor gives a mean value more accurate than WAV and CAN monitors, that underestimate the reference mean radon concentration up to 9%. Considering measurements dispersion, WAV is more sensitive than RSH and CAN monitors.

The analysis of the radon monitors' response time was approached with four different methods. First and simplest one was analysing the time that takes for a monitor to reach a percentage of the final radon concentration during a given interval where variation of radon concentration is known. This method is very easy to implement and it can be applied to different arbitrary concentration steps, but it does not evaluate possible discrepancies in between steps.

The second and third methods were based on the analysis of the relative error from the Atmos 12 reference radon concentration. For method 2, response time was defined as the time when relative error was within the $\pm 10\%$ for each radon monitor. While method 3 compared statistically relative error distributions with a normal distribution with mean 0 and standard deviation 1, defining response time as the time when both distributions cannot be considered different. Method 2 evaluates time differences continuously, unlike method 1, and it presents good results for RE obtained from experimental and smoothed data. However, in the case of RE obtained from data fitted to an exponential equation, the fitting function is averaging out the fluctuations in the data giving unrealistic results. Method 3 is based on the same principle as method 2, but results provided for the particular cases studied are not relevant.

Finally, method 4 consisted in changing analysis from concentration to time and then comparing times with the Atmos 12 reference. This method uses a different way of quantifying response time, based on the frequency of the times where measurements match the reference.

The different approaches show similar results, only method 3 proposed is not suitable for the particular study analysed here, and the slowest response time in any case is found for the WAV monitor and the best for RS1 and RS2 monitors.

To summarise, a range of detectors that are commercially available were analysed and based on the analysis, we can conclude that the choice of a radon detector should depend on the accuracy and response time required for the application needed.

Using the criteria of 10% of the reference monitor, all monitors tested are appropriate for long-term measurements. However, if time-varying concentrations are of interest, RS monitors present a better response time.

The principle of operation for all monitors tested is very similar, based on a passive chamber with a Si detector, HV collection and alpha spectrometry. Therefore, it may be conclude that the variation in performance in term of accuracy and response time is related to a variety in design features including electronics and spectrometry technique.

Acknowledgments

The authors wish to acknowledge the technical staff at LaRUC for the collaboration in the experimental development of the study. This research was partially supported by the OPTI-SDS project, funded by the EPA (Project code: 2015-HW-MS-5).

ORCID iDs

Marta Fuente https://orcid.org/0000-0002-9444-0925
Daniel Rabago https://orcid.org/0000-0002-2285-8767

References

Airthings 2017a Wave Digital Radon Monitor User Manual https://airthings.com/wave/
Airthings 2017b Canary Digital Radon Monitor User Manual https://airthings.com/home/
Ali N, Khan E U and Khan K 2009 Etch induction time in CR-39 detectors etched in Na_2CO_3 mixed NaOH solution *Chin. Phys. Lett.* **26** 092901
Bochicchio F 2011 The newest international trend about regulation of indoor radon *Radiat. Prot. Dosim.* **146** 2–5
Cleveland W S, Grosse E and Shyu W M 1992 Local regression models *Statistical Models in S* ed J M Chambers and T J Hastie (New York: Wadsworth & Brooks/Cole) 309–76
Conover W J 1971 *Practical Nonparametric Statistics* (New York: Wiley)
Council of the European Union 2014 *Laying Down Basic Safety Standards for Protection Against the Dangers Arising from Exposure to Ionising Radiation* Directive 2013/59/EURATOM
Dowdall A, Murphy P, Pollard D and Fenton D 2017 Update of Ireland's national average indoor radon concentration—application of a new survey protocol *J. Environ. Radioact.* **169** 1–8
Espinosa G, Golzarri J I, Gaso M I, Mena M and Segovia N 2013 An intercomparison of indoor radon data using NTD and different dynamic recording systems *Radiat. Meas.* **50** 112–5
Gammadata Instrument AB 2015 Atmos 12: User's Guide www.gammadata.se/products/radiation-detection/radon/radon-instruments/atmos-12/
George A C 1996 State-of-the-art instruments for measuring radon/thoron and their progeny in dwellings—a review *Health Phys.* **70** 451–63
Gillmore G, Wertheim D and Crust S 2017 Effects of etching time on alpha tracks in solid state nuclear track detectors *Sci. Total Environ.* **575** 905–9
Gunning G A, Murray M, Long S C, Foley M J and Finch E C 2016 Inter-comparison of radon detectors for one to four week measurement periods *J. Radiol. Prot.* **36** 104
ICRP 2009 Lung cancer risk from radon and progeny and statement on radon *ICRP Publication 115* **40** (1)
Jilek K and Marušiakova M 2011 Results of the 2010 national radiation protection institute intercomparison of radon and its short-lived decay product continuous monitors *Radiat. Prot. Dosim.* **145** 273–9
Sainz C, Rábago D, Celaya S, Fernández E, Quindós J, Quindós L, Fernández A, Fuente I, Arteche J L and Quindós L S 2018 Continuous monitoring of radon gas as a tool to understand air dynamics in the cave of Altamira (Cantabria, Spain) *Sci. Total Environ.* **624** 416–23
Sainz C, Rábago D, Fuente I, Celaya S and Quindós L S 2016 Description of the behavior of an aquifer by using continuous radon monitoring in a thermal spa *Sci. Total Environ.* **543** 460–6

Sarad GmbH 2016 Radon Scout Home Monitor www.sarad.de/product-detail.php?p_ID=67&cat_ID=2
Sarad GmbH 2017 Radon Scout Monitor www.sarad.de/product-detail.php?p_ID=37&cat_ID=2
Tunno T, Caricato A P, Fernandez M, Leonardi F, Tonnarini S, Veschetti M, Zannoni G and Trevisi R 2017 Critical aspects of remediation in karst limestone areas: some experiences in school of South Italy *J. Radiol. Prot.* **37** 160–75
UNE-EN ISO/IEC 17025 2005 *Conformity assessment. General requirements for the competence of testing and calibration laboratories* AENOR, Spain
UNSCEAR 2006 *Sources and Effects of Ionizing Radiation* (New York: United Nations)
WHO 2009 *Handbook On Indoor Radon: A Public Health Perspective* (Geneva: WHO)

Chapter 3

Paper II

Investigation of gas flow through soils and granular fill materials for the optimisation of radon soil depressurisation systems

Journal of Environmental Radioactivity, 198, pg. 200-209 (2019)

Fuente, M., Muñoz, E., Sicilia, I., Goggins, J., Hung, L.C., Frutos, B., Foley, M.

The work presented in this thesis was conceived on the subject of radon prevention and mitigation, in particular by soil depressurisation technique. From the literature, it is known that there is an impact of the aggregate layer under the slab permeability on the effectiveness of soil depressurisation systems, as mentioned in the introduction (see section 1.2.2).

In order to investigate optimum performance of soil depressurisation systems, an experiment to characterise granular fill materials used in the sub-slab aggregate layer in terms of gas permeability was performed. Following laboratory based tests conducted by Hung et al. (2018) on Irish standard granular fill materials, a similar test apparatus was developed in collaboration with the Eduardo Torroja Institute for Construction Science (IETcc) in Madrid, to test several granular fill materials common to building practices in Spain.

The experiment included analysis of particle size distribution and gas permeability of different uncompacted granular fill material samples. Gas permeability of a soil sample was also tested. Theoretical expressions for permeability were discussed based on the experimental results and Finite Element Method (FEM) numerical simulations conducted. The Spanish aggregates under

study were benchmarked against other standard granular fill materials within the European context, based on works conducted in Ireland and the UK.

Among the findings from the investigation of gas flow through the different aggregates tested, the Darcy-Forchheimer equation was proven to provide the best match to the experimental results. Gas permeability values were found in the order of magnitude of 10^{-8} m^2, lower permeability was obtained for the soil sample tested, in accordance with the literature on soil permeability. Finally, similarities were found between the experimental results compared with British standard granular fill materials.

This work was submitted to the Journal of Environmental Radioactivity and accepted for publication.

Author's contributions

Mark Foley, Borja Frutos, Jamie Goggins and Le Chi Hung contributed to the initial research plan. Marta Fuente and Eduardo Muñoz designed together the experiment, developed and assembled the test set up and conducted the experimental tests with the help from Isabel Sicilia. Marta Fuente analysed the test results and lead the writing of the manuscript. Numerical simulations were performed by Eduardo Muñoz with the contribution from Marta Fuente. Mark Foley, Borja Frutos and Jamie Goggins reviewed the manuscript. All authors read and approved the final manuscript.

Journal of Environmental Radioactivity 198 (2019) 200–209

Contents lists available at ScienceDirect

Journal of Environmental Radioactivity

journal homepage: www.elsevier.com/locate/jenvrad

Investigation of gas flow through soils and granular fill materials for the optimisation of radon soil depressurisation systems

Marta Fuente[a,b,e], Eduardo Muñoz[c,d,*], Isabel Sicilia[c], Jamie Goggins[b,e], Le Chi Hung[a,b,e], Borja Frutos[c], Mark Foley[a]

[a] School of Physics, National University of Ireland Galway, Ireland
[b] Civil Engineering, College of Engineering & Informatics, National University of Ireland Galway, Ireland
[c] Eduardo Torroja Institute for Construction Science IETcc-CSIC, Madrid, Spain
[d] Superior Technical School of Architecture, Technical University of Madrid, UPM, Spain
[e] Centre for Marine and Renewable Energy (MaREI), Ryan Institute, National University of Ireland Galway, Ireland

ARTICLE INFO

Keywords:
Granular fill materials
Permeability
Radon
Soil depressurisation system

ABSTRACT

The purpose of this study is to investigate gas flow through different types of granular fill materials and soil by means of a series of experimental laboratory tests, in relation to soil depressurisation systems for radon reduction under buildings and the soil surrounding the foundation. Gas permeability characterisation of materials used as granular fill material beneath the slab in buildings is a key parameter for the optimum performance of soil depressurisation systems to mitigate radon. A test apparatus was developed, adapted from previous studies, to measure the gas permeability of the samples and Finite Element Method numerical simulations were validated to simulate the flow behaviour through them. Theoretical expressions for permeability were discussed based on the analysis of experimental results and numerical simulations, finding that Darcy-Forchheimer equation provides the best match to the experimental results. Darcy's law also proved to be suitable for low gas velocities, whereas Ergun's equation resulted in a poor fit of the experimental data. Benchmark analysis of the granular fill materials under study and other European standards (Spanish, Irish and British) is also presented.

1. Introduction

Radon (^{222}Rn) is a radioactive gas, product of the decay of ^{226}Ra, which belongs to the decay series of uranium (^{238}U), present in varying amounts across the Earth's crust. It is highly mobile, and its half-life is 3.8 days, emanated from rocks or soil, radon can permeate through the soil and release into the atmosphere. Outdoor radon concentration is not a health problem as it is diluted and dispersed in the atmosphere, but if radon gas enters the air space of a building it can accumulate causing elevated indoor radon concentration. According to the World Health Organization (WHO), radon is classified as the second leading cause of lung cancer in the general population after tobacco smoking (WHO, 2009). Inhaling radon has been shown to cause this disease through the decay of its short lived alpha decay products, such as alpha emitting ^{218}Po and ^{214}Po, which induce pulmonary cell DNA damage. Therefore, reduction of indoor radon levels in buildings is considered an important public health issue and since February 2018, with the implementation of the 2013/59/EURATOM Basic Safety Standards (BSS) Directive, all European Union Member States are required to take action plans against radon in buildings exceeding the reference radon level (Council of the European Union, 2014).

Among the different existing techniques for radon prevention and mitigation, soil depressurisation is considered the most effective solution in radon reduction (Frutos et al., 2011; Long et al., 2013; Jiránek, 2014). It prevents the transfer of radon from the soil towards the building by decreasing the pressure in the granular fill material layer under the concrete slab and thus, reversing the pressure difference between the soil and the occupied space (DELG, 2002). Soil depressurisation systems can be active and passive and include three basic components: a suction point, an exhaust pipe connected to the suction point to draw the soil gas out from the building, and a means of extraction (mechanical or passive).

Several factors affect the performance of a soil depressurisation system, such as permeability of the granular fill material layer beneath the slab and the native soil surrounding the building foundation. Other factors include the thickness of the sub-slab layer, size of the suction

* Corresponding author. Eduardo Torroja Institute for Construction Science IETcc-CSIC, Madrid, Spain.
E-mail addresses: m.fuentelastra1@nuigalway.ie (M. Fuente), emunozlorenzo@ietcc.csic.es (E. Muñoz), borjafv@ietcc.csic.es (B. Frutos), mark.foley@nuigalway.ie (M. Foley).

https://doi.org/10.1016/j.jenvrad.2018.12.024
Received 21 September 2018; Received in revised form 4 December 2018; Accepted 23 December 2018

point, any crack or gap in the floor, moisture content and atmospheric conditions (Jiránek and Svoboda, 2007; Diallo et al., 2015; Muñoz et al., 2017).

Previous studies have highlighted the importance of understanding the permeability degree of the compacted granular fill material layer beneath the slab related to radon mitigation by soil depressurisation (Hung et al., 2018a, b). Characterisation of Irish standardised granular fill materials specified as permeable granular layers beneath the concrete floors and foundations, used for soil depressurisation systems in Ireland was conducted, including grading, compaction, and air permeability tests.

There is no standard technique for gas permeability testing of granular fill materials. Characterisation of granular fill materials' gas permeability can be addressed through different techniques, either experimental or using theoretical calculations. The results obtained from different procedures are not always in agreement and the direct transfer of those results to models for the calculation of depressurisation techniques effectiveness can lead to inaccurate predictive outcomes (Bonnefous et al., 1992).

In terms of soil gas permeability, there is an extended technique for in situ measurements to assess transport through soil using the RADON JOK equipment (Radon v.o.s., www.radon-vos.cz). The principle of this equipment consists of air withdrawal by means of negative pressure. However, this technique is limited to soil field measurements in a range of gas permeability from 10^{-11} m^2 to 10^{-14} m^2 (Castelluccio et al., 2015) and, thus, it is not useful to test granular fill materials and some types of soils.

This paper presents permeability characterisation of different types of granular fill materials commonly used in Spanish building practices. The work includes modelling of gas flow behaviour through soil and granular fill materials to assess permeability and discussion of the equations to calculate gas permeability. Furthermore, benchmarking analysis of European standard granular fill materials is presented.

2. Materials and methods

2.1. Design of the test apparatus

The test apparatus developed for this study was based on the laboratory experimental set-up by Hung et al. (2018a), which, in turn, was based on the operating principle from the standard ASTM-D6539 (2013) and previous works of Gadgil et al. (1991) and BRE (1998). The design consists of three different parts: an inlet chamber, a testing sample chamber and an outlet chamber. Gas is pressurised from a source into the inlet, it goes through the sample and then flows out the outlet chamber. Pressure difference across the sample is measured to obtain permeability.

The apparatus was made of Perspex and PVC pipes with 125 mm diameter, 3.2 mm thick walls and total length of 3050 mm (see Fig. 1). It was divided into different segments to facilitate filling and testing: an inlet segment 1000 mm long, four sample segments of 250 mm length each and an outlet segment 1050 mm long. The segments were joined by flexible couplings to prevent gas leakage. The diameter of the pipe was chosen to suit samples with particle sizes less than 30 mm, for larger particle sizes the pipe diameter should be increased in order to avoid any surface effects.

Several differential pressure sensors were placed at different points along the sample chamber, as well as at the inlet and outlet chambers, to measure pressure drop along the sample and the inlet-outlet pressure difference. The pressure sensors used were DG-700 Pressure & Flow Gauge (measuring range −1250 Pa to 1250 Pa, accuracy ± 1%) and Honeywell model HSCDRRD006MDSA3 (operating pressure ± 6 mbar, accuracy 0.25%). A pitot tube (model Testo 0635 2145, measuring range +1 to +100 m/s) for measuring flow velocity and a hot wire anemometer (model Testo 425, measuring range 0 to +20 m/s, accuracy ± (0.03 m/s + 5% of mv) and resolution 0.01 m/s) were used to measure flow rate in the inlet chamber. The gas source chosen was a compressed air generator and a needle valve was used to regulate the inlet air.

The procedure to conduct the experimental test was as follows:

1) Air leakage was tested prior to any tests.
2) The sample chamber was filled with the uncompact material under study and all the sensors set up.
3) Controlled air flow rate was pressurised into the gas inlet chamber and measurements from pressure sensors and velocity meter recorded.
4) Pressure at the inlet was increased gradually with each sample being tested for a range of pressures from 20 to 600 Pa.

2.2. Gas permeability expressions

Permeability is a property of a porous material, defined as the ability of a fluid or gas to transmit through the porous medium. For gas flow through a porous material, transportation is governed by the gas permeability. In this section, different expressions to determine gas permeability are presented and discussed.

The first equation considered to obtain gas permeability of a porous material is Darcy's law, which is a linear relationship between the fluid flow rate that goes through the porous medium, Q (m^3/s), the cross section, A (m^2), and the hydraulic gradient $\Delta h/\Delta l$ (Lambe and Whitman, 1969).

$$Q = -k\frac{\Delta h}{\Delta l}A \tag{1}$$

where k (m/s) is a constant known as Darcy's permeability coefficient, which depends both on the porous medium and the fluid. Absolute or specific permeability, K_D (m^2), which only depends on the porous medium, can be obtained as:

$$K_D = k\frac{\mu}{\gamma} \tag{2}$$

where μ (Pa.s) is the dynamic viscosity of the fluid, and γ (Pa/m) is the specific weight of the fluid. Combining equations (1) and (2) the following formula is derived,

$$K_D = -\frac{\mu}{\gamma}\frac{Q}{A\frac{\Delta h}{\Delta l}} \tag{3}$$

Finally, knowing that $Q = v{\cdot}A$ and $\Delta h = \Delta P/\gamma$, Darcy's permeability equation can be written as follows:

$$K_D = -\frac{\mu v}{\Delta P/\Delta l} \tag{4}$$

where v (m/s) is the fluid velocity through the porous medium and ΔP (Pa) is the pressure differential between two points of the sample porous material at a distance Δl (m).

Darcy's law has limitations for liquids at high velocities and for gases at very high or very low velocities. In such cases, the relationship between the pressure gradient and gas velocity is not linear. Darcy's law validity is related to the Reynolds' number (Scheidegger, 1958):

$$Re = \frac{\rho v D}{\mu} \tag{5}$$

where ρ (kg/m^3) is the fluid density and D (m) is a diameter related with the porous medium. Scheidegger attributes D the changes in the validity of Darcy's law regarding Reynolds' number.

Darcy's law is valid for models considering low permeability, such as low velocities of the gas through the porous medium (laminar flow). However, in order to develop a suitable model for a larger range of velocities, considering turbulent flow, the Darcy-Forchheimer equation is presented (Forchheimer, 1901).

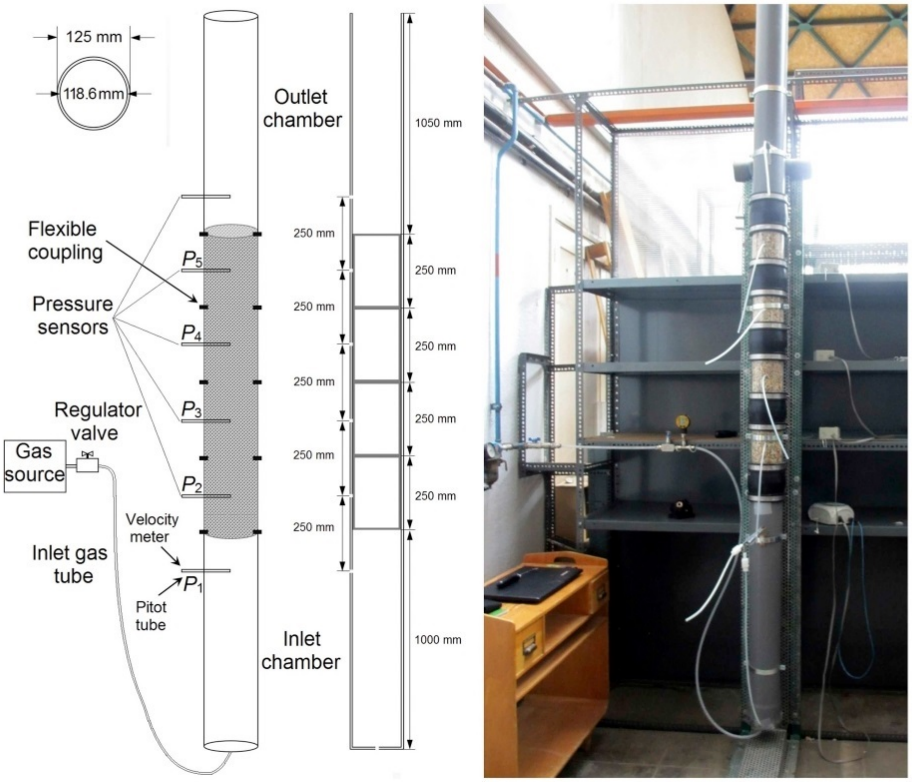

Fig. 1. Diagram of the test apparatus (left) and picture of the test apparatus setup (right).

$$\frac{\Delta P}{\Delta l} = -\frac{\mu}{K_{DF}} v - c\frac{\mu}{K_{DF}} v^2 \tag{6}$$

where K_{DF} (m^2) is Darcy-Forchheimer specific permeability and c (s/m) is a constant called the Forchheimer factor (Gadgil et al., 1991). From equation (6), the following expression for the permeability is obtained:

$$K_{DF} = -\frac{\mu}{\Delta P/\Delta l} v - c\frac{\mu}{\Delta P/\Delta l} v^2 \tag{7}$$

On another note, Ergun (1952) studied fluid flow through beds of granular materials, considering that pressure losses were caused by kinetic and viscous energy losses, as it is shown in equation (8).

$$\frac{\Delta P}{\Delta l} = -150\frac{(1-n)^2\mu}{n^3 d_p^2} v - 1.75\frac{(1-n)\rho}{n^3 d_p} v^2 \tag{8}$$

where n is the porosity of the granular material and d_p (m) is the effective diameter of the granular particles. If velocity tends to the zero, the first term of equation (8), which is the viscous term, dominates and therefore the fluid is considered viscous. At high fluid velocities, kinetic term prevails and the fluid is considered turbulent.

By relating equations (6) and (8), Ergun's permeability expression is obtained as follows:

$$K_E = \frac{n^3 d_p^2}{150(1-n)^2} \tag{9}$$

Unlike previous expressions discussed, equation (9) doesn't require an experimental test to relate fluid velocity to the pressure drop through a granular material sample, but it requires knowledge of the porous material characteristics such as the porosity and the effective diameter of the particles.

2.3. Materials under study

To study the behaviour of gas flow through different porous media, four different materials were tested (see Fig. 2). Two samples were types of gravel, composed of crushed stone with different particle size distribution, sample A: garbancillo 4/12 and sample B: gravel 4/20. Third sample tested, sample C: debris, was composed of loose natural material consisted of broken pieces of demolition waste, normally obtained as a result of building demolitions and commonly used as filler. Last material selected for the study was a type of soil, sample D: soil, which can be classified as coarse grained soil (ASTM-D2487, 2017). The materials were selected in order to cover a wide range of gas permeability.

All samples were tested uncompacted, but sample D was also tested under manual compaction to reproduce field conditions of the soil. Soil was compacted manually using a metal rammer weighing 7.5 kg, by applying 10 blows of the rammer dropping from the controlled height of 200 mm.

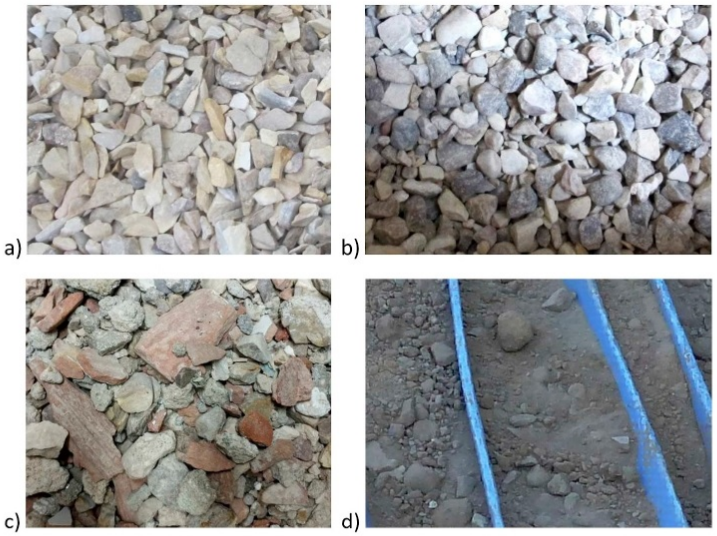

Fig. 2. Pictures of a) sample A: garbancillo 4/12, b) sample B: gravel 4/20, c) sample C: debris and d) sample D: coarse grained soil.

Particle size distribution and porosity are relevant characteristics for the study of porous materials' gas permeability and therefore they were considered for the study. Grading curves of the materials under study were obtained following standard UNE EN-933-1 (UNE-EN 933-1:2012).

Porosity was determined experimentally for all granular fill material samples as the ratio of total volume of pore space within the media divided by the total volume of material (Hung et al., 2018a) using the following expression:

$$n = \frac{V_{total} - V_{solid}}{V_{total}} = \frac{V_{fluid}}{V_{total}} \tag{10}$$

A known volume tank, $V_{total} = 7051\ cm^3$, was filled with the sample material and then water added until the volume was full. Before that, the sample was saturated during 24 h to fill internal porosity. Water mass, Δm, was measured and then fluid volume obtained as $V_{fluid} = \Delta m/\rho_{fluid}$, where ρ_{fluid} is the density of the fluid.

2.4. FEM simulations

Finite Element Model (FEM) simulations were performed to assess gas permeability of the samples and to benchmark the different expressions for permeability calculation. The finite element software COMSOL Multiphysics V5.3 (COMSOL, 2017) was used in this study.

Due to the test apparatus geometry, the axisymmetric analysis was selected for modelling because it uses rotational symmetry to optimise numerical simulation calculations. The Laminar Flow interface, based on the Navier-Stokes equations for conservation of momentum and the continuity equation for conservation of mass, was used for modelling. The simplified equation is

$$\nabla P\boldsymbol{i} = -\frac{\mu}{K}\boldsymbol{v} - \beta\boldsymbol{v}|\boldsymbol{v}| \tag{11}$$

From equation (11), by changing K and β parameters, equations (4), (6) and (8) can be obtained. For Darcy's law $K = K_D$ and $\beta = 0$, for Darcy-Forchheimer equation $K = K_{DF}$ and $\beta = c/K_{DF}$, and for Ergun $K = K_E$ and $\beta = 1.75(1-n)\rho/n^3 d_p$.

Boundary conditions were specified based on the test apparatus setup, with inlet velocity condition at the bottom of the test apparatus. The type of mesh selected was rectangular, with maximum element size of 8.13×10^{-4} m and minimum element size of 9.37×10^{-6} m. All simulations were performed under stationary analysis, with parametric sweep study and using the direct solver MUMPS (MUltifrontal Massively Parallel sparse direct Solver).

3. Results and discussion

3.1. Particle size distribution and porosity of the samples

Fig. 3 shows the grading curves for each sample under study. Based on the particle size distribution, debris can be classified as well-graded material, while garbancillo 4/12, gravel 4/20 and the soil under study are classified as poorly-graded materials.

The effective particle diameter for poorly-graded materials can be taken directly as d_{50} from the grading curve (Hung et al., 2018a). Thus, the effective particle diameter is 9.1 mm for sample A: garbancillo 4/12 and 13.8 mm for sample B: gravel 4/20. For sample C: debris, d_{50} obtained from the grading curve is 10.7 mm and for sample D: soil, d_{50} is 0.64 mm.

Porosity for the granular fill materials samples was obtained experimentally, resulting in $n = 0.46$ for sample A: garbancillo 4/12, $n = 0.40$ for sample B: gravel 4/20 and $n = 0.42$ for sample C: debris. The values obtained are very similar, which can be related to the nature of the materials composition.

3.2. Experimental test results and permeability calculation

Table 1 shows an example of the experimental results obtained for the different materials tested, in this case for sample B: gravel 4/20. Pressure at different points along the test apparatus (see Fig. 1) and the

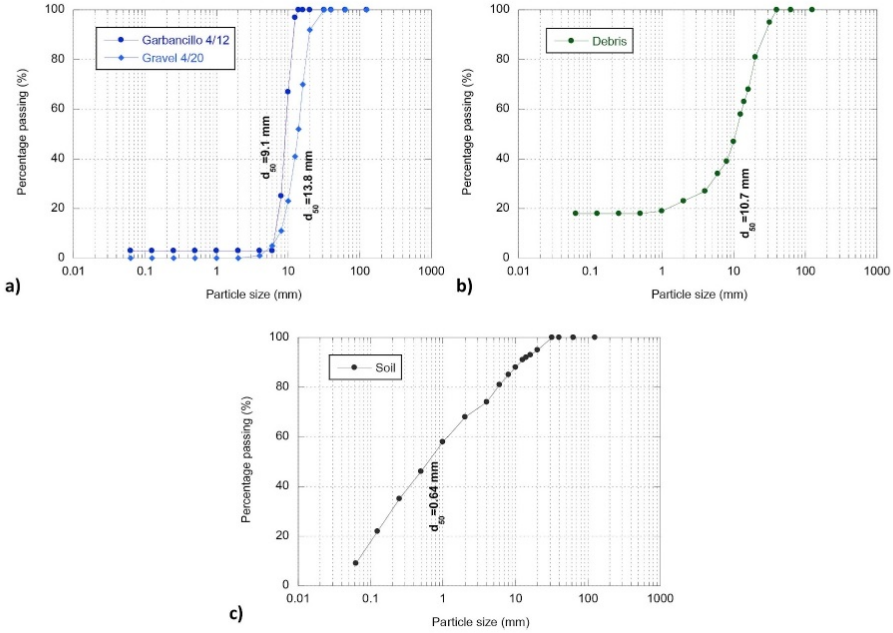

Fig. 3. Particle size distribution of the different materials under study, a) samples A: garbancillo 4/12 and B: gravel 4/20, b) sample C: debris and c) sample D: soil. Particle diameter d_{50} is indicated for all samples.

Table 1
Experimental results for sample B: Gravel 4/20. P_i is the pressure recorded at each i-detector position, v is the gas velocity and $\Delta P/\Delta l$ the pressure gradient over the sample length. The uncertainty in pressure is $u(P_i) = \pm 5$ Pa and for the gas velocity $u(v) = \pm 0.02$ m/s.

Test No.	$P_2 \pm 5$ (Pa)	$P_2 \pm 5$ (Pa)	$P_3 \pm 5$ (Pa)	$P_4 \pm 5$ (Pa)	$P_5 \pm 5$ (Pa)	$v \pm 0.02$ (m/s)	$\Delta P/\Delta l$ (Pa/m)
1	20	25	14	7	4	0.08	28 ± 19
2	40	42	27	13	6	0.12	49 ± 21
3	60	60	41	22	8	0.14	69 ± 20
4	80	77	54	28	10	0.17	90 ± 22
5	100	95	67	35	12	0.21	111 ± 22
6	120	113	80	43	14	0.25	132 ± 23
7	300	268	199	107	32	0.38	314 ± 26
8	415	368	276	149	45	0.48	431 ± 27
9	500	438	331	180	53	0.50	513 ± 28
10	510	448	336	181	55	0.50	524 ± 28

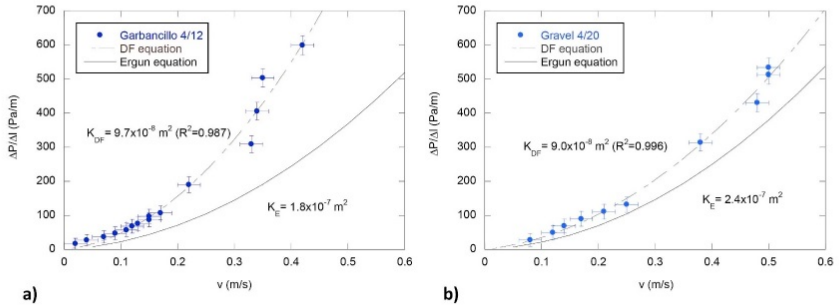

Fig. 4. Pressure difference over length versus gas velocity for a) sample A: garbancillo 4/12 and b) sample B: gravel 4/20.

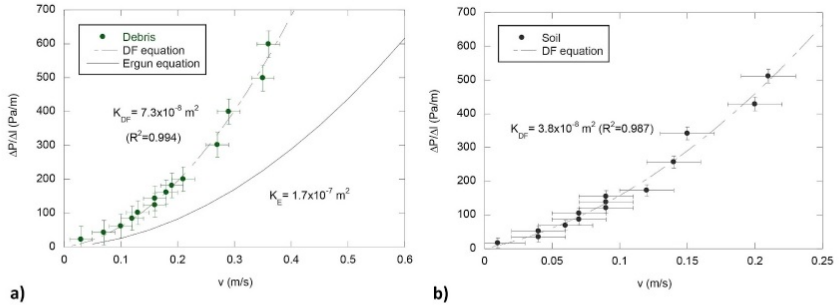

Fig. 5. Pressure difference over length versus gas velocity for a) sample C: debris and b) sample D: soil.

Table 2
Summary of gas permeability values obtained for the samples under study with Darcy's law equation (4), Darcy-Forchheimer equation (7) and Ergun equation (9).

Sample	K_D (m^2)	K_{DF} (m^2)	K_E (m^2)
A: Garbancillo 4/12	$(2.5 \pm 0.8) \times 10^{-8}$	$(9.7 \pm 6.3) \times 10^{-8}$	$(1.8 \pm 0.2) \times 10^{-7}$
B: Gravel 4/20	$(3.1 \pm 1.1) \times 10^{-8}$	$(9.0 \pm 3.5) \times 10^{-8}$	$(2.4 \pm 0.3) \times 10^{-7}$
C: Debris	$(2.0 \pm 0.6) \times 10^{-8}$	$(7.3 \pm 2.6) \times 10^{-8}$	$(1.7 \pm 0.2) \times 10^{-7}$
D: Soil	$(1.2 \pm 0.4) \times 10^{-8}$	$(2.1 \pm 0.4) \times 10^{-8}$	–

gas velocity were recorded. Then, pressure gradient over the sample length was calculated.

Fig. 4 shows test results for samples A and B, where pressure gradient over the sample length is plotted against gas velocity along with trend lines. It can be seen that test results are in good agreement with the Darcy-Forchheimer equation (6), inducing a coefficient of determination $R^2 = 0.987$ and 0.996, for samples A and B, respectively. However, there is very poor agreement between the experimental results and Ergun equation (9).

Fig. 5 shows test results for sample C: debris, similar to the previous granular fill material samples A and B, and sample D: soil. It can be noted that the Darcy-Forchheimer trend line for sample C is in good agreement with experimental results, inducing a coefficient of determination $R^2 = 0.994$, while Ergun trend line doesn't match the experimental data. For sample D, only Darcy-Forchheimer trend line is presented as the porosity value to obtain Ergun trend line was not determined experimentally.

Permeability was determined using the different expressions in section 2.1, the obtained gas permeability values for all samples tested are summarised in Table 2. For each test number of every sample, a value of Darcy's permeability is determined according to equation (4). Then, average Darcy's permeability is obtained and presented in Table 2 for each sample. Darcy-Forchheimer permeability is obtained from the quadratic trend line that fits the experimental data in Figs. 4 and 5, by comparing fitted parameters with equation (6). Ergun permeability is calculated from equation (9), once porosity and effective particle size of the sample are known.

Darcy's permeability values indicate that all samples present a similar gas permeability. From Darcy-Forchheimer permeability values, gravel samples A, B and sample C present a similar permeability in the order of magnitude of 10^{-8} m^2. The Ergun permeability obtained for samples A, B and C is similar in all three cases. However, the order of magnitude found for Ergun permeability is 10^{-7} m^2.

In the case of the soil sample, the Darcy-Forchheimer permeability

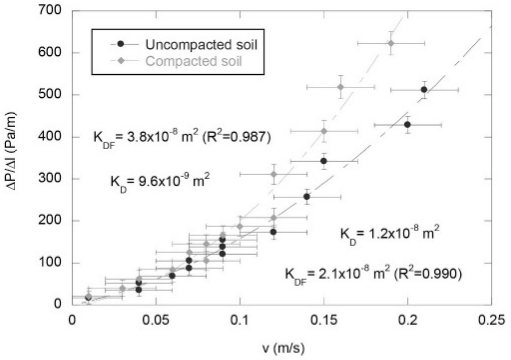

Fig. 6. Pressure difference over length versus gas velocity for sample D: soil, uncompacted and under manual compaction. Dots represent experimental data and the dashed line is the Darcy-Forchheimer equation trendline.

value is approximately 4 times lower than for the granular fill materials, but still is in the same order of magnitude. Soil permeability values reported in other publications are in the range of 10^{-15} to 10^{-9} m^2 (Nielson et al., 1994). A possible explanation for this result is that the sample was taken and then placed in the experimental device, modifying the natural conditions in which is encountered when tested under other type soil permeability tests performed in situ. Sample D was tested again under manual compaction to reproduce field conditions of the soil. Results for this experimental tests are presented in Fig. 6, where the permeability value obtained for the compacted soil sample following Darcy equation (4) was $(9.6 \pm 2.8) \times 10^{-9}$ m^2 and from Darcy-Forchheimer equation (7) it was $(3.8 \pm 2.2) \times 10^{-8}$ m^2.

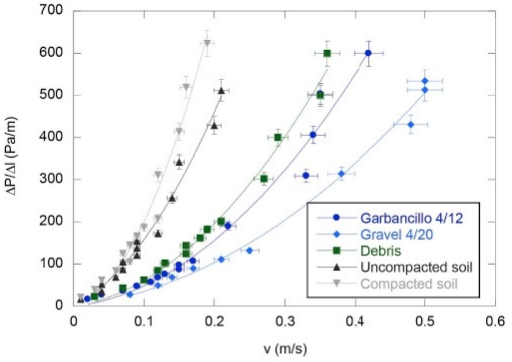

Fig. 7. Comparison of pressure difference over length versus gas velocity experimental results for all samples under study, sample A: garbancillo 4/12, sample B: gravel 4/20, sample C: debris and sample D: soil, tested uncompacted and under manual compaction.

Fig. 6 shows that both the uncompacted and compacted soil samples present very similar permeability, taking into account the uncertainty the data are not significantly different. The value obtained for the Darcy permeability of the compacted soil sample, $9.6 \times 10^{-9}\,m^2$, does reflect a lower permeability than the uncompacted soil and it is more sensible for a soil sample according to the literature (Friske et al., 2010). However, the numerical values for the Darcy-Forchheimer permeability indicate a lower permeability for the uncompacted soil, although considering uncertainty the values for both samples are not significantly different.

Fig. 7 shows experimental results for all samples. It is clear from the figure that the soil sample has lower permeability than the granular fill materials. Within the granular fill materials, it is observed that debris has the lowest permeability, followed by garbancillo 4/12 and then gravel 4/20, which is directly related to the size of the materials and the fact that debris is a well-graded material in contrast with gravel and garbancillo.

3.3. FEM simulations

Simulations were performed using a geometry of the domain based on the test setup, specifying boundary conditions according to Fig. 1. The inlet velocity condition was set at the bottom, the wall condition was defined along the external wall of the apparatus and the outlet pressure condition (0 Pa) was set at the top end. The type of mesh selected was rectangular, with maximum element size of $8.13 \times 10^{-4}\,m$ and minimum element size of $9.37 \times 10^{-6}\,m$.

The physical model implementation for all simulations was the following: laminar flow along porous media domain. Input parameters required for simulations were density and viscosity of the fluid, and the permeability of the sample. Values of the density and viscosity of the gas used for all simulations are $\rho = 1.2\,kg/m^3$ and $\mu = 1.8 \times 10^{-5}\,Pa\,s$.

In the case of the model based on Ergun's equation, the effective particle size and porosity were also required as input parameters. The effective particle diameter was determined from the particle size distribution and the porosity was determined experimentally.

Data from previous works (Gadgil et al., 1991; BRE, 1998) was used to validate numerical simulations (see Fig. 8).

Permeability and Forchheimer factor values used for this purpose are as follows: $k = 1 \times 10^{-7}\,m^2$ and $c = 9.5$ for the ¾" round hardcore sample (Gadgil et al., 1991); $k = 9.9 \times 10^{-8}\,m^2$ and $c = 7.2$ for the 20 mm single sized sample (BRE, 1998).

The results obtained from the simulations are presented in Fig. 9 for the different samples under study. It is observed in all cases that Darcy's simulation only matches experimental data for low gas velocities, and in all cases Darcy-Forchheimer's simulation provides the best match to the experimental data.

Ergun's simulation performed using experimental values of porosity and the effective diameter of the granular particles doesn't match experimental tests, with lower permeability than Darcy-Forchheimer simulation results for all granular fill materials. This finding is in agreement with previous works that state Ergun's equation is not suited for non-uniform particles having non-spherical shape (Olatunde and Fasina, 2018).

3.4. Benchmarking granular fill materials

A benchmark analysis of standard granular fill materials within a European context, looking at works conducted in Spain, Ireland and the UK, is presented below.

Fig. 10 shows the particle size distribution for the granular fill materials tested, together with the grading curves of the Irish standard T1 Struc and T2 Perm granular fill materials published in the work of Hung et al. (2018a) and the grading curves of 20 mm, 40 mm graded and MOT type 1 granular fill materials published in the work of BRE (1998).

It can be seen from Fig. 10 that the particle size distribution of garbancillo 4/12 and gravel 4/20 is similar to Irish T2 Perm and British 20 mm and 40 mm graded materials, all of them classified as poorly-graded materials. Similarly, debris sample size distribution up from

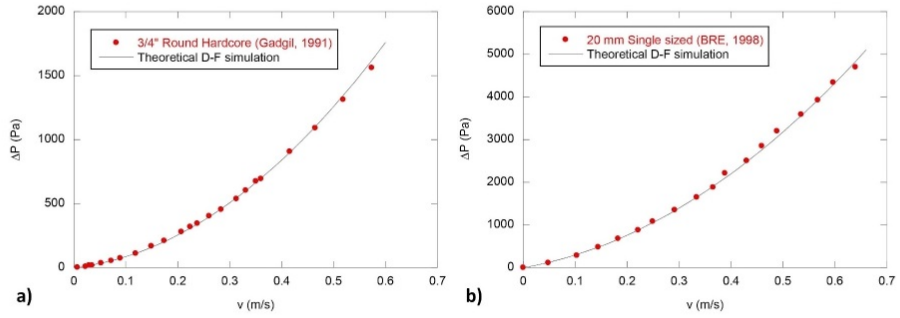

Fig. 8. Experimental data from the literature a) Gadgil et al. (1991), b) BRE (1998) and simulations.

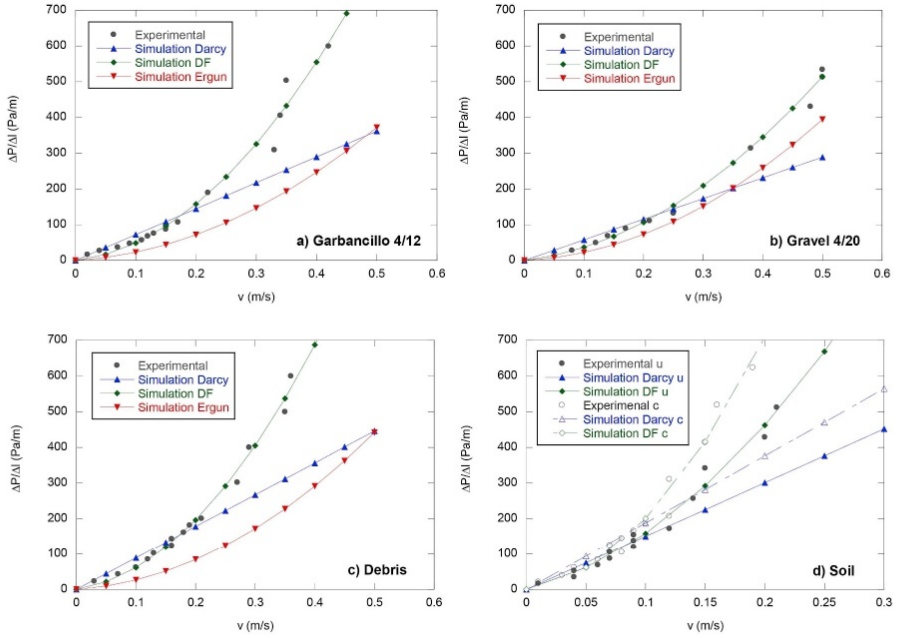

Fig. 9. Comparison of FEM simulations and experimental results for all samples under study, a) sample A: garbancillo 4/12, b) sample B: gravel 4/20, c) sample C: debris and d) sample D: soil (u and c in the legend indicate uncompacted and compacted, respectively).

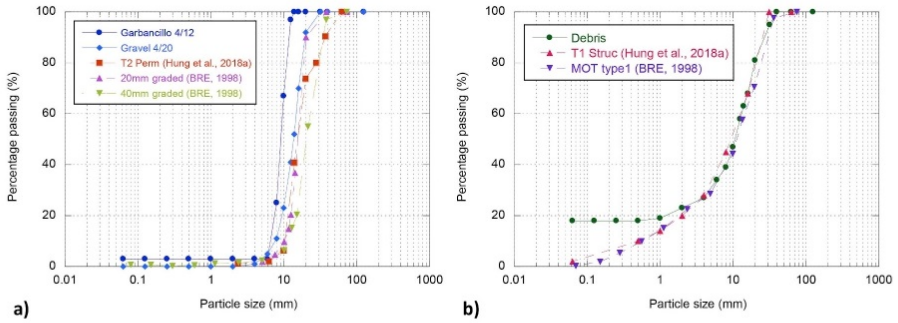

Fig. 10. Particle size distribution of a) poorly-graded and b) well-graded granular fill materials under study (samples A: garbancillo 4/12, B: gravel 4/20 and C: debris), and Irish (T1 Struc and T2 Perm) and British standard granular fill materials, taken from Hung et al. (2018a) and BRE (1998).

1 mm is very similar to T1 Struc and MOT type 1 granular fill materials, both well-graded materials. Therefore, characterisation of the materials presented in this paper could apply to different standards within a European context, based on the tested Spanish materials and comparison with Irish and British granular fill materials.

Comparison of results from permeability tests is presented in Fig. 11 for the samples tested in this study and the British standards (i.e., 20 mm graded, 40 mm graded and MOT type 1). Irish standard (i.e. T1 Struc and T2 Perm) cannot be presented here, as there is only gas permeability tests under compaction reported.

From Fig. 11 a) it can be noted that the poorly-graded granular fill materials analysed present very similar trends, which indicate similar gas permeability values of approximately 9×10^{-8} m^2. Assuming here that the Irish T2 Perm standard would present similar results, and with the knowledge from Hung et al. (2018b), these materials would be suitable to be part of the permeable layer in radon soil depressurisation systems.

However, by looking at Fig. 11 b), debris and MOT type1 material present trends very unalike; results for soil sample are also presented for comparison. The material MOT type 1 present a higher slope than

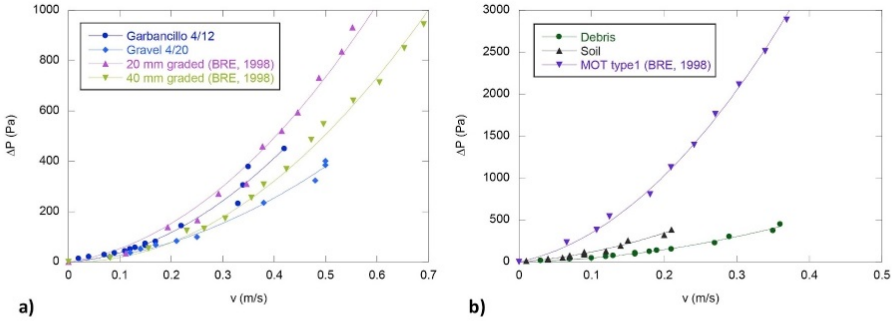

Fig. 11. Comparison of pressure difference versus gas velocity experimental results for samples under study (samples A: garbancillo 4/12, B: gravel 4/20, C: debris and D: soil) with British standards, taken from BRE (1998). a) Poorly-graded materials grouped together and b) well-graded materials.

the soil sample tested in the current study, which means that it presents a significantly lower gas permeability.

4. Conclusions

This paper presents permeability characterisation of different types of granular fill materials through the development of a test apparatus based on the work of Hung et al. (2018a), also based on the operating principle from the standard ASTM-D6539 (2013) and previous works of Gadgil et al. (1991) and BRE (1998).

This test is motivated by the need to establish a standard method for the gas permeability measurement in granular fill materials and soils, given their critical role in radon mitigation in buildings. Characterisation of different granular fill materials is of interest, as well, in order to have a collection of different material characteristics related to the installation of effective soil depressurisation systems for radon mitigation. The method proposed here ensures that reliable and numerically validated results are obtained. Also, through the use of simulations, the behaviour of the material can be extrapolated for higher velocities which can't be easily performed in the laboratory.

From the experimental results, granular fill materials present pressure gradient against gas velocity curves with lower slope, which indicates higher permeability than for the soil sample. Among the granular fill materials tested, a clear relationship between permeability values and the size of the materials is found.

The use of the Darcy-Forchheimer's equation in the numerical simulations provides the best match to the experimental results. In all cases it is observed that Darcy's simulation only matches experimental data for low gas velocities (< 0.1 m/s). For these ranges, experimental data present a linear trend and Darcy's law is correct. But, for higher gas flow velocities Darcy's law shouldn't be used when trying to simulate radon gas behaviour through a porous medium.

Ergun's equation doesn't provide a good fit for experimental results using porosity and effective diameter of granular fill materials as input parameters for the model. A possible explanation for this can be related to the sensitivity when obtaining the porosity values for the samples experimentally, as it is a key parameter on Ergun's equation.

Overall, this work gives an insight into the characterisation of granular fill materials' permeability, which can have applications within the European context. It contributes to the understanding of the specification for soil depressurisation systems performance, in line with the implementation of the 2013/59/EURATOM Basic Safety Standards (BSS) Directive on promoting national action plans for reduction of radon concentration in dwellings with concentrations over the reference level.

Acknowledgements

This research was supported by the OPTI-SDS project, funded by the Irish Environmental Protection Agency [project code 2015-HW-MS-5], and the Spanish National Research Council [BIA2014-58887-R]. The work was performed in the Eduardo Torroja Institute for Construction Science (IETCC), Spain in collaboration with National University of Ireland, Galway.

References

ASTM-D2487, 2017. Standard Practice for Classification of Soils for Engineering Purposes (Unified Soil Classification System). ASTM International, United States.
ASTM-D6539, 2013. Standard Test Method for Measurement of the Permeability of Unsaturated Porous Materials by Flowing Air. ASTM International, United States.
Bonnefous, Y.C., Gadgil, A.J., Fisk, W.J., Prill, R.J., Nematollahi, A.R., 1992. Field study and numerical simulation of subslab ventilation systems. Environ. Sci. Technol. 26 (9), 1752–1759.
BRE, 1998. Modeling and Measurement of Soil Gas Flow. BRE Report IHS BRE Press, United Kingdom, pp. 274.
Castelluccio, M., De Simone, G., Lucchetti, C., Moroni, M., Salvati, F., Tuccimei, P., 2015. A new technique to measure in situ soil gas permeability. J. Geochem. Explor. 148, 56–59.
COMSOL Multiphysics, 2017. Introduction to COMSOL Multiphysics. Version: COMSOL 5.3. COMSOL Ltd.
Council of the European Union, 2014. Council Directive 2013/59/EURATOM, European basic safety standards (BSS) for protection against ionising radiation. Official Journal of the European Union L 13, 17 January 2014, Brussels, ISSN 1977-0677.
Department of the Environment and Local Government (DELG), 2002. Technical Report: *Radon in Existing Buildings. Corrective Options*. Stationery Office, Dublin.
Diallo, T.M.O., Collignan, B., Allar, F., 2015. Air flow models for sub-slab depressurisation Systems design. Build. Environ. 87, 327–341.
Ergun, s., 1952. Fluid flow through packed columns. Chem. Eng. Pro. 48 (2), 89–94.
Forchheimer, P., 1901. Wasserbewegung durch Boden, 45th Edition. Zeitschrift des Vereins deutscher Ingenieure, Düsseldorf.
Friske, P.W.B., Ford, K.L., Kettles, I.M., McCurdy, M.W., McNeil, R.J., Harvey, B.A., 2010. North American Soil Geochemical Landscapes Project: Canadian Field Protocols for Collecting Mineral Soils and Measuring Soil Gas Radon and Natural Radioactivity. Geological Survey of Canada Open File 6282. https://doi.org/10.4095/261633.
Frutos, B., Olaya, M., Santiago, L., Poncela, Q., Sainz, C., 2011. Experimental study of effectiveness of four radon mitigation solutions, based on underground depressurization, tested in prototype housing built in a high radon area in Spain. J. Environ. Radioact. 102 (4), 378–385. https://doi.org/10.1016/j.jenvrad.2011.02.006.
Gadgil, A.J., Bonnefous, Y.C., Fisk, W.J., Prill, R.J., Nematollahi, A., 1991. Influence of Sub-slab Aggregate Permeability on SSV Performance. Lawrence Berkeley Laboratory Report: LBL-31160.
Hung, L.C., Goggins, J., Fuente, M., Foley, M., 2018a. Characterisation of specified granular fill material for radon mitigation by soil depressurisation systems. Constr. Build. Mater. 176, 213–227.
Hung, L.C., Goggins, J., Fuente, M., Foley, M., 2018b. Investigation of sub-slab pressure field extension in specified granular fill materials incorporating a sump-based soil depressurisation system for radon mitigation. Sci. Total Environ. 637–638, 1081–1097.
Jiranek, M., Svoboda, Z., 2007. Numerical modelling as a tool for optimisation of sub-slab depressurisation system design. Build. Environ. 42, 1994–2003.
Jiranek, M., 2014. Sub-slab depressurisation systems used in the Czech Republic and

verification of their efficiency. Radiat. Protect. Dosim. 162 (1–2), 64–67.
Lambe, W.T., Whitman, R.V., 1969. Soil Mechanics. John Wiley & Sons, New York.
Long, S., Fenton, D., Cremin, M., Morgan, A., 2013. The effectiveness of radon preventive and remedial measures in Irish homes. J. Radiol. Prot. 33, 141–149.
Muñoz, E., Frutos, B., Olaya, M., Sanchez, J., 2017. A finite element model development for simulation of the impact of slab thickness, joints, and membranes on indoor radon concentration. J. Environ. Radioact. 177, 280–289.
Nielson, K.K., Rogers, V.C., Rogers, V., Holt, R.B., 1994. The RAETRAD model of radon generation and transport from soils into slab-on-grade houses. Health Phys. 67 (4), 363–377.
Olatunde, G., Fasina, O., 2018. Modified Ergun equation for airflow through packed bed of loblolly pine grinds. KONA Powder Part. J. https://doi.org/10.14356/kona.2019003.
Scheidegger, A.E., 1958. The physics of flow through porous media. Soil Sci. 86, 355.
UNE-EN 933-1, 2012. Tests for Geometrical Properties of Aggregates - Part 1: Determination of Particle Size Distribution - Sieving Method. AENOR, Spain 2012.
World Health Organization, 2009. Handbook on Indoor Radon. A Public Health Perspective. WHO Press, Geneva, Switzerland.

Chapter 4

Conference paper

Radon mitigation in Spanish pilot house: results overview and measurement plan

CERI 2018 Conference Proceedings, pg. 518-522 (2018)
Fuente, M., Hung, L.C., Goggins, J., Foley, M.

Soil depressurisation technique is proven to be the most effective solution for radon prevention and mitigation, as discussed in the introduction Chapter (see section 1.2.2). To investigate ability and efficiency of soil depressurisation for radon reduction, a long-term experiment in a real building constructed for experimental purposes and provided with SDS was formulated.

The experimental building selected to conduct such experiment, referred to as the pilot house, was accessible thanks to collaboration with University of Cantabria. The pilot house was originally built in a high radon area in Spain, to study radon reduction achieved by different radon protective solutions. Description of the facilities was introduced along with the findings from the initial investigation conducted at the experimental house.

Conception of the long-term study, preliminary tests performed at the house and the derived measurement plan designed, considering the experimental set up required to continuous monitor different variables of interest, are outlined.

An overview of the results from the initial radon mitigation study in the pilot house and the monitoring plan intended to investigate the optimum specification for SDS were gathered in a conference paper and published in the proceedings of the Civil Engineering Research in Ireland Conference 2018.

Author's contributions

Marta Fuente reviewed the initial investigation conducted at the pilot house. The measurement plan was formulated by Marta Fuente, Mark Foley and Jamie Goggins in collaboration with the colleagues from the radon group at University of Cantabria, Spain. Preliminary tests were performed by Marta Fuente and Le Chi Hung with the help from the technical staff of the radon group. Marta Fuente wrote the conference paper and all authors read and approved the final version.

Radon mitigation in Spanish pilot house: results overview and measurement plan

Marta Fuente[1, 2], Le Chi Hung[1, 2], Jamie Goggins[2, 3, 4], Mark Foley[1]

[1]School of Physics, National University of Ireland Galway, Ireland
[2]Department of Civil Engineering, College of Engineering & Informatics, National University of Ireland Galway, Ireland
[3]Ryan Institute, National University of Ireland Galway, Galway, Ireland
[4]Centre for Marine and Renewable Energy (MaREI), Galway, Ireland
email: m.fuentelastra1@nuigalway.ie, chihung.le@nuigalway.ie, jamie.goggins@nuigalway.ie, mark.foley@nuigalway.ie

ABSTRACT: Reduction of the indoor radon concentration is an important issue for buildings, as radon is a known carcinogen that can cause lung cancer associated with exposure in homes and workplaces. A pilot house was built in Spain in an area with high radon exhalation to test different radon mitigation techniques back in 2006. After an initial study of the radon concentration inside the house, different radon solutions were implemented such as active and passive soil depressurisation systems, pressurisation, under floor ventilation and radon barriers. An overview of the results from the initial investigation is presented along with on-going research. Pressure field extension under the slab, radon concentration and some atmospheric parameters are being monitored while the soil depressurisation system is in operation under different conditions, in order to assess effectiveness of the soil depressurisation system in relation to building materials impact on the sub slab area.

KEY WORDS: Radon; Mitigation; Soil Depressurisation System.

1 INTRODUCTION

Radon-222 is a radioactive noble gas generated as a decay product of Radium-226 which belongs to the Uranium-238 decay series, the most common natural isotope of uranium, present in all rocks and soils of the Earth's crust in varying amounts. Radon is colourless, odourless and tasteless and has a half-life of approximately 3.8 days. Due to its noble gas character, its behaviour is determined by physical processes instead of chemical interactions. This property, along with its half-life and its gaseous nature, make radon highly mobile and thus it can be released from rocks or soils and move short distances from its origin, therefore being exhaled into the atmosphere [1].

In the outdoor environment radon gas is diluted in the atmospheric air and dispersed. However, if radon gas enters the air space of a building it can be accumulated causing elevated indoor radon concentration, which can result in high radioactive dose when inhaled. As inhaling radon has been shown to cause lung cancer through the decay of its short lived alpha decay products, which induce pulmonary cell DNA damage, reduction of the indoor radon concentration is an important issue for buildings [2].

Pressure driven airflow is considered the dominant mechanism of radon transport from the ground into the indoor air, but also it is generally accepted that a very small percentage of the indoor radon concentration is due to building materials. Pressure gradients created either by thermal differences, wind or mechanical systems cause the soil air to flow into buildings through cracks, holes and other leakage routes existing in the foundation structures [3][4][5].

Ingress of radon from the soil is affected by different factors such us the ground potential, influenced by air permeability, porosity and moisture content of the soil, the characteristics of the building (e.g. the infiltration features in the foundation and wall below the ground level) and the ventilation, related to meteorological conditions and behaviour of occupants [6]. Also, as radon comes from the ground and is a heavier gas than air, it is not normally a problem in the upper stories or high rise buildings.

There are different radon prevention and mitigation techniques, aimed at either preventing radon entry or removing it after. Radon protection strategies include reduction of radon entry by sealing of surfaces, installation of barriers or membranes, soil depressurisation systems (active and passive), pressurisation and ventilation of spaces to dilute indoor radon concentration with external air [2][7].

Sealing soil gas routes is the first approach in order to avoid radon infiltration, but it may be very demanding as radon can enter through cracks and openings that are too small to locate and effectively close off. Radon barrier systems involve placing a membrane of a special radon proof material over the ground that is in contact with the soil under the occupied space of the building, taking special care at joints and leakage points during the installation [8]. Soil depressurisation systems (SDS) reverse the normal flow of soil gas by means of a fan (active) or a cowl (passive) and piping which draw air out from a suction point under the slab. The withdrawal of air causes the sub slab area to be at lower pressure than the air in the building and this prevents the soil gas entry. An alternative approach to a soil depressurisation system is to use a fan system to provide positive pressure throughout the building and in that way reverse the normal inflow of soil gas from under the floor. Thus, radon is forced through other paths to reach the surface far from the building [2][7]. Ventilation gradually replaces the internal air with air from outside and it is the simplest method to reduce relatively low levels of radon concentration.

Among the existing radon prevention and mitigation techniques, some studies have proven that soil depressurisation is the most effective measure to reduce air radon levels and prevent radon entry into houses [3][4][9]. The effectiveness of SDS is influenced by several different variables such as the air permeability of the granular fill material in the sub slab area

and the native soil surrounding the foundation, the suction point size, which is normally a sump, moisture content, fan speed (active SDS) and atmospheric conditions [10][11][12][13][14].

To study different radon mitigation techniques back in 2006, a prototype house was built in Spain in an area with high radon exhalation [15]. Currently, new investigations are conducted at this pilot house, focused on SDS performance to mitigate radon. The present paper presents an overview of the results from the initial investigation carried out at the pilot house by B. Frutos and collaborators from University of Cantabria, and the on-going research.

2 PILOT HOUSE

2.1 Location, design and construction

An area with high radon concentration in the soil, so as to perform accurate tests on mitigation solutions, was selected to build the experimental dwelling. The site chosen is located within the land of the Saelices el Chico former uranium mine, in the province of Salamanca (Spain), nowadays under reclamation activities to monitor and control the dismantled radioactive facilities, managed by ENUSA Industrias Avanzadas S.A. [16].

A radiological characterisation of the on-site soil was carried out prior to the construction works, resulting in 1012 Bq/kg average ^{226}Ra concentration activity of the soil, which significantly exceeds the normal range (around 50 Bq/kg), and an average radon gas concentration of 250 kBq/m^3 at 1 m depth [17]. Air permeability of the native soil surrounding the house was also measured on-site recently, estimated in the order of magnitude of 10^{-11} m^2.

The prototype home was designed to reproduce a typical Spanish single family house. It consists of two storeys: a ground storey at grade level and a basement below grade with an area of 5 x 5 m^2. There is a single access door and two windows placed on opposite walls at the ground level storey. The floor area (25 m^2) is not representative of a real home, but it is sufficient to study radon behaviour in a large room (see Figure 1) [18].

The house was built using materials and methods that follow Spanish standard construction practices. The basement walls were built with 25 cm clay brick and the floor consisted of a 10 cm thick concrete slab over a 15 cm granular fill material layer. Initially, foundation was not properly sealed in order to get the worst radon conditions inside [17].

Figure 1. Picture of the Spanish pilot house.

2.2 Mitigation solutions

After construction, the house remained closed for a period of three months to allow radon gas concentration increase inside in absence of mitigation solutions, in order to establish initial indoor radon reference levels.

Following the initial study of the radon concentration inside the pilot house, soil gas routes were sealed and different mitigation solutions were implemented: active and passive SDS, positive pressurisation, under floor ventilation and a radon barrier.

SDS were put into practice by installing two underground sumps, one underneath the basement floor slab and another outside the foundation wall, each one fitted with an evacuation pipe running to above roof level, see Figure 2. Both sumps are 1 m^2 and their walls were built with conventional perforated brick, for the piping work standard 110 mm PVC pipes were used [18].

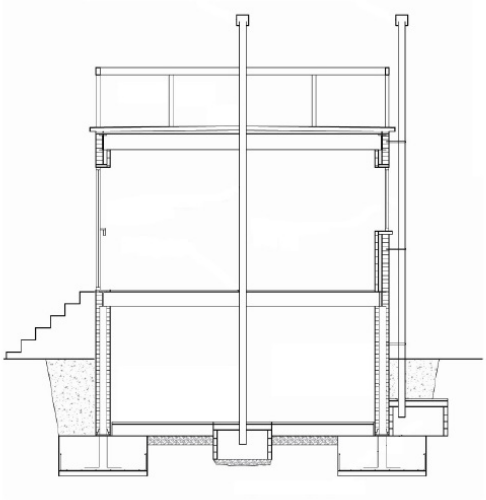

Figure 2. Cross-section along centreline of the pilot house. Modified from [18].

Central and side sumps for the SDS were tested independently from each other, to study the effectiveness in relation to the area of influence. Tests were performed under active and passive operation. A mechanical fan was employed for the active SDS operation and for the passive natural extraction, a wind force based rotating cowl was set on top of the exhaust pipe.

Mitigation by positive pressurisation was studied using the facility of the SDS system through the central sump and pipework, by setting the mechanical fan on reverse flow mode.

Under floor ventilation solution was tested using the basement as a crawl space, therefore the extractor fan was installed in one of the basement walls to force air ventilation inside the basement through an opening placed in the opposite wall.

Finally, to test a radon barrier system, a membrane was installed using an elastomer liquid system. It was placed in the basement's floor and walls in contact with soil [15]. Sometime after testing, it was completely removed from the house.

3 RESULTS' OVERVIEW OF THE INITIAL INVESTIGATION

As mentioned above, for the first three months after the pilot house was built, it remained closed building up the radon concentration. As a result, reference radon levels for the basement and the ground floor under no mitigation were stablished as 39385 Bq/m^3 and 6855 Bq/m^3 respectively [15].

Mitigation by soil depressurisation was the first radon solution tested. Central and side underground sumps were tested individually, while the central sump SDS was in operation, the side sump and pipe stayed closed and sealed, and vice versa. Active soil depressurisation was tested with an 80 Watt electric fan, able to develop a maximum suction pressure of -280 Pa [15]. For the operation of the passive SDS, a rotating cowl was used, developing suction pressures derived from the wind speed.

Results for the SDS tests are summarised in

Table 1. SDS effectiveness summary, #1 refers to the central sump and #2 to the side sump, modified from [19].

. Reduction percentage is obtained from the radon concentration, C_{Rn}, compared to the initial reference values.

Table 1. SDS effectiveness summary, #1 refers to the central sump and #2 to the side sump, modified from [19].

		C_{Rn} (Bq/m^3)		Reduction (%)	
		Basement	*Ground floor*	*Basement*	*Ground floor*
Active	#1	349	479	99	93
	#2	327	480	99	93
Passive	#1	1742	603	96	91
	#2	16607	3213	58	53

The same 80 Watt extractor fan was used in the central sump to test positive pressurisation mitigation solution by reversing the flow. Meanwhile, the side sump and pipe stayed closed and sealed.

Under floor ventilation solution was implemented by placing the mechanical fan in one of the basement's walls while another opening was installed in the opposite wall to allow circulation of air from outside. Both pipes connected to the sumps were closed and sealed during under floor ventilation testing.

Finally, all pipes and openings were closed and sealed to install and test a radon barrier. A liquid elastomer membrane was applied in three layers in the basements' floor and walls in contact with the soil. Results from these mitigation solutions' are summarised in Table 2.

Table 2. Positive pressurisation, under floor ventilation and radon barrier effectiveness summary, modified from [19].

	C_{Rn} (Bq/m^3)		Reduction (%)	
	Basement	*Ground floor*	*Basement*	*Ground floor*
Pressurisation	271	388	99	94
Under floor ventilation	10072	307	74	96
Radon barrier	1446	434	96	94

Overall, by looking at the results from Table 1 and Table 2, most of the mitigation solutions tested were effective, exceeding 90% radon reduction in 5 out of 7 of the solutions tested. The active depressurisation and the positive pressurisation were the most effective radon mitigation solutions and the least effective solution was the passive depressurisation through the side sump.

From Table 1, a significant difference in the reduction percentage was found in the basement compared to the ground floor, reaching highest radon reductions in the basement. Also, from central (#1) to side (#2) sump tests, there is a remarkable difference for the passive operation of the system.

From Table 2, similar to the results from Table 1, reduction percentages found are higher in the basement, except for underfloor ventilation with the highest reduction in the ground floor.

4 ON-GOING RESEARCH

Within the scope of the on-going research on the optimum specification for soil depressurisation systems related to Irish building practices (OPTI-SDS project), the accessibility to the pilot house is a great opportunity to study SDS effectiveness through collaboration with European partners.

In order to design a measurement plan, preliminary tests were performed at the house in 2017. Radon monitors were set up in the house, one in the basement and another one in the ground floor. Radon levels have been monitored continuously over different periods since then, an example of the radon concentration recorded during months February to April 2018 is shown in Figure 3.

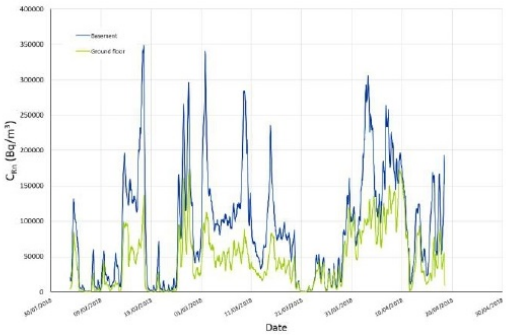

Figure 3. Radon concentration in the pilot house over time from February to April 2018. Dark blue line is for the basement and light green line for the ground floor.

The house remained closed with both pipes sealed building up radon levels for the period shown in Figure 3. Average radon concentration in the basement was found to be 89968 Bq/m^3 and 45073 Bq/m^3 in the ground floor, which are higher values than the reference levels established in the initial investigation.

In November 2017, first initial pressure field extension measurements were carried out under the concrete slab of the pilot house. Different holes drilled through the slab at various distances from the centre were tested in terms of pressure while SDS was in operation. Central and side sumps were studied under active soil depressurisation using a 30 Watt extractor fan [20].

Results from the pressure field extension study under the slab showed a good performance of the central sump SDS. Suction pressure developed under the slab was found to be relatively constant and uniform, causing a homogenous suction pressure in the room when SDS was operated through the central sump and pipe. However, the side sump performance didn't show such a good pressure field extension, since no pressure development was observed under the slab. This phenomenon could be due to the obstruction of the foundation beside the sump, but additional measurements may be required to confirm this result.

The findings of the pressure field extension led to focus the investigation on the central sump for soil depressurisation. The plan proposed consists of continuously monitoring radon concentration and pressure field extension at several different points in the house, while operating SDS under different conditions. Also, it is planned to measure locally different atmospheric parameters that influence both radon entry in the building and the performance of the SDS. A study timeline for the tests proposed is shown in Figure 4.

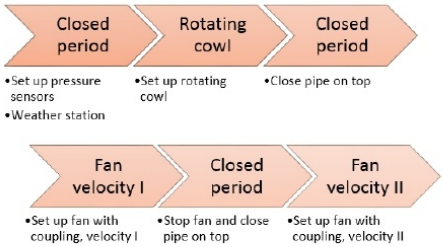

Figure 4. Study timeline for the monitoring plan.

The measurement plan includes long term testing, alternating periods of building up radon concentration in the house and then testing the active and passive performance of the soil depressurisation, controlling the power of the mechanical fan in the active SDS operation.

To monitor the pressure field extension in the pilot house, a pressure sensor system was developed by a group from ITEFI-CSIC (Spain). It is an acquisition system designed with segmented architecture and capacity up to 15 pressure sensors. It consists of an adapter board for pressure sensor units and it contains Honeywell pressure sensors with SPI communication (see Figure 5). The adapter board for units is connected to a PC with an input/output USB card type Lab Jack U3, and all connections between pressure sensor units use Ethernet cables connected in parallel.

The actual system, set up in the house in April 2018, consists of 9 pressure sensor units, distributed along the slab in the basement of the house and in other key points (see Figure 6). There are 5 sensors placed at gravel layer depth under the slab, one in the sump (S06) and another one inside the exhaust pipe (S03). A sensor placed in the soil outside the house at 0.6 m depth (S01) and the last one is placed in the ground floor (S02), connecting both storeys of the house.

Distribution of the sensors across the slab will give an idea of the suction pressure extension in the room area. Sensor S01 placed in the soil is also important to see if the suction pressure is extended beyond the foundation of the house.

Figure 5. Pressure sensor unit (up). Zoom in Honeywell pressure sensor within PSI (down).

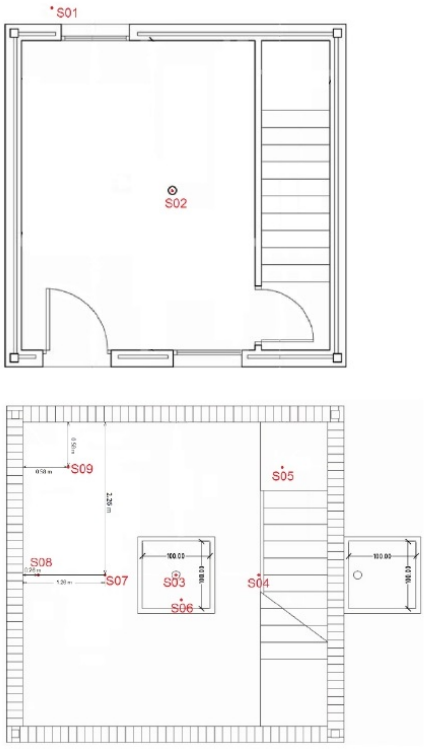

Figure 6. Ground floor and basement plan drawing (cm-unit) with pressure sensor units locations indicated.

To measure atmospheric parameters, a local weather station was installed in the roof of the pilot house (see Figure 7). Among the data recorded by this local weather station, are wind speed and direction, temperature, atmospheric pressure, humidity and precipitation values. Wind variables are the most important to record locally while assessing passive SDS performance.

Apart from the local weather station, there is a professional weather station in the mine site, about 2 km far from the house,

from which data of variables such as temperature, atmospheric pressure or precipitation can be compared.

Figure 7. Picture of the local weather station installed in the roof of the pilot house.

Among the objectives of the monitoring plan, from which data of radon concentration, pressure field extension under the slab and in some other points in the house and atmospheric parameters will be gathered, is to assess the effectiveness of the SDS performance under different conditions. Thus, the reduction percentage obtained in the initial investigation could be compared and contrasted.

Besides, monitoring pressure during the periods while the house stays closed and pipes sealed it is interesting to see the natural pressure distribution under the slab, related to the behaviour of the radon concentration indoors, which is related to the atmospheric conditions as well.

Overall analysis of the pressure field extension data recorded during the different testing periods will give us information on the real distribution of the soil gas and its behaviour. As well, any possible correlation with the atmospheric parameters will be studied.

Computational fluid dynamic simulations are envisaged within the project, to investigate the behaviour of the sub-slab pressure field extension developed by the SDS. Therefore, the data gathered will be also useful to develop a model and validate numerical simulations on the behaviour of the soil gas.

5 CONCLUSIONS

The prototype house under study is a great facility to perform tests on radon mitigation solutions in a controlled environment.

The initial investigation showed that among the different radon mitigation solutions implemented in the pilot house, the most effective radon concentration reduction was found during active soil depressurisation system performance.

On-going tests on the pilot house will give us insight on the pressure distribution under the slab and the behavior of soil gas. The performance of the active and passive soil depressurisation will be assessed by looking at the radon concentration measurements, along with the analysis of the suction pressure extension data from the sump and also taking into account the influence of the atmospheric conditions.

Results from this work can be incorporated into numerical models which will enhance our knowledge of indoor radon dynamics.

ACKNOWLEDGMENTS

This research is a part of the OPTI-SDS project, which is funded by the Irish Environmental Protection Agency through Grant No. 2015-HW-MS5. The authors wish to acknowledge technical staff from Radon Group (University of Cantabria, Spain) and also thank ENUSA Industrias Avanzadas S.A. for their support during test preparation and measurements in the pilot house. Finally, acknowledge IETcc-CSIC research group in Spain for the experimental data.

REFERENCES

[1] Quindos, L.S., Fernandez, P.L. and Soto, J. (1994), 'Radiactividad natural y radón', *Boletín Sociedad Española Hidrológica Médica*, volume IX, 133-137.

[2] World Health Organization, *Handbook on Indoor Radon. A public health perspective*, WHO Press, Geneva, Switzerland, 2009.

[3] Abdelouhab, M., Collignan, B. and Allard, F. (2010), 'Experimental study on passive Soil Depressurisation System to prevent soil gaseous pollutants into building'. *Building and Environment,* 45(11), 2400-2406.

[4] Jelle, B.P. (2012), 'Development of a model for radon concentration in indoor air', *Science of the Total Environment,* 416, 343-350.

[5] Arvela, H. (2001), 'Experiences in radon-safe building in Finland', *The Science of the Total Environment*, 272, 169-174.

[6] Wang, F. and Ward, I.C. (2002), 'Radon entry model for a house with a cellar', *Building and Environment,* 37, 1153-1165.

[7] Department of the Environment and Local Government, Technical report: *Radon in existing buildings. Corrective Options*, Dublin, Ireland, 2008.

[8] United States Environmental Protection Agency, Technical report: *Building Radon Out: A step-by-step guide on how to build radon-resistant homes*, Office of Air and Radiation, USA, 2001.

[9] Jiranek, M. (2014), 'Sub-slab depressurisation systems used in the Czech Republic and verification of their efficiency', *Radiation Protection Dosimetry,* 162(1-2), 64-67.

[10] Hung, L.C., Goggins, J., Fuente, M., Foley, M. (2018), 'Characterisation of specified granular fill materials for radon mitigation by soil depressurisation systems', *Construction and Building Materials*, 176, 213-227.

[11] Robinson, A.L. and Sextro, R.G. (1997), 'Radon entry into buildings driven by atmospheric pressure fluctuations', *Environmental Science & Technology*, 31, 1742-1748.

[12] BRE, BRE report: *Modelling and Measurement of Soil Gas flow,* HIS BRE Press, United Kingdom, 1998.

[13] Jiranek, M. and Svoboda, Z. (2007), 'Numerical modelling as a tool for optimisation of sub-slab depressurisation systems design', *Building and Environment*, 42, 1994-2003.

[14] Diallo, T.M.O., Collignan, B. and Allard, F. (2015), 'Air flow models for sub-slab depressurisation systems design', *Building and Environment*, 87, 327-341.

[15] Frutos, B. (2009), *Estudio experimental sobre la efectividad y la viabilidad de distintas soluciones constructivas para reducir la concentración de gas radón en edificaciones*, PhD Thesis, Universidad Politécnica de Madrid, Spain.

[16] ENUSA Industrias Avanzadas S.A., http://www.enusa.es/en/areas-de-negocio/medioambiental/restauracion-de-antiguas-instalaciones-mineras/ (accessed 10-05-2018)

[17] Frutos, B., Olaya, M and Esteban, J.L. (2011), 'Rehabilitation Measures against radon gas entry', *Revista Ingeniería de Construcción*, 26, 95-121.

[18] Frutos, B., Olaya, M., Quindos, L.S., Sainz, C., Fuente, I. (2011), 'Experimental study of effectiveness of four radon mitigation solutions, based on underground depressurisation, tested in prototype housing built in a high radon area in Spain', *Journal of Environmental Radioactivity*, 102, 378-385.

[19] Frutos, B., Presentation: '*The Spanish experience: Approaches, optimization, and singularities concerning to energy saving*' at International Workshop 'Radon for building professionals', Salamanca, Spain, November 2017.

[20] Hung, L.C., Goggins, J., Fuente, M., Foley, M. (2018), 'Investigation of sub-slab pressure field extension in specified granular fill material incorporating a sump-based soil depressurisation system for radon mitigation', *Science of the Total Environment*, 637-638,1081-1097.

Chapter 5

Paper III

Radon mitigation by soil depressurisation case study: Radon concentration and pressure field extension monitoring in a pilot house in Spain

Science of the Total Environment, 695, 133746 (2019)

Fuente, M., Rábago, D., Goggins, J., Fuente, I., Sainz, C., Foley, M.

As outlined in Chapter 4, a case study to investigate effectiveness of soil depressurisation was conducted in a pilot house in Spain. The purpose was to improve understanding of the factors that influence optimum performance of soil depressurisation systems for radon protection in new and existing buildings, considering that indoor radon reduction is an important public health issue.

A long-term monitoring study was carried out in the pilot house, which has very high radon levels. The monitored variables included radon concentration, several atmospheric parameters and the induced pressure in the aggregate layer under the slab as a consequence of soil depressurisation, measured through holes drilled into the slab of the house. The experiment consisted of different testing phases, alternating active and passive performance of the SDS with periods to foster accumulation of radon indoors in order to evaluate the pressure induced, its distribution and the resulted radon reductions.

The different variables recorded were analysed, indoor radon behaviour in the house was examined and also the influence that atmospheric parameters have on it. The pressure field extension under the slab, correlation of the extraction airflow with the induced depressurisation and radon reductions achieved were analysed and also discussed.

From the analysis of the data recorded, pressure distribution under the slab was found to be quite homogeneous, but it was noted that pressure drop with distance from the suction point is linearly proportional to depressurisation. Permeability characterisation of the pilot house was examined from the analysis of the depressurisation induced as function of the extraction airflow for active SDS operation, the behaviour obtained was similar to previous studies. On the analysis of passive SDS performance using a rotating cowl, a relationship between wind velocity and effective extraction airflow was obtained. Finally, overall radon reductions achieved for all the tested soil depressurisation cases were over 85%.

The findings were submitted to Science of the Total Environment, peer-reviewed and accepted for publication.

Author's contributions

The initial research plan and the conception of the monitoring study were formulated by Marta Fuente, Mark Foley, Jamie Goggins and Carlos Sainz. Marta Fuente, Carlos Sainz, Ismael Fuente and Daniel Rábago evaluated and reviewed the testing plan. The experimental development of the study was conducted by Marta Fuente and Daniel Rábago with the help from the radon group technical staff (Enrique Fernández, Jorge Quindós and Luis Quindós) and the support of ENUSA Industrias Avanzadas S.A. Marta Fuente processed the experimental data, analysed the results with the help from Daniel Rábago, and wrote the manuscript. Mark Foley, Jamie Goggins, Ismael Fuente and Carlos Sainz reviewed and edited the manuscript for the final version. All authors read and approved the final manuscript.

Science of the Total Environment 695 (2019) 133746

Contents lists available at ScienceDirect

Science of the Total Environment

journal homepage: www.elsevier.com/locate/scitotenv

Radon mitigation by soil depressurisation case study: Radon concentration and pressure field extension monitoring in a pilot house in Spain

Marta Fuente [a,b,c], Daniel Rábago [d], Jamie Goggins [b,c], Ismael Fuente [d], Carlos Sainz [d], Mark Foley [a,*]

[a] School of Physics, National University of Ireland Galway, Ireland
[b] Civil Engineering, School of Engineering, National University of Ireland Galway, Ireland
[c] MaREI Centre for Marine, Climate and Energy, Ryan Institute, National University of Ireland Galway, Ireland
[d] Radon Group, University of Cantabria, Spain

HIGHLIGHTS

- Active and passive soil depressurisation (SD) ability was studied in a pilot house.
- Radon concentration and pressure field extension (PFE) under slab were monitored.
- Radon behaviour was analysed under the influence of atmospheric parameters.
- Pressure drop with distance was found proportional to depressurisation under slab.
- Over 85% radon reduction was achieved for active and passive SD.

GRAPHICAL ABSTRACT

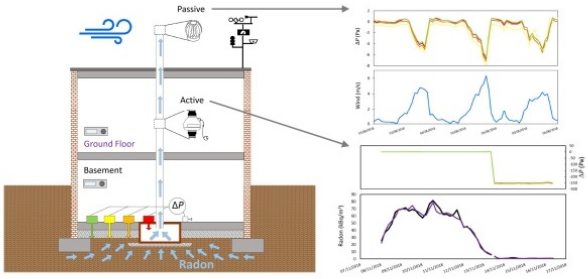

ARTICLE INFO

Article history:
Received 20 May 2019
Received in revised form 14 July 2019
Accepted 1 August 2019
Available online 05 August 2019

Editor: Pavlos Kassomenos

Keywords:
Radon mitigation
Soil depressurisation
Pressure field extension
Permeability

ABSTRACT

A one-year monitoring study was conducted in a pilot house with extremely high radon levels to investigate the ability and efficiency of radon mitigation by soil depressurisation (SD) both active and passive. The study included monitoring of radon concentration, pressure field extension (PFE) under the slab and some atmospheric parameters for different testing phases. Periods in which the house remained closed to foster radon accumulation were alternated with phases of active and passive soil depressurisation under different conditions. The behaviour of the radon concentration in the pilot house was analysed along with the influence of atmospheric variables, significant correlations were found for the radon concentration with atmospheric pressure, outdoor temperature and wind. From the PFE analysis it was proven that the pressure drop with distance from the suction point of the SD system is proportional to the depressurisation generated. A behaviour law was found for the permeability characterisation of the house based on the active SD performance and also, the relationship between wind velocity and extraction airflow during passive SD operation by means of a rotating cowl was obtained. Radon reductions in excess of 85% were achieved for the different testing phases in all cases. Finally, from the results it was

* Corresponding author.
E-mail addresses: m.fuentelastra1@nuigalway.ie (M. Fuente), mark.foley@nuigalway.ie (M. Foley).

https://doi.org/10.1016/j.scitotenv.2019.133746

postulated that a fan power of 20 W is sufficient to ensure radon reductions over 85% for dwellings with similar aggregate layer and soil permeability.

1. Introduction

Radon (^{222}Rn) is a colourless, odourless, radioactive gas formed in the ground by the radioactive decay of uranium (^{238}U), which is present in all rocks and soils of the Earth's crust. With a half-life of 3.8 days together with its noble gas condition, radon can move through interconnected pores in the soil, reach the Earth's surface and penetrate into buildings. Radon is the greatest natural source of exposure to ionising radiation for the general public and it is also the leading cause of lung cancer after smoking, as stated by the World Health Organisation (WHO, 2009). Poor ventilation conditions, gaps or cracks in the construction systems favour the accumulation of radon inside buildings, leading to health risks related to the inhalation of the radon decay products. 9% of deaths from lung cancer per year are attributable to residential radon exposure in the European Union, which accounts for more than 20,000 deaths each year (Darby et al., 2004; WHO, 2018).

There are various prevention and mitigation measures that might be considered to minimise indoor radon concentration, in order to address the radon problem both in new and existing buildings. Radon protection strategies include reduction of radon entry by sealing of surfaces, barriers or membranes, soil depressurisation (SD) techniques to reverse the air pressure differences between the indoor occupied space and the soil underneath the building, and ventilation of spaces to dilute indoor radon concentration with external air (Long et al., 2013; Jiranek, 2014; WHO, 2018).

The active and passive SD techniques have proven to be the most effective strategy for indoor radon prevention and mitigation. SD systems include three basic components: a suction point, ideally located in a continuous and uniform permeable aggregate layer under the slab, an exhaust pipe to extract the soil gas and a means of extraction, which can be a mechanical fan in the case of forced extraction or a chimney or cowl for passive depressurisation using natural extraction and wind effect. The suction point is normally a sump placed under the slab or on a side of the building, connected to a permeable aggregate layer, but perforated pipes beneath the existing floors can be an alternative to sumps. The building characteristics (airtightness of the building, exhaust pipe diameter and height, type of extractor, etc.) have an impact in the SD performance; likewise, it can be affected by the stack effect due to temperature difference, meteorological conditions, ventilation systems and occupancy behaviour (DELG, 2002; Abdelouhab et al., 2010; Long et al., 2013; Diallo et al., 2015).

Previous works discuss the importance of the aggregate layer in the design of SD systems for radon mitigation. The impact of the granular fill materials permeability of such aggregate layer and the soil permeability beneath and surrounding the building on the SD effectiveness has been investigated and permeability characterisation of aggregates within the European context conducted (Hung et al., 2018a, b; Fuente et al., 2019). But there is a lack of evidence in testing efficiency of SD techniques in relation with the pressure distribution in actual buildings with elevated radon concentration where radon reduction can be quantified with confidence.

This paper outlines a case study on radon mitigation by soil depressurisation in an unoccupied real building built for experimental purposes. A one-year monitoring study was conducted in a pilot house with very high radon levels to investigate the ability and efficiency of active and passive SD. The work includes the behaviour analysis of the radon concentration inside the experimental building. Also, it presents the analysis of the SD effectiveness, looking at the pressure distribution induced under the building slab, in relation to the permeability characterisation of the aggregate layer beneath the slab, and the achievable radon reduction in such conditions.

2. Materials and methods

2.1. Pilot house: location and design

The pilot house chosen for the case study is located in Saelices el Chico, Salamanca (Spain) within the land of a former uranium mine managed by the company ENUSA Industrias Avanzadas S.A. (see Fig. 1) now under reclamation activities. The location of the experimental house was selected due to the high radon exhalation rate and the high radium content in the soil of the area, which would provide high radon levels accumulated inside the building. An average radium concentration of 1600 Bq/kg was quantified from different soil samples taken onsite, this value is 40 times in excess of the average worldwide concentration, approximately 40 Bq/kg (Frutos et al., 2011). The experimental house was built in an area where there was no mining activity. In terms of the geology characteristics, the site belongs to the Iberian Massif and the predominant host rocks are schist and quartzite (IGME, 2015).

The experimental house was designed to reproduce a space large enough to be representative of a room in a typical dwelling house. It consists of two storeys, a partially below grade so-called basement of 2 m height and a ground floor (2.41 m height) connected by a standard door. The dimensions of the rooms are 5×5 m^2 (see Fig. 2). There are two windows at the ground floor level, one in the front wall next to the main door and another one in the opposite wall. The front wall of the house is facing the North.

In 2006 when the pilot house was built for a different study, several mitigation measures were investigated (Frutos, 2009). As a result, there are two soil depressurisation systems installed in the house. Both SD systems consist of a 1 m^2 and 0.5 m deep sump and an exhausting pipe of 125 mm diameter, one system is located in the centre of the experimental house with the sump placed in the aggregate layer below the concrete slab and the other system is placed on a side of the house (see Fig. 2).

Materials used for the construction of the house were according the Spanish building practices, a 15 cm thick aggregate layer was placed below a 10 cm thick concrete slab. Standard clay bricks were used for the walls and conventional perforated clay bricks to build the sumps of the SD systems (Frutos et al., 2011).

2.2. Monitoring system

To continuously monitor radon concentration several active radon monitors were used, including the Radon Scout (SARAD GmbH), Radon Scout Home (SARAD GmbH) and AlphaE (Bertin Instruments) detectors. Performance of the radon monitors used in the experiment at the pilot house was tested previously in a purpose-built radon chamber (Fuente et al., 2018). Radon concentration was recorded in the basement and in the ground floor.

For some measurement periods, the radon monitors used were contaminated due to the high radon exposure levels at the pilot house. These monitors were then replaced. There were also some problems due to memory of the devices in some cases, so there is radon data missing for some of the testing phases.

A pressure sensor system was installed to monitor the distribution of pressure under the slab of the house. The pressure system was

Fig. 1. Map of Spain and plan of the mining facilities indicating the location of the pilot house and a recent picture of the building.

specifically developed for this experiment at the pilot house in collaboration with a research group of the ITEFI-CSIC, Madrid (Spain). It is an acquisition system designed with segmented architecture and capacity up to 15 pressure sensors. It consists of an adaptor board for the pressure sensor units and contains a series of Honeywell pressure sensors (HSCDRRD006MDSA3 model, operating pressure $\pm$ 6 mbar, accuracy 0.25%) with SPI communication. The connections between the units use Ethernet cables connected in parallel and the adaptor board needs to be connected to a PC by an input/output USB card type Lab Jack U3. The actual system installed in the house for this experiment consists of a total of 8 pressure sensor units. There are 5 of them distributed along the basement area in different holes drilled through the concrete slab to measure pressure difference in the aggregate layer under the slab and the inhabited volume of the basement, at distances $d = 1, 2$

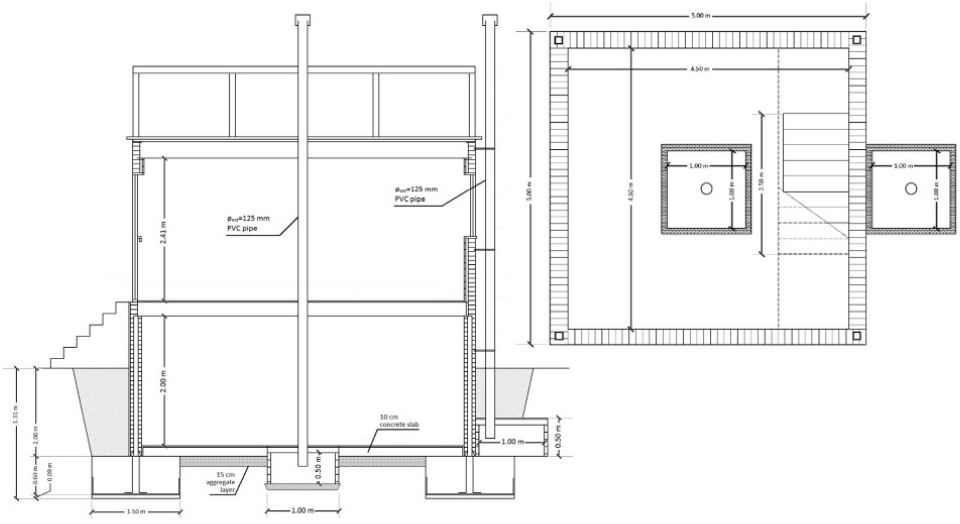

Fig. 2. Section view of the house and plan of the basement after installation of mitigation measures, modified from Frutos et al. (2011).

and 2.4 m from the central sump. The remaining 3 pressure sensors are placed at the sump and pipe of the central SD system and at room level for reference.

To record atmospheric conditions locally at the house site, a local weather station (PCE-FWS20, PCE Instruments) was installed on the rooftop. Variables recorded were wind velocity, indoor and outdoor temperature, atmospheric pressure, relative humidity and accumulated rain. Both the pressure sensor system and the weather station are remotely accessible, which facilitates data collection.

2.3. Experimental methodology

The initial monitoring plan was alternating testing phases of SD performance (active or passive) with periods in which the house remained completely closed, in order to record radon increase and reduction over the different phases along with the pressure field extension induced under the slab, hereinafter referred as PFE.

The monitoring study commenced in June 2018 with a first phase of the house closed to foster accumulation of radon gas. All testing phases with this setting, in which the house remains closed and the pipes of the SD systems capped to foster radon accumulation in the building, will be henceforth referred as closed periods. During the closed periods, there is no ventilation mechanism apart from the natural ventilation due to air leakage of the house and there is no heating mechanism used. After the first closed period (phase 1), a phase 2 involved passive SD performance evaluation. Then a subsequent series of closed periods followed by active SD performance was conducted up to 9 phases, with different active SD settings, ending in April 2019.

Only the central SD system was used for the investigation of the soil depressurisation during the SD testing phases. A rotating cowl was used for the passive SD operation and for the active SD performance, a mechanical fan (RP145i, RadonAway with 80 W max) was installed in the central SD system pipe. The mechanical fan was modified by adding a potentiometer to control the extraction airflow, which in terms of velocity ranges from 0 to 4 m/s. A hot wire anemometer (Testo 440, measuring range 0 to 30 m/s, accuracy $\pm(0.3\ \text{m/s} + 4\%\ \text{of mv})$ and resolution 0.01 m/s) was used to measure extraction velocity of the mechanical fan punctually, to obtain the relationship between the extraction airflow and the mechanical fan power. A schema of the experimental house settings for the different phases is shown in Fig. 3.

The duration of the different phases varied, depending on the access to the site and technical problems experienced with the sensors or the power supply. The monitoring study was stopped at some times and later resumed.

From February 2019, a stage of the monitoring study focused on the investigation of the mechanical fan extraction impact on the SD

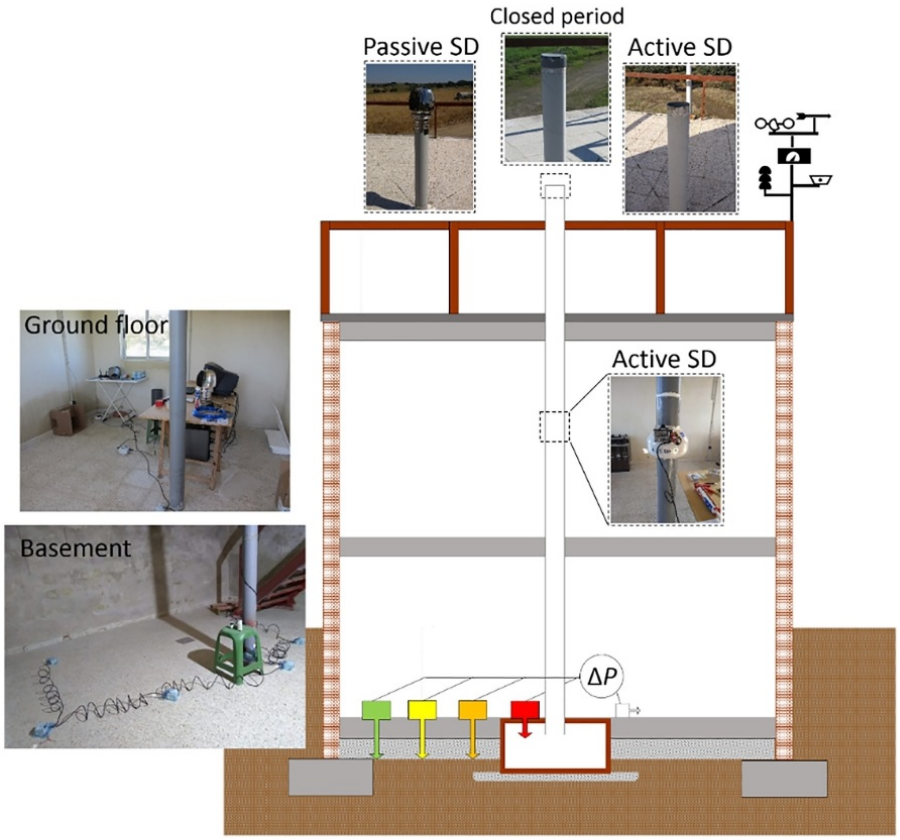

Fig. 3. Schema of the pilot house for the closed periods, active SD and passive SD testing phases. Section view of the experimental house shows the pressure sensors system in the basement (same for all phases), the mechanical fan installed on the central pipe (for the active SD performance) and the top of the exhaust pipe in the house rooftop, with a cap, a rotating cowl or opened, depending on the testing phase.

Table 1
Summary of testing phases at the pilot house.

Phase	Description	Dates
1	Closed period	25/06/2018–26/07/2018
2	Passive SD	26/07/2018–end of August
No measurements (issues related with the pressure sensors)		
3	Closed period	10/10/2018–13/11/2018
4	Active SD (v_{ext} = 0–4 m/s)	13/11/2018–16/11/2018
No measurements (issues related to power supply in the house)		
5	Closed period	13/12/2018–19/02/2019
6	Active SD (v_{ext} = 1.5 m/s)	19/02/2019–06/03/2019
7	Closed period	06/03/2019–14/03/2019
8	Active SD (v_{ext} = 2 m/s)	14/03/2019–02/04/2019
9	Closed period	02/04/2019–30/04/2019

effectiveness was conducted. It consisted of short periods (1–2 weeks) of active SD followed by closed periods, gradually increasing the mechanical fan extraction for the SD performance by controlling the airflow rate.

A summary of the testing phases including dates and incidents are presented in Table 1.

Radon levels were monitored continuously, but also, passive radon detectors were used for some testing periods. However, due to the high radon concentration, the passive track etched detectors were saturated in the most cases.

3. Radon concentration behaviour in the pilot house

There is a long term record of the radon concentration fluctuations in the experimental house measured during the different testing phases. Before looking at the radon reductions generated as a result of the soil depressurisation, it is important to try to understand the natural behaviour of the radon concentration inside the house. To do so, the closed testing periods when there were no mitigation measures in operation and the house remained closed with the exhaust pipes of the SD systems capped are analysed.

Indoor radon levels in the experimental house depend on three features: the radon source, the entry rate and the air exchange between the building and the outdoor air, all of which, in turn, depend on many other variables and especially atmospheric conditions.

The radon source is constituted by the soil beneath and surrounding the house, which contains high radium levels. Therefore, it is expected to find higher radon levels in the basement, which is partially below grade and in direct contact with the soil, than in the ground floor. An overview of the radon levels recorded is presented in Fig. 4.

An average radon concentration of 55 kBq/m^3 is found in the basement for the closed house conditions, while for the ground floor there is an average radon concentration of 26 kBq/m^3 under the same house settings. Both values are obtained from the radon records available during the closed testing periods. The average radon concentration values from the initial study conducted in 2006 are 40 kBq/m^3 for the basement and 7 kBq/m^3 for the ground floor. These values were obtained from a three month measurement period (January–April) in which the experimental house remained closed building up the radon concentration, before the installation of any mitigation measures (Frutos et al., 2011). The difference may be related to the deterioration of the basement slab associated with thermal dilation or other analogous phenomenon, therefore leading to the formation of new cracks or radon pathways. The higher increase of the ground floor radon concentration compared to the basement's with regard to the initial levels by Frutos et al. (2011) could also be due to the fact that the door between floors was not closed during all the testing phases as it was for the initial study.

The concentration ratio between floors found for the closed house testing configuration is approximately two, which means that the concentration recorded in the basement is approximately double the concentration in the ground floor. This result is according to expectation, as the basement is in direct contact with the soil and the main radon gas entry is through gaps or cracks in the foundation, while the radon in the ground floor comes from the radon in the basement. The infiltration through the main door and the windows could be considered as a source of radon gas, but the outdoor air radon concentration at the site is much lower, approximately 300 Bq/m^3. Then, assuming that radon in the ground floor comes only from the basement, the lower radon concentration in the ground floor is explained by the radioactive decay and the exchange of outdoor air through infiltration.

3.1. Radon behaviour and atmospheric parameters

Fluctuations of radon concentration are daily and seasonal, and they are related to atmospheric conditions and the air exchange between the building and the outdoor air. There is also a seasonal component related to the outdoor temperature changes and the associated atmospheric pressure variations that directly affects radon entry in the building (Nero et al., 1990; Scivyer and Jaggs, 1998).

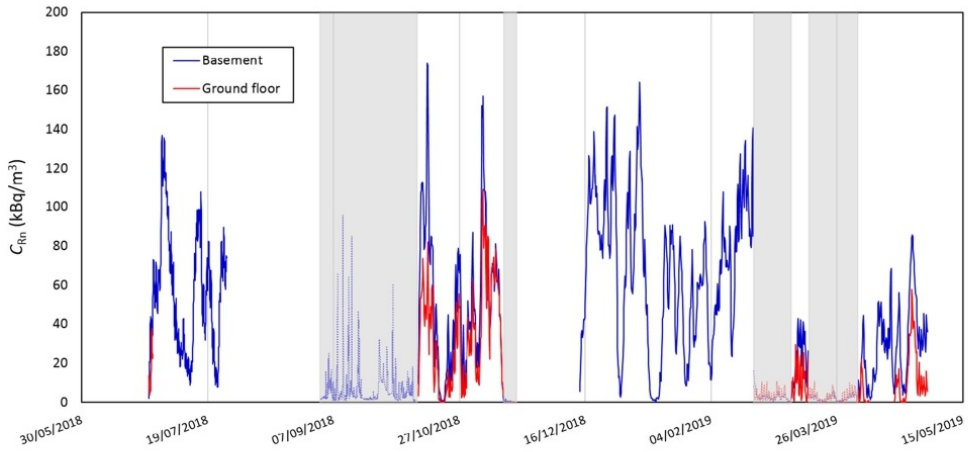

Fig. 4. Radon concentration recorded in the basement and ground floor of the pilot house. The solid line indicates the closed testing periods and the dashed line (shaded areas) indicates the periods of SD performance.

The air exchange rate in the experimental house reaches its minimum value during the closed testing periods as there is no ventilation mechanism, apart from the air leakage through the windows and main door frames. Thus, the radon levels in the house basically depend on the atmospheric conditions, which determine the soil gas pressure-driven flow from the ground into the building.

Multiple atmospheric conditions influence radon concentrations and it is possible to find correlations between the trends in radon concentration and atmospheric variables (Schubert et al., 2018; Garcia-Tobar, 2019). The radon concentration trends as a function of the different atmospheric parameters recorded were analysed for the closed testing periods in the pilot house. Selected measurement periods where statistically significant correlation was found between the radon concentration in the pilot house and a specific atmospheric variable are presented below.

The differences between indoor and outdoor temperature in a building can generate a pressure gradient due to the stack effect, leading to an increase of the soil gas flow from the ground into the basement through the existing entry routes. Pressure gradient due to stack effect is described as follows:

$$\Delta P = c\,P_{\mathrm{atm}} h\left(\frac{1}{T_{\mathrm{out}}} - \frac{1}{T_{\mathrm{in}}}\right) \quad (1)$$

where ΔP is the indoor-outdoor pressure difference, $c = 0.0342$ K/m is a constant, P_{atm} is the atmospheric pressure in Pa, h is the height or distance in m, T_{out} and T_{in} correspond to outdoor and indoor temperature respectively (Frutos, 2009).

Fig. 5 depicts an example of the pressure difference generated as a result of the stack effect in the pilot house along with the radon concentration recorded for a time period when the house was closed. Pressure difference was calculated from the indoor and outdoor temperature records (see Fig. 5) following Eq. (1), using the height of the house $h = 4.7$ m and assuming a constant atmospheric pressure $P_{\mathrm{atm}} = 10^5$ Pa.

From Fig. 5, positive correlation between outdoor temperature and radon concentration is found at a daily scale, agreeing with previous studies (Mentes and Eper-Papao, 2015; Schubert et al., 2018). A Pearson's correlation coefficient of $r = 0.44$ with a 95% confidence level is obtained.

Looking at the pressure difference ΔP result of the stack effect, fluctuations are within the range of −1 to 3 Pa. A Pearson's correlation coefficient of $r = -0.48$ is obtained between radon concentration in the ground floor and the pressure difference ΔP generated due to the indoor temperature at the ground floor and outdoor temperature difference. As the pressure difference increases, radon concentration decreases. The negative pressure difference ΔP means that indoor pressure in the house is lower than the pressure in the soil and thus, the radon in the soil flows into the house, while when ΔP is positive the pressure inside the house is higher and the entry of soil gas is reduced.

The wind effect can generate a pressure gradient too, due to the pressure changes and suction generated in the walls, which can modify the indoor pressure relative to that in the ground. But also, the wind causes the opposite effect as it fosters ventilation through infiltration that lower the radon levels (Burke et al., 2010; Baskaran, 2016). A negative correlation between the radon concentration and the wind was found, as wind velocity increases the radon level decreases as observed in Fig. 6(a). For this case an $r = -0.59$ Pearson's correlation coefficient is obtained with 95% confidence level. This result is also consistent with the literature (Riley et al., 1996; Schubert et al., 2018).

Theoretically, pressure variation inside a dwelling is almost simultaneous with atmospheric pressure changes, but pressure changes in the soil pores beneath the building reach the atmospheric pressure values with a time delay that depends on the soil characteristics (e.g. porosity). Thus, there is a pressure gradient generated between the soil and inside the building that determines the soil gas airflow into the building (Frutos, 2009). If the atmospheric pressure decreases and so it does indoor pressure of the house, indoor pressure in the house is lower than the pressure in the soil beneath, which leads to an increase of the radon flow into the house. From the analysis of the experimental data

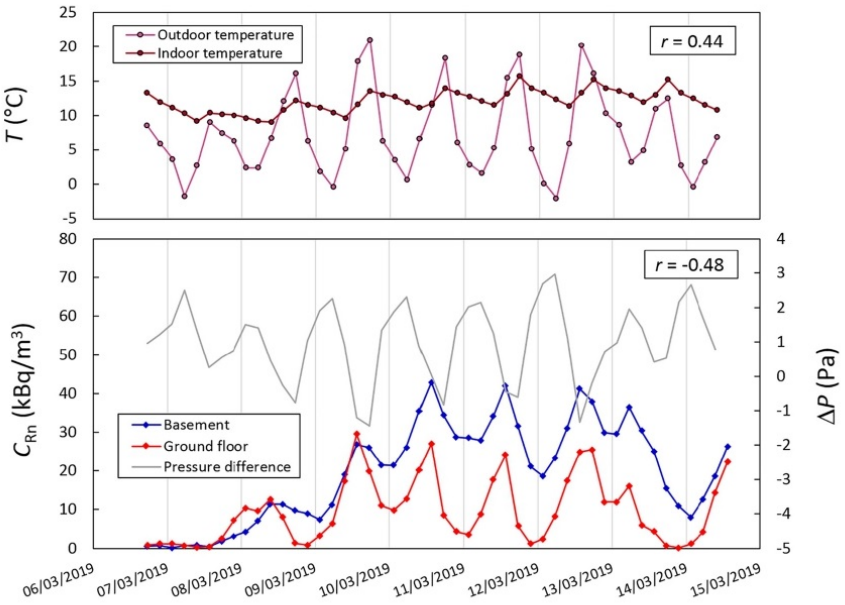

Fig. 5. Radon concentration recorded in the basement and ground floor of the pilot house along with the pressure difference ΔP obtained as a result of the indoor – outdoor temperature for a time period while the house was closed. Pearson's correlation coefficient r between the radon concentration, pressure difference and outdoor temperature are indicated.

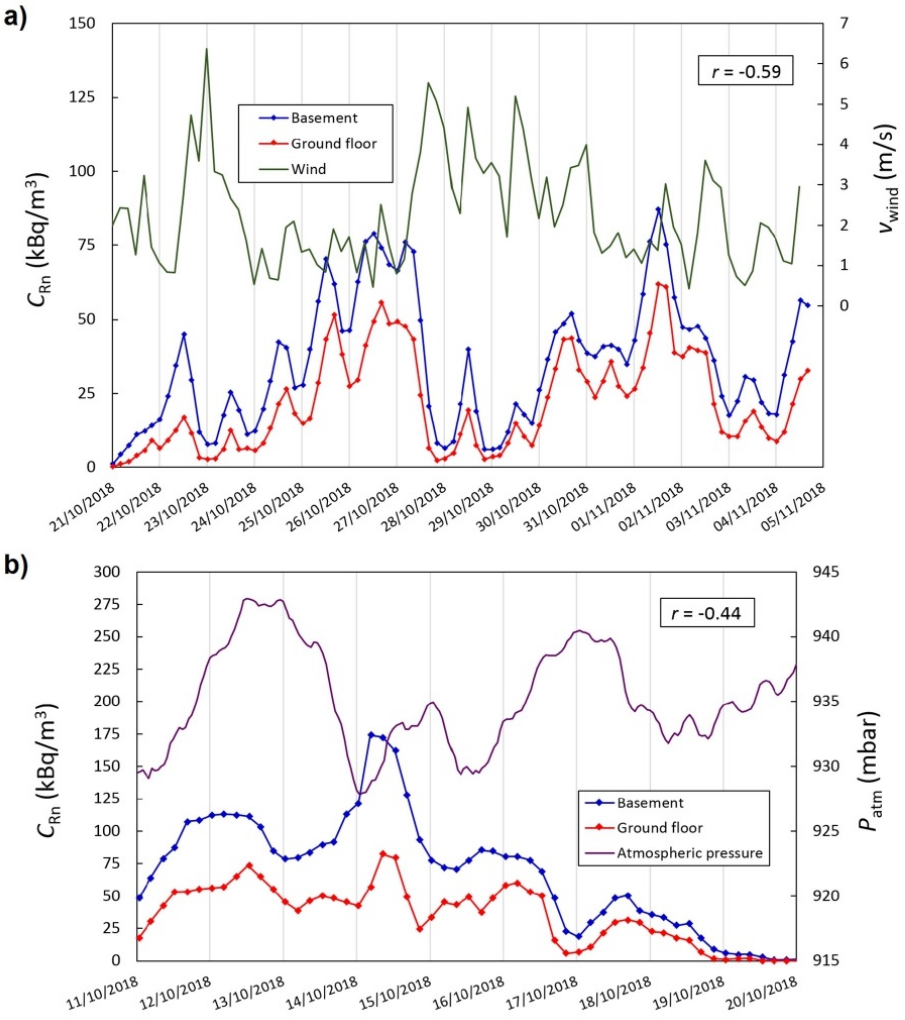

Fig. 6. Radon concentration recorded in the basement and ground floor of the pilot house along with atmospheric variables, a) wind velocity and b) atmospheric pressure, for different time periods while the house was closed. Pearson's correlation coefficient *r* between radon concentration in the basement and the corresponding atmospheric variable is indicated.

recorded, a negative correlation is found between the atmospheric pressure and radon levels, which is consistent with results from other investigations (Mentes and Eper-Papao, 2015). An example of such correlation between radon and atmospheric pressure is presented in Fig. 6(b), where radon concentration decreases with the increase of the atmospheric pressure with a time delay. Pearson's correlation coefficient found for this particular case is $r = -0.44$ with a 95% confidence level. No significant correlation with radon levels was found for the other two atmospheric parameters monitored in the study, relative humidity percentage and accumulated rain.

From the initial study conducted at the pilot house in 2006, the pressure difference created due to indoor-outdoor temperature differences is below 3 Pa, which is small compared to the pressure gradient created by other parameters such as the wind or atmospheric pressure. However, both temperature and wind are usually associated to atmospheric pressure changes, which is the key parameter affecting the radon levels in the pilot house, creating pressure differences in the order of magnitude of a few thousand Pa (Frutos, 2009).

This case study was focused on the impact of the soil depressurisation, so further investigation extended in time would be required to understand the radon behaviour in detail at the pilot house, as a function of all the atmospheric parameters and their time variations.

4. Soil depressurisation effectiveness analysis

The distribution of the pressure induced under the slab as a consequence of the soil depressurisation system performance, correlation between the extraction airflow and the depressurisation, and radon reduction are analysed below.

4.1. Pressure field extension

The pressure distribution under the pilot house was studied for different depressurisation induced at the central sump of the SD system, both by active and passive performance of the system. Prior to the depressurisation analysis, it was found that the pressure difference between the indoor air and the measurement points under the slab fluctuates around 0 Pa for the closed testing periods when there is no SD in operation. During the passive SD testing period, the pressure induced under the slab as a consequence of the wind force reached levels of approximately −20 Pa, for wind velocities up to 8 m/s. For the active SD operation, the pressure induced at the sump was up to −250 Pa for the highest power of the mechanical fan.

The analysis of the pressure data recorded under the slab for the different testing phases at distances $d = 1, 2$ and 2.4 m from the suction point, using the centre of the sump as the reference, leads to obtain the rate of pressure drop with distance across the slab, which is also related to the depressurisation generated (see Fig. 7).

Fig. 7 shows that the pressure drop with distance results are consistent for the measurements recorded at the different distances $d = 1, 2$ and 2.4 m from the suction point. The trend of the pressure drop with distance is linear with the depressurisation under the slab; therefore the lower the pressure induced under the slab, the higher the pressure drop with the distance. However, a quite homogenous PFE, not exceeding 1 Pa/m pressure drop rate was found with distance for the highest depressurisation tested, induced by the highest extraction airflow rate permitted by the fan during the active SD operation.

4.2. Depressurisation induced as function of the extraction airflow

Some results of the pressure induced under the slab as a function of the extraction velocity during the active SD performance are presented in Fig. 8. As mentioned above, the active SD testing depressurisation was generated by means of a mechanical fan and the extraction velocity was measured in the exhaust pipe directly under the extractor fan.

The highest depressurisation recorded under the slab during the active SD operation is approximately −250 Pa, induced by the highest extraction airflow rate of the mechanical fan equivalent to 4 m/s.

Abdelouhab et al. (2010) conducted a study of this kind in France at the MARIA (Mechanized house for Advanced Research on Indoor Air) experimental house, built with a 40 cm thick aggregate layer beneath the slab and two sumps, one centred and another decentred placed on the aggregate layer. They calculated two behaviour laws to relate the extraction airflow Q with the pressure difference induced between the aggregate layer and the inhabited volume ΔP for the natural and mechanical extraction. A similar behaviour law is obtained from the active SD experimental data of the monitoring study at the pilot house, the extraction airflow in this case is obtained from the mechanical fan velocity based on the exhaust pipe diameter (see Fig. 9).

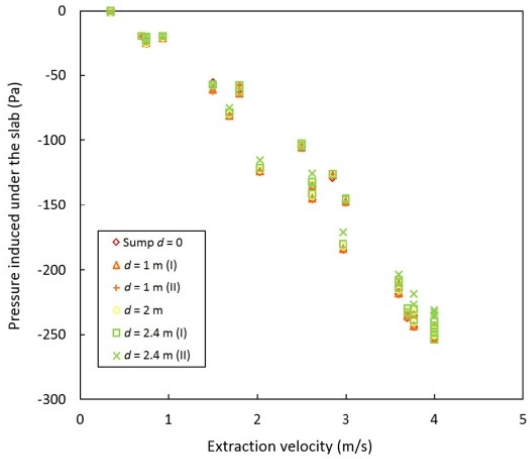

Fig. 8. Pressure induced under the slab during active SD operation against the extraction velocity of the mechanical fan for the different measurement points at different distances from the suction point.

The trendline fitting the experimental data for the active SD performance represents the permeability characterisation of the pilot house comprising the aggregate layer, ground and concrete slab, and is described by the following power law:

$$Q = (2.1 \pm 0.2)\Delta P^{(0.79 \pm 0.02)} \quad (2)$$

Experimental data obtained for the active SD performance in the pilot house are similar to the results for the active depressurisation in Abdelouhab et al. (2010). From Fig. 9 it is observed that the behaviour

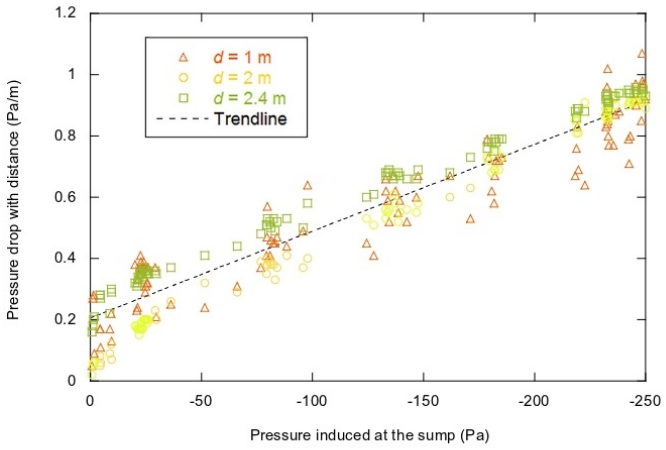

Fig. 7. Pressure drop with distance against pressure induced at the sump. Symbols represent the experimental data obtained from pressure records at distances $d = 1, 2$ and 2.4 m from the sump, both for active and passive SD testing phases. The dashed line is the linear trend obtained from all the experimental data, with a coefficient of determination $R^2 = 0.95$.

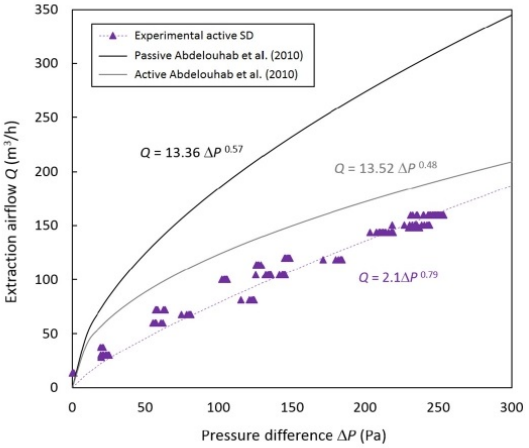

Fig. 9. Extraction airflow through the central exhaust pipe as function of the pressure difference generated between the aggregate layer under the slab and the inhabited volume of the basement. Symbols represent the experimental data for the active SD, the dashed line is the trend obtained from the experimental data and the solid lines represent the law relating extraction airflow with depressurisation for active and passive SD from Abdelouhab et al. (2010).

law differs for the active and passive SD operation in Abdelouhab et al. (2010), these results are explained by the fact that the permeability of the slab was modified due to works on it between tests. For the passive extraction the slab was leakier and higher extraction flow from the ground was induced to obtain the same depressurisation below the slab.

For a given airflow extraction rate from the ground, the depressurisation generated under the slab in the pilot house is the same no matter the phenomenon generating the extraction from the ground (active or passive), as it is determined by the permeability of the domain (aggregate layer, ground and slab). By solving Eq. (2), the theoretical extraction airflow required in the exhaust pipe of the pilot house to obtain a certain depressurisation under the slab can be calculated.

An example of the depressurisation generated under the slab by means of a rotating cowl during the passive SD operation is shown in Fig. 10(a) along with the wind velocity. There are no measurements of the extraction airflow generated in the exhaust pipe during the passive SD testing as a result of the wind effect. There are only records of the wind velocity, measured at the rooftop of the pilot house at a similar height to the rotating cowl and at a distance of approximately 3.5 m from the centre of the exhaust pipe. Fig. 10(b) shows the pressure induced at the sump as function of the wind velocity.

From data in Fig. 10(b) and using Eq. (2), a linear relationship between the wind velocity and the theoretical extraction airflow required in the exhaust pipe to induce such pressure under the slab is obtained (see Fig. 11). This relationship is only applicable to the type of rotating chimney cowl used during passive SD testing.

Following the results shown in Fig. 11, further passive SD testing phases would be required to investigate different type of extractors and chimney cowls in order to evaluate their performance at the pilot house, with known permeability from Eq. (2), and in line with research on the topic by Allard et al. (2018) and Hung et al. (2019).

4.3. Radon reduction

The radon reductions obtained for the different testing phases are summarised in Table 2, relative to the average radon concentration in the basement and ground floor calculated from the closed testing phases. It should be emphasised that the outdoor radon concentration in the area surrounding the pilot house is very high, approximately 300 Bq/m^3, while the average outdoor radon concentration globally is between 5 and 15 Bq/m^3 (WHO, 2016).

In all cases the radon reductions obtained are over 85%, and the highest reduction is found for the testing phase 4 reaching a radon concentration in the ground floor of 328 Bq/m^3, which is comparable to the outdoor radon concentration at the site, and a radon concentration of 662 Bq/m^3 in the basement. During phase 4 the mechanical fan was tested varying the extraction airflow and up to the highest power permitted (80 W).

From phase 6 experimental results, it can be highlighted that a 30 W mechanical fan, which is the equivalent power for the extraction airflow used during testing phase 6, is sufficient to reach radon reductions up to 94% in the basement and 86% in the ground floor in a house of these permeability characteristics. In terms of pressure induced under the slab, the average value at the sump recorded for testing phase 6 is −55 Pa.

Although it depends on the atmospheric conditions (mainly wind and temperature) and the occupant behaviour, the typical pressure difference found between indoors and the soil in a dwelling oscillates

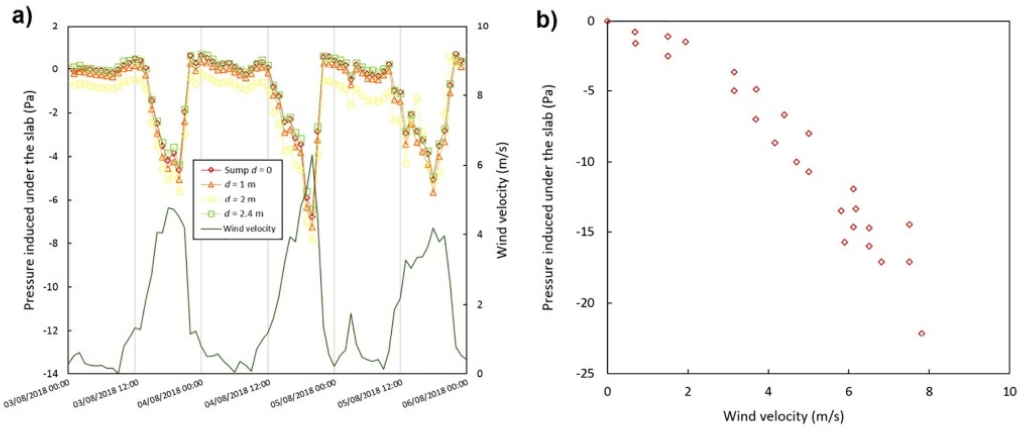

Fig. 10. (a) Hourly averaged pressure induced under the slab at the sump and the different measurement points with distances indicated from the central pipe along with hourly averaged wind velocity recorded at the site. (b) Pressure induced at the sump during passive SD operation against the wind velocity.

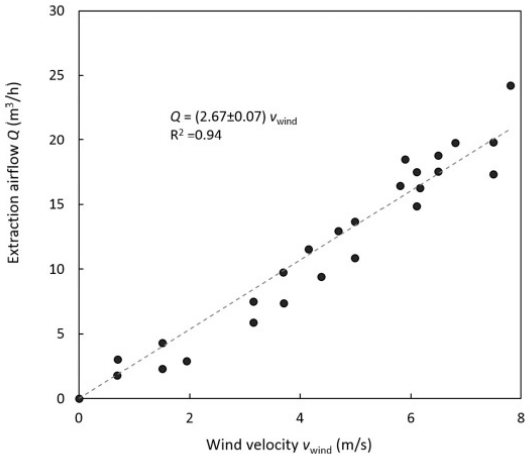

Fig. 11. Extraction airflow expected in the central exhaust pipe of the pilot house SD system against wind velocity, from measurements during passive SD testing by means of a rotating cowl. Dots represent the experimental data and the dashed line is the trendline obtained from the experimental data.

between 1 and 5 Pa. Thus, the depressurisation system should be designed to induce at least −6 Pa in every point of the slab area (Fowler et al., 1991; Broadhead, 2018; Dumais, 2018). Looking at Fig. 8, it can be observed that such pressure is obtained for extraction velocities below 1 m/s that correspond to 20 W power of the mechanical fan. Therefore, it could be postulated that a 20 W mechanical fan is sufficient to achieve an optimum soil depressurisation reaching radon reductions above 85% for dwellings with similar permeability characteristics to the experimental house studied here.

5. Conclusions

A monitoring study was conducted in a pilot house with extremely high radon levels to investigate the ability and efficiency of radon mitigation by both active and passive soil depressurisation. The study was motivated by the need to quantify SD effectiveness in terms of pressure field extension and also quantify significant radon reductions.

The testing plan consisted of different testing phases, alternating closed periods of the house to foster radon accumulation in the experimental house with SD operation phases. The variables monitored over the different testing periods were radon concentration in the basement and ground floor of the house, pressure field extension under the slab, and atmospheric parameters such as wind velocity, indoor and outdoor temperature, atmospheric pressure, relative humidity and accumulated rain.

Table 2
Radon concentration C_{Rn} found in the basement and ground floor for the SD testing phases indicated and radon reduction, respect to the average radon levels for the closed periods.

	C_{Rn} (Bq/m^3)		Radon reduction	
	Basement	Ground floor	Basement	Ground floor
Average closed	54,625	26,421		
Phase 2: passive SD	7417	–	86%	–
Phase 4: active SD (v_{ext} = 0–4 m/s)	662	328	99%	99%
Phase 6: active SD (v_{ext} = 1.5 m/s)	3326	3689	94%	86%
Phase 8: active SD (v_{ext} = 2 m/s)	3701	2279	93%	91%

Radon concentration behaviour was analysed for the closed testing periods, where an average radon concentration of 55 kBq/m^3 was found in the basement, while for the ground floor there was an average radon concentration of 26 kBq/m^3. Atmospheric variables influence on the radon behaviour in the house was also studied, finding significant correlations between outdoor temperature, atmospheric pressure and wind velocity with the radon concentration in the house. Impact of the indoor-outdoor temperature difference was discussed as well, significant negative correlation between pressure difference created as result of the temperature gradient with the radon concentration in the ground floor was obtained.

From the analysis of the pressure distribution under the slab, it was proven that the pressure drop with distance from the suction point of the SD system is linear with the depressurisation generated under the slab. Still, it was found that the distribution of the pressure under the slab in the pilot house is quite homogeneous, not exceeding 1 Pa/m pressure drop with distance for the highest depressurisation generated under the slab by active SD.

Permeability characterisation of the pilot house (including the aggregate layer, ground and concrete slab) was conducted, finding a behaviour law from the experimental data for the active SD performance, similar to previous works published on the characterisation of granular fill materials for radon soil depressurisation systems across Europe. Also, a relationship between the wind velocity and the extraction airflow from the ground was found for the passive SD performance by means of the particular rotating cowl used.

Finally, radon reductions in excess of 85% were achieved for the different testing phases in all cases. Based on the radon reduction results associated with the depressurisation generated under the slab as function of the extraction airflow for the active SD conditions considered, it was found that 20 W power for a mechanical fan is sufficient to achieve an optimum soil depressurisation reaching radon reductions above 85%.

To summarise, the case study presented contributes to the specification for optimum soil depressurisation systems performance and the findings encountered have applicability within similar building type dwellings with comparable aggregate layer permeability characteristics within the European context.

Authors' contributions

Mark Foley, Jamie Goggins, Carlos Sainz and Marta Fuente contributed to the initial research plan and the conception of the monitoring study. Marta Fuente, Carlos Sainz, Ismael Fuente and Daniel Rábago also evaluated and reviewed the testing plan. The experimental development of the study was conducted by Marta Fuente and Daniel Rábago with the help from the radon group technical staff (Enrique Fernández, Jorge Quindós and Luis Quindós) and the support of ENUSA Industrias Avanzadas S.A. Marta Fuente processed the experimental data, analysed the results with the help from Daniel Rábago and wrote the manuscript. Mark Foley, Jamie Goggins, Ismael Fuente and Carlos Sainz reviewed and edited the manuscript for the final version. All authors read and approved the final manuscript.

Declaration of Competing Interest

The authors declare that they have no known competing financial interests or personal relationships that could have appeared to influence the work reported in this paper.

Acknowledgments

This research was supported by the OPTI-SDS project carried out at the National University of Ireland Galway in collaboration with University of Cantabria, Spain. The OPTI-SDS project is funded by the Irish Environmental Protection Agency (EPA) [project code 2015-HW-MS-5].

The work was performed at the ENUSA Industrias Avanzadas S.A. facilities in Spain, thanks to the collaboration with the radon group at University of Cantabria. The authors would like to acknowledge ENUSA Industrias Avanzadas S.A. for the support and help while conducting the experiment and the technical staff of the radon group for their work on the experimental development of the study.

References

Abdelouhab, M., Collignan, B., Allard, F., 2010. Experimental study on passive soil depressurisation system to prevent soil gaseous pollutants into building. Build. Environ. 45, 2400–2406. https://doi.org/10.1016/j.buildenv.2010.05.001.

Allard, F., Abadie, M., Romani, Z., Burlot, M., Collignan, C., Druette, L., Peigné, P., Nicolle, J., 2018. Evaliation de la Performance des Systemes de Dépressurisation du Sol a Fonctionnement Natural (106 pages).

Baskaran, M., 2016. Radon: A Tracer for Geological, Geophysical and Geochemical Studies. Springer International Publishing https://doi.org/10.1007/978-3-319-21329-3 January.

Broadhead, B., 2018. Radon Mitigation in the US. WPB-Radon Inc. at ROOMS (Radon Outcomes on Mitigation Solutions) Conference (27th–28th September 2018, Lugano, Switerland). SUPSI.

Burke, O., Long, S., Murphy, P., Organo, C., Fenton, D., Colgan, P.A., 2010. Estimation of seasonal correction factors through Fourier decomposition analysis – a new model for indoor radon levels in Irish homes. J. Radiol. Prot. 30, 433–443. https://doi.org/10.1088/0952-4746/30/3/002.

Darby, S., Hill, D., Auvinen, A., Barros-Dios, J.M., Baysson, H., Bochicchio, F., ... Doll, R., 2004. Radon in homes and risk of lung cancer: collaborative analysis of individual data from 13 European case-control studies. BMJ 330 (7485), 223. https://doi.org/10.1136/bmj.38308.477650.63.

DELG, 2002. Radon in Existing Buildings. Corrective Options. Technical Report. Department of the Environment and Local Government, Stationery Office, Dublin.

Diallo, T.M.O., Collignan, B., Allard, F., 2015. Air flow models for sub-slab depressurization systems design. Build. Environ. 87, 327–341. https://doi.org/10.1016/j.buildenv.2015.01.017.

Dumais, C., 2018. The Canadian approach to radon mitigation and design. Radonwest Inc. at ROOMS (Radon Outcomes on Mitigation Solutions) Conference (27th–28th September 2018, Lugano, Switzerland). SUPSI.

Fowler, C.S., Williamson, A.D., Pyle, B.E., Belzer, F.E., Coker, R.N., 1991. Handbook: Sub-slab Depressurization for Low-permeability Fill Material. Design & Installation of a Home Radon Reduction System. US EPA, Washington, DC, USA.

Frutos, B., 2009. Estudio experimental sobre la efectividad y la viabilidad de distintas soluciones constructivas para reducir la concentración de gas radón en edificaciones. Universidad Politécnica de Madrid, Madrid.

Frutos, B., Olaya, M., Santiago, L., Poncela, Q., Sainz, C., 2011. Experimental study of effectiveness of four radon mitigation solutions, based on underground depressurization, tested in prototype housing built in a high radon area in Spain. J. Environ. Radioact. 102 (4), 378–385. https://doi.org/10.1016/j.jenvrad.2011.02.006.

Fuente, M., Rabago, D., Herrera, S., Quindos, L., Fuente, I., Foley, M., Sainz, C., 2018. Performance of radon monitors in a purpose-built radon chamber. J. Radiol. Prot. 38, 1111–1127. https://doi.org/10.1088/1361-6498/aad969.

Fuente, M., Muñoz, E., Sicilia, I., Goggins, J., Hung, L.C., Frutos, B., Foley, M., 2019. Investigation of gas flow through soils and granular fill materials for the optimisation of radon soil depressurisation system. J. Environ. Radioact. 198, 200–209. https://doi.org/10.1016/j.jenvrad.2018.12.024.

Garcia-Tobar, J., 2019. Weather-dependent modelling of the indoor radon concentration in two dwellings using CONTAM. Indoor Built Environ. 0 (0), 1–9. https://doi.org/10.1177/1420326X19841119.

Hung, L.C., Goggins, J., Fuente, M., Foley, M., 2018a. Characterisation of specified granular fill material for radon mitigation by soil depressurisation systems. Constr. Build. Mater. 176, 213–227. https://doi.org/10.1016/j.conbuildmat.2018.04.210.

Hung, L.C., Goggins, J., Fuente, M., Foley, M., 2018b. Investigation of sub-slab pressure field extension in specified granular fill materials incorporating a sump-based soil depressurisation system for radon mitigation. Sci. Total Environ. 637–638, 1081–1097. https://doi.org/10.1016/j.scitotenv.2018.04.401.

Hung, L.C., Goggins, J., Croxford, C., Foley, M., 2019. Large-scale experimental investigation of specified granular fill materials for radon mitigation by active and passive soil depressurisation. J. Environ. Radioact. 207, 27–36. https://doi.org/10.1016/j.jenvrad.2019.05.018.

IGME (Instituto Geológico y Minero de España), 2015. http://info.igme.es/ielig/LIGInfo.aspx?codigo=CI079, Accessed date: 1 July 2019 (Updated 30 June).

Jiranek, M., 2014. Sub-slab depressurisation systems used in the Czech Republic and verification of their efficiency. Radiat. Prot. Dosim. 162 (1–2), 64–67. https://doi.org/10.1093/rpd/ncu219.

Long, S., Fenton, D., Cremin, M., Morgan, A., 2013. The effectiveness of radon preventive and remedial measures in Irish homes. J. Radiol. Prot. 33, 141–149. https://doi.org/10.1088/0952-4746/33/1/141.

Mentes, G., Eper-Papao, I., 2015. Investigation of temperature and barometric pressure variation effects on radon concentration in the Sopronbanfalva geodynamic observatory, Hungay. J. Environ. Radioact. 149, 64–72. https://doi.org/10.1016/j.jenvrad.2015.07.015.

Nero, A.V., Gadgil, A.J., Nazaroff, W.W., Revzan, K.L., 1990. Indoor Radon and its Decay Products: Concentrations, Causes and Control Strategies. Technical report. Lawrence Berkeley Laboratory. University of California, Berkeley, CA, USA.

Riley, W.J., Gadgil, A.J., Bonnefous, Y.C., Nazaroff, W., 1996. The effect of steady winds on radon-222 entry from soil into houses. Atmos. Environ. 30, 1167–1176. https://doi.org/10.1016/1352-2310(95)00248-0.

Schubert, M., Mussolff, A., Weiss, H., 2018. Influences of meteorological parameters on indoor radon concentrations (^{222}Rn) excluding the effects of forced ventilation and radon exhalation from soil and building materials. J. Environ. Radioact. 198, 81–85.

Scivyer, C.R., Jaggs, M.P.R., 1998. A BRE Guide to Radon Remedial Measures in Existing Dwellings. Dwellings With Cellars and Basements. BRE.

WHO, 2016. https://www.who.int/news-room/fact-sheets/detail/radon-and-health, Accessed date: 4 May 2019 (Updated 30 June).

World Health Organization, 2009. Handbook on Indoor Radon. A Public Health Perspective. WHO Press, Geneva, Switzerland.

World Health Organization, 2018. WHO Housing and Health Guidelines.

Chapter 6

Conclusions

This thesis presented a study on the soil depressurisation technique for radon prevention and mitigation. The effectiveness of soil depressurisation systems was examined through laboratory based work and a case study conducted in a pilot house. Additionally, research on active radon detectors performance in a radon chamber was carried out. The research conducted was presented as three separate research articles in Journal of Radiological Protection, Journal of Environmental Radioactivity and Science of the Total Environment, and a conference paper in the proceedings of the Civil Engineering Research in Ireland 2018.

Chapter 2 addressed the evaluation of instrumentation for radon in air measurements by means of a benchmarking study of different types of active radon detectors, some of which are aimed for house testing available for the general public, while other are intended for diagnostic or research purposes. The evaluation of reliability and accuracy of the radon monitors was achieved through exposure to a stable controlled radon concentration inside a purpose-built radon chamber. The mean radon concentration obtained for all the monitors under study was found to be within the $\pm 10\%$ of the reference radon concentration given by the reference monitor. Response time to fluctuations in the radon concentration was investigated by controlling variations of the radon concentration in the chamber. Four analysis methods to assess response time of the monitors were proposed: two were based on the analysis of the relative error, one was based on the evaluation of time that a monitor takes to reach a certain percentage of the final concentration within a selected period and the last one considered frequency analysis of the occasions when measurement recorded matched the reference. The main conclusion drawn is that the selection of the radon monitor should be based on the application considered and the related accuracy and response time required for such purpose. In general, all the

active detectors tested were found to be appropriate for long-term measurement, but differences were found when investigating time-varying concentrations due to slight different response time of the detectors.

Characterisation of granular fill materials was investigated in Chapter 3, various types of aggregates commonly used in Spanish building practices were tested in terms of permeability, for which a test apparatus was adapted from our previous work. Gas permeability values for the samples under study were obtained from several theoretical expressions, of which the Darcy-Forchheimer equation was found to best fit experimental results and numerical simulations. From the analysis, air permeability coefficients of the order of magnitude of 10^{-8} m^2 were obtained for the different granular fill materials tested. A soil sample was also tested in the same test apparatus, the analysis of the experimental data led to verify that soil permeability is lower compared to that for the aggregates. Granular fill materials under study were benchmarked against Irish and British standards finding similarities among them. Overall, this research contributes to the understanding of specification for granular fill materials, which influence soil depressurisation and have applicability within the European context.

The main research of this thesis was conducted over a year in an experimental house provided with a soil depressurisation system and located in a high radon area, presented and explained in Chapters 4 and 5. Behaviour of the radon concentration in the pilot house was analysed, average radon levels found in the basement and ground floor of the house for the testing periods during no operation of the soil depressurisation system were 55 kBq/m^3 and 26 kBq/m^3, respectively. Analysis of the radon behaviour in relation to the atmospheric parameters monitored at the house site was carried out, resulting in significant correlation between outdoor temperature, atmospheric pressure and wind velocity with the indoor radon levels. Also, significant negative correlation between the pressure difference created due to indoor-outdoor temperature gradients and radon concentration was found. From the pressure field extension analysis, it was stated that the pressure drop with distance from the suction point is linearly proportional to depressurisation induced under the slab.

Performance of active and passive soil depressurisation was investigated, passive SDS was tested using a rotating cowl as the means of extraction, while a controlled power mechanical fan was used for the active SDS. Depressurisation induced

under the slab as a function of the extraction airflow was examined and, from the data recorded for active SD performance, an expression to describe permeability characterisation of the pilot house was found. From the experimental data for passive SDS operation, a relationship between the wind velocity and the extraction airflow generated in the exhaust pipe was obtained. This relationship helps to quantify effectiveness of passive soil depressurisation in direct relation to the wind velocity for the particular extractor employed and it is of interest for further investigation of different types of passive extractors.

Radon reductions achieved for the different testing phases considered were over 85%, thus confirming the high effectiveness reported for soil depressurisation techniques. From the analysis of radon reduction resulting from the depressurisation generated under the slab in relation to the extraction flow required, it was postulated that a 20 W electric fan used for active soil depressuristion could suffice to achieve optimum radon reduction. This finding is relevant for similar building type with comparable aggregate layer permeability characteristics.

To summarise, this thesis presents novel research on permeability characterisation of granular fill materials that influence performance of soil depressurisation systems and significant specification of factors that affect soil depressurisation effectiveness for radon reduction in buildings. As well as novel evaluation of radon monitor performance, addressing response time assessment.

The research conducted was developed within a theoretical scientific framework considering laboratory based experiments and a case study in an experimental pilot house, subject to the characteristics of the building and the local atmospheric conditions. Particularly, the pilot house is an experimental scenario not realistic in terms of pressure conditions and occupancy behaviour when comparing with an occupied dwelling. However, the findings can be extrapolated to real building scenarios taking into account the specific characteristic of each case.

This work can be used to form guidance for key stakeholders, such as housing authorities, radiation protection and public health authorities, architects, builders, radon prevention and mitigation service providers and other construction industry professionals. The findings can influence policy makers to inform the potential amendments of building regulations and also feed into the training of building professionals and radon mitigation service providers within national radon control

programmes. In this way, contributing to the development of the national radon action plan required by the 2013/59/EURATOM BSS Directive for the member states of the European Union. Overall, this research contributes to knowledge in the field of radon mitigation and it has implications within the European context.

6.1 Future work

Further research is recommended, including investigation into the passive soil depressurisation technique. Continuation of the case study conducted at the pilot house would be of interest to investigate the impact of different passive extractors under different weather conditions on the effectiveness of the soil depressurisation system. This proposed work could prove cost-effectiveness of passive soil depressurisation systems installation against other radon measures, which would constitute a low-cost, passive and sustainable strategy to minimise radon levels in buildings.

Future work could be carried out also regarding the effect of energy efficiency in buildings on indoor radon levels, addressing one of the identified knowledge gaps for Phase 2 of the National Radon Control Strategy for Ireland. In line with the implementation of recent EU Directive 2010/31/EU on energy performance of buildings, aimed at reaching high energy efficiency and sustainability, new buildings have airtightness and ventilation requirements that affect indoor radon levels. Investigation of performance of radon prevention and mitigation techniques taking into consideration the airtightness and air exchange rates required for the new energy efficient buildings would be timely and very important given the changes in the building practices. An example of proposed research in relation to this could be continuing the monitoring study at the pilot house to examine effectiveness of the soil depressurisation system by controlling the air exchange rate of the house.

Leverage of international collaborations, which allow access to valuable world class facilities for controlled studies on radon mitigation, should be continued. Future research could be conducted building upon existing relations, contributing to the development and strengthening of a research network for radon prevention and mitigation with collaborators across Europe.

Bibliography

2010/31/EU. Council of the European Union Directive 2010/31/EU on the Energy Performance of Buildings. Official Journal of the European Union 18.6.2010 L 153/13, 2010.

2013/59/EURATOM. Council of the European Union Directive 2013/59/EURATOM European Basic Safety Standards for Protection Against Ionising Radiation. Official Journal of the European Union L 13/17.1.2014.

M. Abdelouhab, B. Collignan, and F. Allard. Experimental study on passive Soil Depressurisation System to prevent soil gaseous pollutants into building. *Building and Environment*, 45(11):2400–2406, 2010.

Airthings. *Canary Digital Radon Monitor User Manual*, Accesed date: 28 August 2019.

M.C. Akis, H. Stadtmann, and P. Kindl. Computer simulation of air pressure modification in radon laden sub-floor soil. Graz University of Technology. Institute of Technical Physics. Austria, 2004.

W.J. Angell. *Encyclopedia of Environmental Health*, chapter Indoor Radon Prevention and Mitigation, pages 208–217. Elsevier, 2011.

H. Arvela. Experiences in radon-safe building in Finland. *The Science of the Total Environment*, 272:169–174, 2001.

G. Audi, F. G. Kondev, Meng Wang, W.J. Huang, and S. Naimi. The NUBASE2016 evaluation of nuclear properties. *Chinese Physics C*, 41(3):030001, 2017. doi: 10.1088/1674-1137/41/3/030001.

F. Bochicchio. The newest international trend about regulation of indoor radon. *Radiation Protection Dosimetry*, 146:2–5, 2011.

Y. Bonnefous. *Etude numerique des systemes de ventilation du sol pour diminuer la concentration en radondans l'habitat*. PhD thesis, Genie Civil: sols, materiaux,

Structures et Physique du batiment. Institut National des Sciences Apliquees de Lyon, 1992.

R. P. Chauhan and A. Kumar. A comparative study of indoor radon contributed by diffusive and advective transport through intact concrete. *Physics Procedia*, 80: 109–112, 2015.

B. Collignan, C. Lorkowski, and R. Améon. Development of a methodology to characterize radon entry in dwellings. *Building and Environment*, 57:176 – 183, 2012. doi: 10.1016/j.buildenv.2012.05.002.

B. Collignan, E. Le Ponner, and C. Mandin. Relationships between indoor radon concentrations, thermal retrofit and dwelling characteristics. *Journal of Environmental Radioactivity*, 165:124 – 130, 2016. doi: 10.1016/j.jenvrad.2016.09.013.

M. Collins and S. Dempsey. Residential energy efficiency retrofits: potential unintended consequences. *Journal of Environmental Planning and Management*, 2018. doi: 10.1080/09640568.2018.1509788.

S. Darby, D. Hill, A. Auvinen, Barros-Dios ..., E. Whitley, H.E. Wichmann, and R. Doll. Radon in homes and risk of lung cancer: collaborative analysis of individual data from 13 European case-control studies. *BMJ*, 330(7485):223, 2005. doi: 10.1136/bmj.38308.477650.63.

C. de Oliveira Loureiro. *Simulation of the steady-state transport of radon from soil into houses with basements under constant negative pressure*. PhD thesis, University of Michigan, 1987.

G. De Pin, S. Dulla, and M. Esposito. General expression of the calibration curve for the cr-39 radon track detectors. *Radiation Measurements*, 89:1 – 7, 2016. doi: 10.1016/j.radmeas.2016.04.001.

DEHLG. S.I. No. 497 of 1997. Building Regulations 1997. Technical report, Department of the Environment, Heritage and Local Government, Stationery Office, Dublin, 1997.

DEHLG. Technical Guidance Document C - Site Preparation and Resistance to Moisture. Technical report, Department of the Environment, Heritage and Local Government, Stationery Office, Dublin, 2004.

DELG. Radon in existing buildings. Corrective Options. Technical report, Department of the Environment and Local Government, Stationery Office, Dublin, 2002.

S. Dempsey, S. Lyons, and A. Nolan. High radon areas and lung cancer prevalence: Evidence from Ireland. *Journal of Environmental Radioactivity*, 182:12 – 19, 2018. doi: 10.1016/j.jenvrad.2017.11.014.

A. R. Denman, R.G.M. Crockett, and C.J. Groves-Kirkby. An assessment of the effectiveness of UK building regulations for new homes in Radon Affected Areas. *Journal of Environmental Radioactivity*, 192:166 – 171, 2018. doi: 10.1016/j.jenvrad.2018.06.017.

A. Denman et al. Do radon-proof membranes reduce radon levels adequately in new houses? In *Proc. 7th SRP International Symposium 'Change and continuity in Radiation Protection'*, Cardiff, UK, 2005.

T. M. O. Diallo, B. Collignan, and F. Allard. Air flow models for sub-slab depressurization systems design. *Building and Environment*, 87:327–341, 2015.

A. Dowdall, P. Murphy, D. Pollard, and D. Fenton. Update of Ireland's national average indoor radon concentration - application of a new survey protocol. *Journal of Environmental Radioactivity*, 169-170:1–8, 2017.

B.A. El-Badry and T.I. Al-Naggar. Estimation of indoor radon levels using etched track detector. *Journal of Radiation Research and Applied Sciences*, 11(4):355 – 360, 2018. doi: 10.1016/j.jrras.2018.07.002.

J. Elio, Q. Crowley, J. Scanlon, J. Hodgson, and S. Long. Logistic regression model for detecting radon prone areas in Ireland. *Science of the Total Environment*, 599-600:1317–1329, 2017.

EPA. Understanding Radon Remediation A Householder's Guide. Technical report, Irish Environmental Protection Agency, Dublin, 2019.

US EPA. Building Radon Out: A step-by-step guide on how to build radon-resistant homes. Technical report, United States Environmental Protection Agency, Office of Air and Radiation, 2001.

G. Espinosa, J.I. Golzarri, M.I. Gaso, M. Mena, and N. Segovia. An intercomparison of indoor radon data using NTD and different dynamic recording systems. *Radiation Measurements*, 50:112 – 115, 2013.

Ll. Font. *Radon generation, entry and accumulation indoors*. PhD thesis, Universitat Autonoma de Barcelona, 1997.

B. Frutos Vázquez. *Estudio experimental sobre la efectividad y la viabilidad de distintas soluciones constructivas para reducir la concentración de gas radón en edificaciones*. PhD thesis, Universidad Politécnica de Madrid, 2009.

B. Frutos Vázquez, M. Olaya Adán, L.S. Quindós Poncela, C. Sainz Fernández, and I. Fuente Merino. Experimental study of effectiveness of four radon mitigation solutions, based on underground depressurization, tested in prototype housing built in a high radon area in Spain. *Journal of environmental radioactivity*, 102 (4):378–385, 2011.

A. J. Gadgil. Models of radon entry. *Radiation Protection Dosimetry*, 45(1-4): 373–379, 1992.

A. J. Gadgil, Y. C. Bonnefous, and W. J. Fisk. Relative effectiveness of sub-slab pressurization and depressurization systems for indoor radon mitigation: Studies with an experimentally verified numerical model. *Indoor Air*, 4(4):265–275, 1994.

A.C. George. State-of-the-art instruments for measuring radon/thoron and their progeny in dwellings-a review. *Health Physics*, 70:451–463, 1996.

G.A. Gunning, D. Pollard, and E.C. Finch. An outdoor radon survey and minimizing the uncertainties in low level measurements using CR-39 detectors. *Journal of Radiological Protection*, 34:457–467, 2014.

G.A. Gunning, M. Murray, S.C. Long, M.J. Foley, and E.C. Finch. Inter-comparison of radon detectors for one to four week measurement periods. *Journal of Radiological Protection*, 36:104, 2016.

S.A. Hodgson and V. Pudner. Passive Remediation for Radon in UK Homes. Technical Report PHE-CRCE-045, PHE, Oxfordshire, UK, January 2019.

O. Holmgren and H. Arvela. Assessment of current techniques used for reduction of indoor radon concentration in existing and new houses. Technical report, Radiation and Nuclear Safety Authority (Stuk) Finland, 2011.

C.B. Howarth. PHE Intercomparison of Passive Radon Detectors. Technical Report PHE-CRCE-036, PHE, Public Health England, London, UK, 2017.

L.C. Hung, J. Goggins, M. Fuente, and M. Foley. Characterisation of specified granular fill material for radon mitigation by soil depressurisation systems. *Construction and Building Materials*, 176:213–227, 2018.

ICRP. Statement on radon. Technical report, International Commission on Radiological Protection, 2009. Ref 00/902/09.

Y. Ishimori, K. Lange, P. Martin, Y.S. Mayya, and M. Phaneuf. Measurement and calculation of radon releases from NORM residues. Technical Report Series No 474, International Atomic Energy Agency (IAEA), Viena, 2013.

B. P. Jelle. Development of a model for radon concentration in indoor air. *Science of The Total Environment*, 416:343–350, 2012.

M. Jiránek. Sub-slab depressurisation systems used in the Czech Republic and verification of their efficiency. *Radiation Protection Dosimetry*, 162(1-2):64–67, 2014.

M. Jiránek and J. Hulka. Applicability of various insulating materials for radon barriers. *Science of The Total Environment*, 272(1):79 – 84, 2001. doi: 10.1016/S0048-9697(01)00668-4. Radon in the Living Environment.

M. Jiránek and V. Kacmarikova. Dealing with the increased radon concentration in thermally retrofitted buildings. *Radiation Protection Dosimetry*, 160:43 – 47, 2014. doi: 10.1093/rpd/ncu104.

M. Jiránek and Z. Svoboda. Numerical modelling as a tool for optimisation of sub-slab depressurisation systems design. *Building and Environment*, 42(5): 1994–2003, 2007.

M. Jiránek, M. Neznal, and M. Neznal. Sub-slab depressurisation systems: effectiveness and soil permeability. In *Radon in the Living Environment*, Athens, Greece, 19-23 April 1999.

K. Jílek and M. Marušiaková. Results of the 2010 National Radiation protection institute intercomparison of radon and its short-lived decay product continuous monitors. *Radiation Protection Dosimetry*, 145(2-3):273–279, 2011.

S.M. Khan, J. Gomes, and D.R. Krewski. Radon interventions around the globe: A systematic review. *Heliyon*, 5(5):e01737, 2019. doi: 10.1016/j.heliyon.2019.e01737.

C-F Lin, J-J Wang, S-J Lin, and C-K Lin. Performance comparison of electronic radon monitors. *Applied Radiation and Isotopes*, 81:238 – 241, 2013. 6th

International Conference on Radionuclide Metrology - Low Level Radioactivity Measurement Techniques.

S. Long and E. Smyth. The impact of energy retrofitting on radon levels in local authority homes. EPA study, Irish National Radon Forum 2015, 2015.

S. Long, D. Fenton, M. Cremin, and A. Morgan. The effectiveness of radon preventive and remedial measures in Irish homes. *Journal of Radiological Protection*, 33:141–149, 2013.

I. Makelainen, H. Arvela, and A. Voutilainen. Correlations between radon concentration and indoor gamma dose rate, soil permeability and dwelling substructure and ventilation. *The Science of the Total Environment*, 272:283–289, 2001.

B. McCarron, X. Meng, and S. Colclough. A pilot study of radon levels in certified passive house buildings. *Building Services Engineering Research and Technology*, 40(3):296–304, 2019. doi: 10.1177/0143624418822444.

J.A. McGrath and M.A. Byrne. UNVEIL: Understanding ventilation and radon in energy-efficient buildings in Ireland. Technical Report 273, EPA, Ireland, 2019.

W. Meyer. Impact of constructional energy saving measures on radon levels indoors. *Journal of Environmental Radioactivity*, 29:680 – 685, 2019. doi: 10.1111/ina.12553.

J. Miles. Methods of radon measurement and devices. Proceedings of the 4th European conference on protection against radon at home and at work Conference programme and session presentations, Czech Republic, 2004.

L. Minkin. Is diffusion, thermodiffusion, or advection a primary mechanism of indoor radon entry? *Radiation Protection Dosimetry*, 102(2):153–162, 2002.

E. Muñoz, B. Frutos, M. Olaya, and J. Sánchez. A finite element model development for simulation of the of slab thickness, joints and membranes on indoor radon concentration. *Journal of Environmental Radioactivity*, 177:280–289, 2017.

W.W. Nazaroff. Radon transport from soil to air. *Reviews of Geophysics*, 30(2): 137–160, 1992.

A.V. Nero, Nazaroff W.W. Gadgil, A.J., and K.L. Revzan. Indoor radon and decay products: concentrations, causes and control strategies. Technical report, Lawrence Berkeley Laboratory, University of California, 1990.

P. Nilson. Radon diagnostics and radon corrective actions – Scandinavia experience. ROOMS conference, October 2017.

NRCS. National Radon Control Strategy. Report of interagency group established by the Minister for the Environment, Community and Local Government, to develop a NRCS for Ireland. Technical report, Dublin, Ireland, 2014.

NRCS. National Radon Control Strategy year 4 report. Technical report, Dublin, Ireland, 2019a.

NRCS. National Radon Control Strategy review of knowledge gaps paper 2014-2018. Report of the National Radon Control Strategy Coordination Group. Technical report, Dublin, Ireland, 2019b.

NRCS. National Radon Control Strategy Phase two: 2019-2024. Report of the National Radon Control Strategy Coordination Group. Technical report, Dublin, Ireland, 2019c.

C. Organo and P. Murphy. The Castleisland radon survey-follow-up to the discovery of a house with extremely high radon concentrations in County Kerry (SW Ireland). *Journal of Radiological Protection*, 27:275–285, 2007.

F. Pacheco-Torgal. Indoor radon: an overview on a perennial problem. *Building and Environment*, 58:270–277, 2012.

L. Pampuri, P. Caputo, and C. Valsangiacomo. Effects of buildings' refurbishment on indoor air quality. results of a wide survey on radon concentrations before and after energy retrofit interventions. *Sustainable Cities and Society*, 42:100 – 106, 2018. doi: 10.1016/j.scs.2018.07.007.

K.G. Pennell, O. Bozkurt, and E.M. Suuberg. Development and application of a three-dimensional finite element vapor intrusion model. *Air and Waste Management Association*, 59(4):447–460, 2009.

A. Poffijn, O. Tonet, B. Dehandschutter, M. Roger, and M. Bouland. A pilot study on the air quality in passive houses with particular attention to radon, 2012.

L.S. Quindós. *Radón. Un gas radiactivo de origen natural en su casa.* CSN, 1995.

L.S. Quindós, P.L. Fernández, and J. Soto. Radiactividad natural y radón. In *Boletín Sociedad Española Hidrológica Médica*, volume IX, pages 133–137. 1994.

L.S. Quindós-Poncela, P.L. Fernández, C. Sainz, J. Arteche, J.G. Arozamena, and A.C. George. An improved scintillation cell for radon measurements. *Nuclear Instruments and Methods in Physics Research Section A: Accelerators, Spectrometers, Detectors and Associated Equipment*, 512(3):606 – 609, 2003. doi: 10.1016/S0168-9002(03)02049-7.

D. Rábago. Aplicación de un sistema de monitorización de la concentración de gas radón en el agua de una instalación termal. Universidad de Cantabria, 2013.

T.A. Reddy, K.J. Gadsby, H.E. Black, D.T. Harrje, and R.G. Sextro. Modeling air flow dynamics in radon mitigation systems: a simplified approach. *Air and Waste Manage Association*, 41(11):1476–1482, 1991.

W. Ringer. Monitoring trends in civil engineering and their effect on indoor radon. *Radiation Protection Dosimetry*, 160:38 – 42, 2014. doi: 10.1093/rpd/ncu107.

W. Ringer and J. Graser. Radon and energy efficient building construction. ROOMS conference, October 2011.

RPII. Radon in dwellings - The Irish National Radon Survey. Technical report, RPII 02/1, 2002.

C. Sainz, L.S. Quindós, Fernández ..., and J.M. Matarranz. Spanish experience on the design of radon surveys based on the use of geogenic information. *Journal of Environmental Radioactivity*, 166:390–397, 2017.

M. Schubert, A. Musolff, and H. Weiss. Influences of meteorological parameters on indoor radon concentrations (222Rn) excluding the effects of forced ventilation and radon exhalation from soil and building materials. *Journal of Environmental Radioactivity*, 192:81 – 85, 2018. doi: 10.1016/j.jenvrad.2018.06.011.

H. Synnot et al. A survey of the impact of amending building regulations on radon concentrations in Irish homes. In *11th congress of the International Radiation Protection Association (IRPA11)*, Madrid, 2004.

B.H. Turk, J. Harrison, and R.G. Sextro. Performance of radon control systems. *Energy and Buildings*, 17:157–175, 1991.

UNSCEAR. Sources and effect of ionizing radiation. Technical report, United Nations Scientific Committe on the Effects of Atomic Radiation, 2000.

A.V. Vasilyev and M.V. Zhukovsky. Determination of mechanisms and parameters which affect radon entry into a room. *Journal of Environmental Radioactivity*, 124:185 – 190, 2013. doi: 10.1016/j.jenvrad.2013.04.014.

F. Wang and I.C Ward. The development of a radon entry model for a house with a cellar. *Building and Environment*, 35:615–631, 2000.

F Wang and I.C. Ward. Radon entry, mitigation and reduction in houses with cellars. *Building and Environment*, 37:1153–1165, 2002.

J.M. Wasikiewicz, Z. Daraktchieva, and C.B. Howarth. Passive etched track detectors application in outdoor radon monitoring. *Perspectives in Science*, 12: 100416, 2019. doi: 10.1016/j.pisc.2019.100416.

WHO. *WHO Handbook on Indoor Radon. A public health perspective*. WHO Press, World Health Organization, Avenue Appia, Geneva, Switzerland, 2009.

Y. Yao, R. Shen, K.G. Pennell, and E.M. Suuberg. A review of Vapor Intrusion Models. *Environmental Science & Technology*, 47:2457–2470, 2013.